The Effect of Irisin on Orthodontic Tooth Movement and Human Cells in Tooth-Supporting Apparatus

Yang Yang

Doctoral Thesis for the Degree of Philosophiae Doctor (Ph.D)

Department of Biomaterials

Institute of Clinical Dentistry

Faculty of Dentistry

University of Oslo

Norway

2023

Series of dissertations submitted to the
Faculty of Dentistry, University of Oslo

ISBN 978-82-8327-078-5

Cover: UiO.
Print production: Graphic center, University of Oslo.

1 ACKNOWLEDGEMENTS

The current research work was carried out at Department of Biomaterials, Institute for Clinical Dentistry, Faculty of Dentistry, University of Oslo, partly in collaboration with Comparative Medicine Core Facility, Norwegian University of Science and Technology (NTNU).

It's incredible how quickly the time has passed and how much has changed. Finally, the moment has arrived to pay tribute to all those who have helped and supported me along the amazing journey! Looking back, I can't help but feel a sense of nostalgia for all these years spent in Norway, but I also realize that every moment, no matter how fleeting, has shaped me into the person I am today.

In the beginning, I wish to express my deepest gratitude to my principal supervisor professor Janne Elin Reseland for her exceptional guidance throughout the entire PhD project, including the instructions on lab work and the meticulous article editing, as well as all the support she has given me in both study and personal life over the past years.

I would further extend my heart-felt gratefulness to my secondary supervisor Helen Pullisaar from Department of Orthodontics for her detailed revisions on my research papers and tremendous help in animal study conducted in Trondheim, which definitely could not have been possible without her assistance.

I am grateful to Athina Samara for her superb analysis and interpretation of my research data. Thank Maria A. Landin, her skillful techniques and easy-going personality always inspire me. Many thanks to Catherine Anne Heyward, for sharing the expertise in histology and providing support in confocal imaging. Gratitude should also go to Astrid Kamilla Stunes for her assistance in the animal experiments in Trondheim. Thank Liebert Parreiras Nogueira for his help in micro-CT scanning, I am truly amazed at his vast knowledge equipment. Thank Professor Vaska Vandevska Radunovic from Department of Orthodontics for her professional instructions on establishment of animal models. I would also like to express my profound thanks to professor Unni Syversen from NTNU for generously funding the animal study.

Scientific inputs and technical support have been gratefully received from all my other collaborators and co-authors, including Anne Eriksson Agger, Bjørn Helge Skallerud, Jianying He, Maria Schröder, Maria Grano, Ole Kristoffer Olstad and Tianxiang Geng, I am deeply appreciative of their contribution in this PhD thesis.

Sincere thanks should also go to the staffs at Department of Biomaterials. I would like to thank Aina Mari Lian, Alejandro Barrantes Bautista, Mousumi Sukul and Sonny Margaret Langseth for their great effort in maintaining the lab. Meanwhile, special acknowledgement goes to professor Håvard Jostein Haugen for his excellent leadership.

My earnest gratitude goes to my dear friends in Oslo, they are Congying Zheng, Tianxiang Geng and Yuping Fu, I will remember all the joyous weekend parties and every fantastic moment we have shared in Norway, how serendipitous it is to get to know you all!

Moreover, I highly appreciate the financial support from China Scholarship Council (CSC) and Faculty of Dentistry, University of Oslo, which have substantially supported my academic stay in Norway.

Finally, and above all, I would like to acknowledge my family members for their unwavering mental support, I could not have been able to go through this journey without their constant love and care.

Oslo, April 2023

Yang Yang

2 LIST OF PUBLICATIONS

The present PhD thesis is based on the following three papers, which will be further referred to according to their Roman numerals in the text of the thesis.

Paper I

Yang Y, Pullisaar H, Landin MA, Heyward CA, Schröder M, Geng TX, Grano M, Reseland JE. FNDC5/irisin is expressed and regulated differently in human periodontal ligament cells, dental pulp stem cells and osteoblasts. *Archives of Oral Biology*. 2021; 124: 105061.

Paper II

Yang Y, Pullisaar H, Stunes AK, Nogueira LP, Syversen U, Reseland JE. Irisin reduces orthodontic tooth movement in rats by promoting the osteogenic potential in the periodontal ligament. Manuscript submitted to *European Journal of Orthodontics, 2023.*

Paper III

Yang Y, Geng TX, Samara A, Olstad OK, He JY, Agger AE, Skallerud BH, Landin MA, Heyward CA, Pullisaar H, Reseland JE. Recombinant irisin enhances the extracellular matrix formation, remodeling potential, and differentiation of human periodontal ligament cells cultured in 3D. *Journal of Periodontal Research*. 2023; 00: 1- 14. doi:10.1111/jre.13094.

3 LIST OF ABBREVIATIONS

ALP	alkaline phosphatase
Asn	asparagine
ATRA	all-trans retinoic acid
BAT	brown adipose tissue
BRC	bone remodeling compartment
BVF	bone volume fraction
CMPs	common myeloid progenitors
DEG	differentially expressed gene
ECM	extracellular matrix
E. coli	escherichia coli
EDTA	ethylenediaminetetraacetic acid
ELISA	enzyme-linked immunosorbent assay
FNDC5	fibronectin type III domain-containing protein 5
GAPDH	glyceraldehyde-3-phosphate dehydrogenase
GlcNAc	N-acetylglucosamine
GM-CSF	granulocyte/macrophage stimulating factor
GMPs	granulocyte/macrophage progenitors
GO/KEGG	Gene Ontology/Kyoto Encyclopedia of Genes and Genomes
hDPCs	human dental pulp cells
H&E	hematoxylin and eosin
HIER	heat-mediated epitope retrieval
hOBs	human osteoblasts
HSCs	hematopoietic stem cells
IF	immunofluorescence
IL	interleukin
IPA	Ingenuity pathways analysis
LCS	lacuno-canalicular system
M-CSF	macrophage colony-stimulating factor
micro-CT	micro computed tomography
MMPs	metalloproteinases
MSCs	mesenchymal stem cells
NFATc1	nuclear factor-activated T cells c1
OCN	osteocalcin
OPG	osteoprotegerin
OTM	orthodontic tooth movement
PDL	periodontal ligament
PGC-1α	peroxisome proliferator-activated receptor γ coactivator 1α
PPAR-α	peroxisome proliferator-activated receptors α
qPCR	quantitative polymerase chain reaction
RANKL	receptor activator of nuclear factor-κB ligand
RUNX2	runt-related transcription factor 2

TAS2R	bitter taste-sensing type 2 receptor family subtypes
TNF-α	tumor necrosis factor α
TRAP	tartrate-resistant acid phosphatase
UCP1	uncoupling protein 1
VEGF	vascular endothelial growth factor
VOI	volume of interest
vWF	von Willebrand factor
WAT	white adipose tissue
2D	two dimensional
3D	Three dimensional

TABLE OF CONTENTS

4 INTRODUCTION

4.1 FNDC5/irisin

In the year of 2002, two independent groups of researchers discovered a previously unknown gene, which was originally termed as peroxisomal protein (1) or fibronectin type III repeat containing protein 2 (2) because of its specific motif. This particular gene, which is now termed as fibronectin type III domain-containing protein 5 (FNDC5), regained much attention 10 years later as it has been defined as one of the target genes for peroxisome proliferator-activated receptor γ coactivator 1α (PGC-1α), a transcriptional coactivator induced in response to physical activities in skeletal muscle. PGC-1α expression in muscle then stimulates expression of FNDC5, which is subsequently proteolytically cleaved and released into circulation as a newly identified hormone irisin, thus affecting energy metabolism by promoting browning of white adipose cells (3, 4).

FNDC5 is a glycosylated type I membrane protein, with a mass varying from 20 to 32 kDa dependent on the number and structure of oligosaccharides (glycans) bound to it in post-translational process of N-glycosylation (5). FNDC5 contains an N-terminal signal peptide (amino acid (aa) 1-28), an FNIII domain (aa 33-124), a transmembrane domain (aa 150-170) and a C-terminal cytoplasmic segment (aa 171-209). The C-terminal part is localized in cytoplasm, whereas the N-terminal portion is proteolytically cleaved, glycosylated and secreted into circulation. This secreted part is termed as irisin (Figure 1), the enzyme which cleaves the FNDC5, however, has not been identified yet (6, 7). The irisin peptide is highly conserved in human, mouse and rat, although the signal peptide and segments from C-terminal to irisin exhibit some variability. A notable exception is that the human FNDC5 gene possesses a mutant start codon, ATA, instead of the canonical ATG. Among the six genes with ATA as start codon, FNDC5 is the only described gene that is not conserved in other species than humans (4).

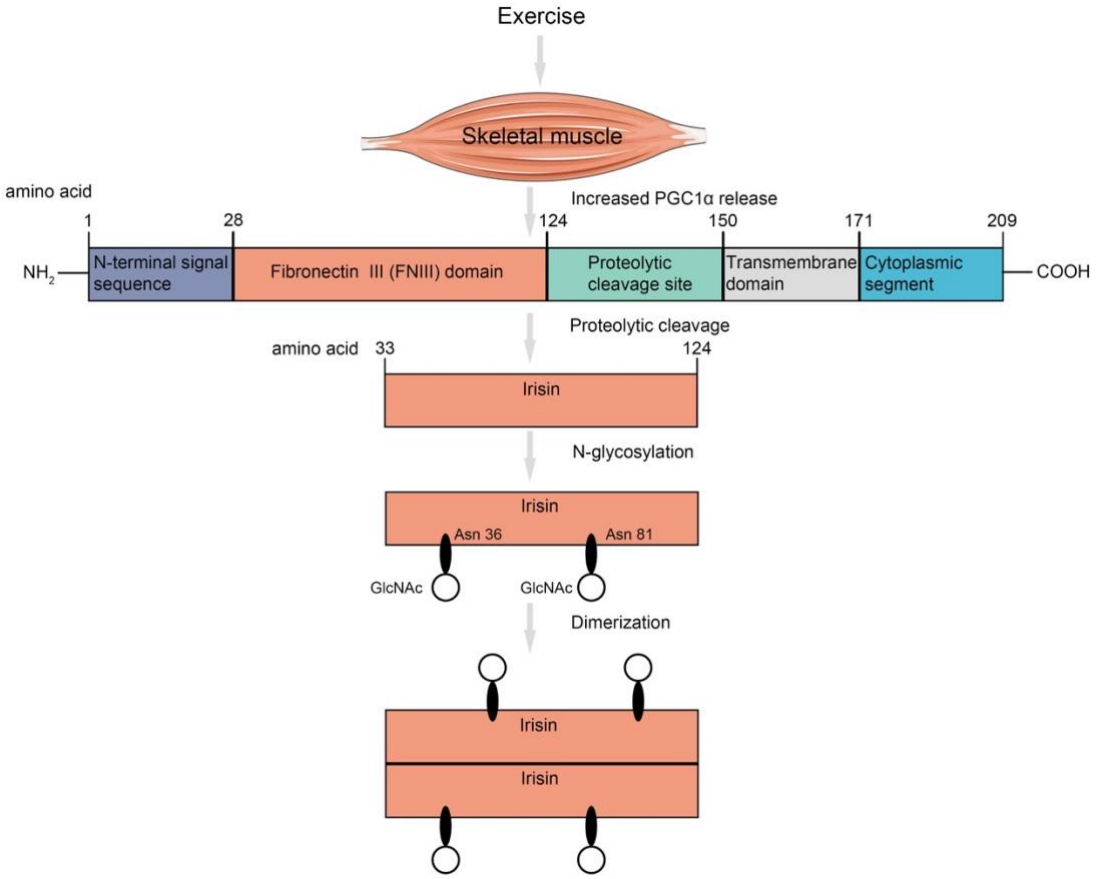

Figure 1. Schematic illustration for mechanism of irisin release from FNDC5 and their structures. Exercise promotes the release of PGC-1α from skeletal muscles, increasing the FNDC5 expression, and irisin is thus cleaved from FNDC5 by unknown protease and secreted into circulation. Through the bond which is formed between N-acetylglucosamine (GlcNAc) and the nitrogen derived from the amide group of asparagine (Asn36 and Asn81), irisin is glycosylated and subsequently dimerized. This figure is adapted from Panati et al. (8) and Pinkowska et al. (9).

The binding of oligosaccharides (glycans) to proteins or lipids is referred to as glycosylation, which is a common post-translational modification that results in a wide range of functions from a limited set of genes (10). Glycans can affect the physical and chemical characteristics of proteins, which are essential in acquiring accurate proteins conformation, providing proteolysis protection and are vital for their biological roles in certain metabolic processes (11). FNDC5 is an N-glycosylated protein with oligosaccharides verified to be N-glycosylated at Asn^{36} and Asn^{81} sites, and the glycosylation process is essential in the stabilization of FNDC5 and secretion of irisin (12). Irisin

has a molecular weight of 12 kDa as a monomer, and its molecular weight can be further increased up to 20-32 kDa through glycosylation and dimerization, according to the number of glycans bound to the protein molecule during N-glycosylation (3, 13). Additionally, irisin crystal structure shows that the FNIII-like domain forms a continuous intersubunit β-sheet dimer, which may present a possible mechanism for ligand and receptor activation (14).

4.1.1 Irisin receptors

Until now, the receptors for irisin still have not been elucidated, however, a research conducted by Kim et al. defined a subunit of integrin complexes as presumptive receptor for irisin in osteocytes and adipose tissues (15). Their conclusions were based on the following findings. First, quantitative mass spectrometry revealed that irisin can attach to osteocytes, which allows chemical cross-linking to β1 integrin. Second, protein-protein binding analysis that uses purified irisin and integrin complexes exhibited that irisin binds to multiple complexes, among which αV/β5 has the highest apparent affinity. Third, it was proved that irisin bind to integrin αV/β5, and this analysis allowed the mapping of binding sites on both irisin and integrin complex. Fourth, irisin induced enhanced integrin signal in HEK293T cells transfected with αV/β1 integrin or αV/β5 integrin compared with control cells. Finally, inhibitors or antagonistic antibody targeted against αV/β5 integrin suppressed almost all irisin-mediated signaling and its downstream gene expression (5, 15). It should be pointed out that identification of irisin receptors in osteocytes and adipose tissues suggests that αV family of integrin complexes are possible major receptors in all cells/tissues, but it does not rule out the possibility of existence of other potential receptors for irisin in both integrin family or even outside of integrins (15). Anyway, the identification of receptors for irisin would promote future research on both its upstream regulation and its down-stream signaling cascades, with implications in its potential therapeutic approaches (16). However, one major problem with the identification of this receptor may be the dearth of specificity: the initial quantitative mass spectrometry screen had identified β1 to be the only integrin, but it was abandoned in all following experiments. Currently, the favored receptor is αV/β5, which induced the best response in the screen of integrins (4). The identification of αV/β5 as the irisin receptor has been supported by several subsequent studies. A recent research reported that CD81 can form a complex with αVβ1 and αVβ5, the authors found that CD81 sensitized the HEK293T cells against irisin, further, it is required for proliferation of

beige adipocyte progenitor cells and mediates the activation of integrin-FAK signaling in response to irisin (17). Another study revealed that an antibody inhibiting αVβ5 deprived the response of osteoclasts to irisin, which confirms this receptor (18). However, the main integrin determined on osteoclasts is αVβ3 while αVβ5 integrin has not been identified on osteoclasts previously (19, 20).

4.1.2 Physiological roles of FNDC5/irisin

Irisin plays vital role in energy metabolism by acting on the browning of white adipose tissue (WAT) to promote energy consumption (21). Generally, the adipose tissue comprises of two elements called WAT and brown adipose tissue (BAT), WAT functions to store lipids, while BAT is involved in thermogenesis via uncoupled respiration (22). WAT adipocytes are featured by unilocular lipid droplets, less mitochondria and relatively low metabolic rate, by contrast, adipocytes in BAT are featured by multilocular lipid droplets, ample mitochondria and relatively high metabolic rate, which is induced by mass production of uncoupling protein 1 (UCP1), whereas its expression is rarely observed in WAT (23). The mechanism with which irisin regulates energy metabolism can be summarized as follows: physical activities increase the expression of PGC-1α, leading to upregulation of FNDC5 (24). Irisin then attaches to the receptors on white adipocytes, and partly through upregulating the expression of peroxisome proliferator-activated receptor α (PPAR-α), irisin enhances the expression of UCP1 in mitochondria, resulting in increased thermogenesis and ultimately the energy consumption in skeletal muscles and BAT (25-27). Based on its effects in enhancement of metabolic profile, irisin is considered to be a potential therapeutic agent to treat metabolic diseases, especially the ones that can be alleviated by exercise (26, 28).

Apart from its role in energy metabolism, FNDC5/irisin also plays important roles in an array of other biological processes. FNDC5/irisin may have a developmental role in neuronal differentiation and maturation (7, 29, 30). Overexpression of FNDC5 by lentiviral vector transduction enhances the expression of several important markers for both neuronal precursor and mature neurons in mouse embryonic stem cells (31), while knockdown of FNDC5 in mouse embryonic stem cells significantly undermines the maturation of both neurons and astrocytes (32). In addition to its role in neural differentiation, FNDC5/irisin has been shown to be able to promote angiogenesis in several cell types (33-35). Furthermore, recent studies have documented that FNDC5/irisin participates in

the occurrence and development of an array of tumors (36). For example, FNDC5/irisin may be utilized as a biomarker for renal cancer diagnosis (37); FNDC5 expression may be a prognostic factor to predict survival rate in patients with non-small cell lung cancer (38); in breast cancer, serum level of irisin functions as a potential candidate to evaluate spinal metastasis in patients (39). Moreover, FNDC5/irisin is shown to exert an anti-inflammatory effect in multiple tissues and cells including adipose tissue (40), liver (41), murine hippocampus (42), macrophages (43) and neural cell line (44). FNDC5/irisin has also been reported to play a vital role in osteogenesis, irisin may target osteoblasts directly to enhance the differentiation potential through P38/ERK MAP kinase signaling cascades activation (45, 46); recombinant irisin is able to prevent reduction of osteoblast differentiation caused by microgravity (47); additionally, weekly injection of irisin remarkably stimulates the cortical bone mass and strength in mice (48).

4.1.3 Expression sites of FNDC5/irisin

FNDC5/irisin is best known for being present in skeletal muscle and blood plasma by Boström *et al.*'s study (24). The systematic distribution of FNDC5/irisin in other tissues was first comprehensively studied by Aydin *et al.*, who verified that FNDC5/irisin was expressed in the brain, cardiac and skeletal muscle, skin tissues and kidney from male rats by immunohistochemical staining. On the other hand, FNDC5/irisin signal was found to be present in human skeletal muscle, testis, pancrea, liver, spleen and stomach tissues, in addition, they also confirmed that FNDC5/irisin was mainly produced in the nerve sheaths that spread within the skeletal muscle (49, 50). Further, FNDC5/irisin has been observed to be expressed in retina, pineal, thyroid gland, heart, lung and adipose tissues from rats (51-54). Moreover, irisin, the secreted form of FNDC5, was also found in several human body fluids including cerebrospinal fluid, saliva and urine (55, 56).

In oral tissues, the expression of FNDC5/irisin has been rarely examined to date. As far as we know, FNDC5/irisin has been reported to be expressed in three major salivary glands (submandibular gland, sublingual gland and parotid gland) (57). Furthermore, our research has proved that it is also expressed in human periodontal ligament cells (hPDL cells), human dental pulp cells (hDPCs) and periodontium and dental pulp tissues from rats (58).

4.2 Tooth supporting tissues

The tooth supporting tissues (Figure 2) refer to the periodontal tissues that surround and support the teeth, it consists of four components, namely periodontal ligament, alveolar bone, cementum and gingiva. Together these tissues function as a united system to help maintain the teeth in position in the alveolar bone and their destruction may eventually lead to tooth loss (59-61).

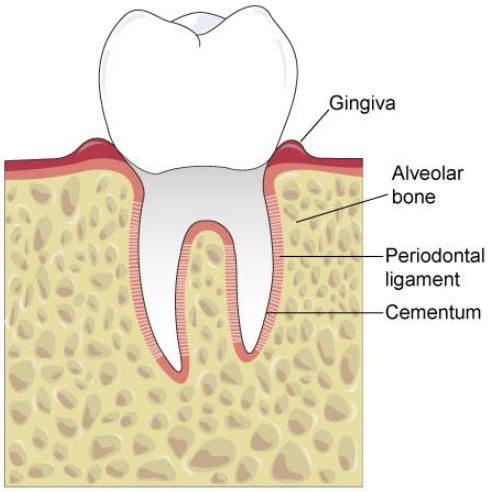

Figure 2. The longitudinal section of a tooth displaying healthy tooth supporting tissues.

4.2.1 Periodontal ligament

The periodontal ligament (PDL) is an aligned fibrous meshwork that is sandwiched between cementum-root dentin and inner wall of alveolar socket. By providing mechanical stability and working as a shock buffer, PDL mainly functions to protect both tooth and alveolar bone from damage caused by excessive forces related to mastication, further, PDL may collaborate with gingiva to form a protective barrier against pathogens from within the oral cavity (62, 63). The PDL has a vital role in responding to loading caused by mastication and thus constantly undergoing remodeling, hence the PDL should be strong and flexible to fulfill this unique function (64). Compared with other ligaments which mainly function in tensional environment, the PDL undergoes multiaxial loading and is thus capable of functioning under tension, compression, shear stress and torsion (64-66).

PDL is a highly vascularized connective tissue with a subpopulation of diverse cell types embedded

in an extracellular matrix (ECM) that is abundant in proteins (67). The ECM of PDL consists of collagens and non-collagenous elements, in addition, growth factors, cytokines and matrix degradation enzymes, metalloproteinases (MMPs) are also found to be part of the periodontal ECM (68). Collagen type I and III are two major components in PDL collagenous ECM, whereas proteoglycans and glycoproteins, including versican, dextran sulphated biglycan, decorin, fibronectin, periostin, vitronectin, thrombospondin, tenascin and osteopontin constitute the composition of non-collagenous ECM of PDL (67, 69-71). Out of all the PDL components, collagen type I is the most predominant one (72), it is able to facilitate the osteogenic differentiation and matrix mineralization and considered to largely determine the mechanical strength of ligament and tendon through its molecular structure and physical arrangement into fibers (73-75).

The PDL contains a remarkably heterogeneous cell population (76). The major cell type of PDL cell population is fibroblast, which is able to concurrently synthesize and degrade collagen to remodel the collagen fibrils (77, 78). Epithelial cells in PDL, also known as epithelial cell rests of Malassez, occur abundantly around cementum and furcation areas, their function may be related to periodontal regeneration (76, 78). Further, cementoblasts and osteoblasts were also found to be present in the PDL (79, 80). By migration, differentiation and interaction with soluble mediators, endothelial cells, cementoblasts and osteoblasts make contribution to periodontal regeneration (81). The diversity of cell types within PDL has led to a hypothesis that PDL possibly contains stem cell population capable of maintaining periodontal homeostasis and regeneration (79, 82). In 2004, Seo BM *et al.* successfully isolated the stem cells from PDL tissues (83), which could differentiate into cementoblast-like cells, adipocytes, collagen-forming cells, chondrogenic phenotypes and osteogenic phenotypes (83, 84). These findings suggest that PDL stem cells may not only participate in maintenance of PDL tissues, but also may be important for repair, remodeling and regeneration of the surrounding alveolar bone and cementum tissues (76, 85).

4.2.2 Alveolar bone

The alveolar bone is a complicated structure resting on the basal bone of maxilla and mandible, and the teeth are situated in the sockets formed in it (86). Alveolar bone is connected to the teeth by PDL, similar to bone in other sites, alveolar bone generally functions as a mineralized supporting

tissue to provide mechanical strength, an environment for bone marrow and a reservoir for calcium ions, however, the main functions of alveolar bone are housing the tooth roots, absorbing and dispersing forces induced by oral functions (87, 88). The alveolar bone is a dynamic tissue that is constantly exposed to mechanical stimulation and undergoes continuous cycle of bone remodeling by coordinated bone resorption, which is induced by bone-resorbing cells such as osteoclasts; and bone formation, which is achieved by osteoblast lineage cells including osteoblasts, osteocytes and bone-lining cells (89, 90). Generally, the bone remodeling process (Figure 3) is initiated at a specific site via recruitment of osteoclast precursors from circulation into a closed space termed as bone remodeling compartment (BRC), then bone resorption takes place through active osteoclast differentiation and function, while recruitment of mesenchymal stem cells (MSCs) and osteoprogenitors happen simultaneously. After that, the bone formation is induced by osteoblast differentiation and functions such as osteoid synthesis. Finally, the osteoids are mineralized as new bone which replace the old one, hence a cycle of bone remodeling is concluded (91, 92). Further, through the regulation of diverse hormones, cytokines, proteins and enzymes, bone resorption and bone formation are well-balanced, which ensures a stable bone volume after each remodeling cycle (89, 93).

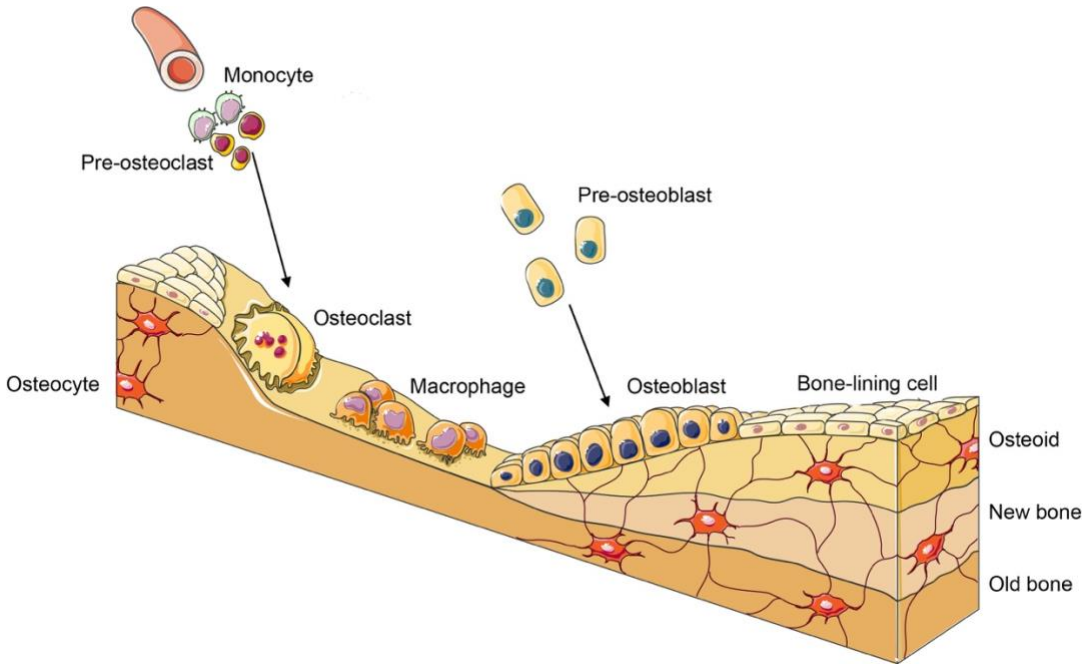

Figure 3. The schematic illustration of the bone remodeling cycle. The bone remodeling is initiated by bone resorption induced by osteoclasts, followed by bone formation, in which osteoblasts lay down new bone matrix and eventually become mineralized until the resorbed bone is completely refreshed. The figure was generated using Servier Medical Art, provided by Servier, licensed under a Creative Commons Attribution 3.0 unported license (94).

Similar to the other bone tissues, osteoclasts, osteoblasts and osteocytes are the major cell types that make contribution to the homeostasis and functions of the alveolar bone (95). Osteoclasts are large, multinucleated cells that stem from hematopoietic stem cells (HSCs) and are responsible for bone resorption. The HSCs give rise to common myeloid progenitors (CMPs), which, under the stimulation of granulocyte/macrophage stimulating factor (GM-CSF), subsequently differentiate into granulocyte/macrophage progenitors (GMPs). Further, the GMPs differentiate into monocyte/macrophage lineage and become the osteoclast progenitors, which fuse after traveling to the bone surfaces through blood circulation. Eventually, the osteoclast progenitors mature as multinucleated osteoclasts which secrete acid and lytic enzymes capable of degrading mineral and protein structures to regulate bone resorption (88, 95, 96). The differentiation of monocytes/macrophages into osteoclasts is mediated by two important cytokines: macrophage colony-stimulating factor (M-CSF) and receptor activator of nuclear factor-κB ligand (RANKL). The M-CSF attaches to its receptor c-Fms on myeloid progenitors to promote their proliferation

(97), while RANKL attaches to its receptor RANK to potentiate NF-kB and MAPK signaling pathways, leading to activation of osteogenic transcription factors c-Fos and nuclear factor-activated T cells c1 (NFATc1), by activation, these two factors in turn regulate osteoclastic markers including tartrate-resistant acid phosphatase (TRAP) and cathepsin K, which are essential in osteoclastic differentiation (88, 98, 99). Osteoprotegerin (OPG) is a soluble decoy receptor, it acts by blocking the docking of RANKL to its receptor RANK to blunt the osteoclastogenesis, therefore the balanced expression of osteoclastogenic stimulator RANKL and inhibitor OPG together determine the quantity of resorbed bone (100). In periodontal tissues, both gingival fibroblasts and PDL cells have been reported to be able to produce RANKL and OPG, hence controlling the activity of osteoclasts to regulate alveolar bone remodeling (101, 102).

In contrast to osteoclasts that originate from hematopoietic/monocyte lineage, osteoblasts are mononucleated cells derived from mesenchymal/mesodermal lineage and are involved in bone apposition (95). The differentiation of osteoblasts from mesenchymal cells requires sequential action of the transcription factors runt-related transcription factor 2 (RUNX2) and osterix. The osteoblasts create densely packed sheets on the surface of bone, from which they extend cellular processes throughout the newly formed bone, in order to lay down new bone successfully, osteoblasts produce a variety of enzymes, growth factors and hormones including alkaline phosphatase (ALP), collagen type I, osteocalcin (OCN), collagenase, TGF β and IGFs (103, 104). Osteoblasts also produce RANKL/OPG to regulate osteoclasts, and the amount of secreted RANKL/OPG relies on the differentiation stage of osteoblasts, pre-osteoblasts express relatively more RANKL than OPG, which stimulates osteoclast differentiation and function, while more mature osteoblasts express higher levels of OPG than RANKL, which suppresses the osteoclast differentiation and function (105). Osteoblasts have a limited lifespan, once the bone formation is completed, they are faced with three potential fates: some become flattened and elongated bone lining cells that remain quiescent on the bone surface, some undergo cell death by apoptosis, whereas the majority of osteoblasts gradually become embedded in bone matrix, undergo structural changes, and further differentiate into osteocytes (106).

Osteocytes are a long-lived cell type that account for most majority of the bone cells, they stem

from the terminally differentiated osteoblasts that are buried in mineralized bone structures in the process of bone formation. Osteocytes always reside in microscopic cavities also known as lacunae, after being embedded in mineralized matrix, the osteocytes maintain its contact with adjacent cells by the dendritic cellular processes radiating from the cell body and spreading through the canaliculi within the bone mineral matrix, the lacunae and canaliculi together are termed as lacuno-canalicular system (LCS) (89, 95, 107). Osteocytes are also actively involved in bone remodeling via multiple mechanisms. To begin with, osteocytes are primary sources of both RANKL and OPG, which indicates that they can affect osteoclasts in either stimulatory or inhibitory manner (108, 109). The dying osteocytes can also regulate bone resorption by detecting microdamage within bones, thus initiating osteoclastogenesis through apoptosis (110). Further, the location and the cellular network structure of osteocytes render them the ability to sense mechanical stimulation and transduce these signals into biochemical cues to control bone remodeling through gene regulation. Upon mechanical stimulus, the secretion of negative mediators of osteoblast differentiation such as sclerostin and Dickkopf-1 are inhibited, leading to promoted bone formation (111, 112).

4.3 Orthodontic tooth movement

Orthodontic treatment is achieved on the basis of the fact that tooth can be moved within the alveolar bone when a proper amount of orthodontic force is applied, in this condition, some areas in the PDL are compressed and termed as so-called compression sides, while some other areas are subjected to tensile force and thus termed as tension sides (113) (Figure 4). The PDL cells can perceive the mechanical signals exerted by orthodontic force and transduce them into molecular events in the progenitor cells, which subsequently differentiate into osteoclasts and osteoblasts, therefore resulting in the bone remodeling and orthodontic tooth movement (OTM) (114). Generally, the biological events regarding the OTM are as follows: on the side subjected to compression, PDL displays disorganization due to the pressure force, and blood flow is disturbed, causing cell death, also known as hyalinization, further, the hyalinized tissues are resorbed by macrophages and bones are resorbed by osteoclasts near the hyalinized tissues. While on the side subjected to tensional force, the PDL fibers are aligned with the direction of tensile force in an organized manner, and the blood flow is boosted, leading to promoted osteogenic activity and ECM deposition, which consequently mineralizes. Consequently, PDL and alveolar bone are degraded to make space for the tooth to move,

whereas new PDL and bone tissue are formed simultaneously (115, 116).

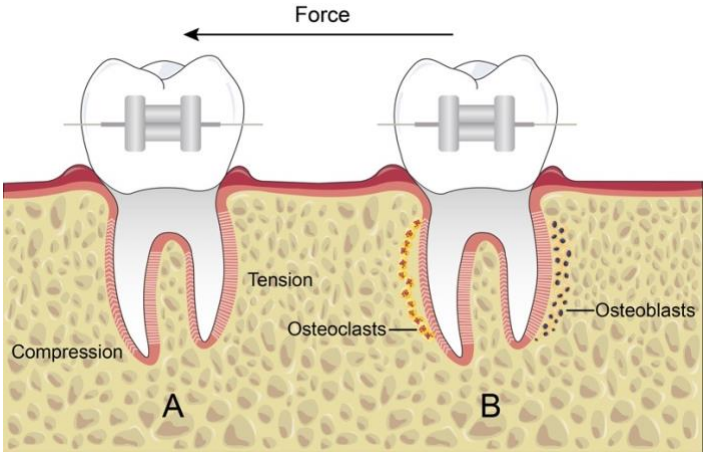

Figure 4. A tooth having orthodontic appliance on (A and B) with compression side and tension side indicated explicitly (A). As the orthodontic force is applied, osteoclasts which resorb bone tissue are recruited on the compression side, while osteoblasts which are responsible for new bone formation are present on the tension side (B). The arrow points the direction of force.

Generally, the entire temporal course of OTM can be divided and sequenced into four phases: initial phase, lag phase, acceleration phase and post lag phase. The initial phase can be interpreted as rapid tooth movement immediately after orthodontic force application. Due to the orthodontic force, the width of the periodontal ligament is decreased on the compression side, hence the initial rapid movement can be largely attributed to the tooth displacement within the PDL space. The lag phase happens immediately after the initial phase and is characterized by relatively low rate of tooth movement or no tooth movement at all due to the hyalinization areas in the PDL compression side. Besides, no more tooth movement will occur until the hyalinized tissues are completely removed. Moreover, the duration of lag phase appears to have a large individual variation fluctuating between 0-35 days, this suggests that individual differences in bone density and metabolic activities in bone or PDL may play an important role in such large variation. The acceleration phase is featured by gradual or sudden increase in the tooth movement rate and may be interpreted as a period in which the biological processes involved in the remodeling of PDL and bone have reached their maximum capacity. This may also explain why constant linear tooth movement is observed in the so-called post lag phase, which is the last phase of OTM (117-121).

It has been documented that the initial phase of OTM is often accompanied by an acute inflammatory response as a result of hypoxia and decreased nutrient level caused by deformation of blood vessels and disarrangement of periodontal tissues (122). However, by functioning in concert with the mechanical stimulation applied to periodontal tissues, this aseptic inflammation is essential for OTM to occur (123). In PDL, the vasodilatation of capillaries is induced by inflammation, which allows the leukocytes to migrate out of the capillaries in the PDL tissue, where they are subsequently stimulated by biochemical signals to produce and secrete multiple proinflammatory cytokines, chemokines and growth factors. Finally, these biological agents generate a complicated multifactorial sequence of biological events culminating in bone remodeling and thus facilitate tooth movement (124-126). On the compression side, which is dominated by bone resorption, a significantly higher expression of TNF-α, IL-1β, RANKL, MMP-1 has been observed, while the tension side, which is featured by osteogenesis, possesses a significantly increased expression of IL-10, VEGF, OPG, collagen type I, RUNX2 and OCN (123, 125-128). The tissue and cellular responses to orthodontic force application are summarized and illustrated below in Figure 5.

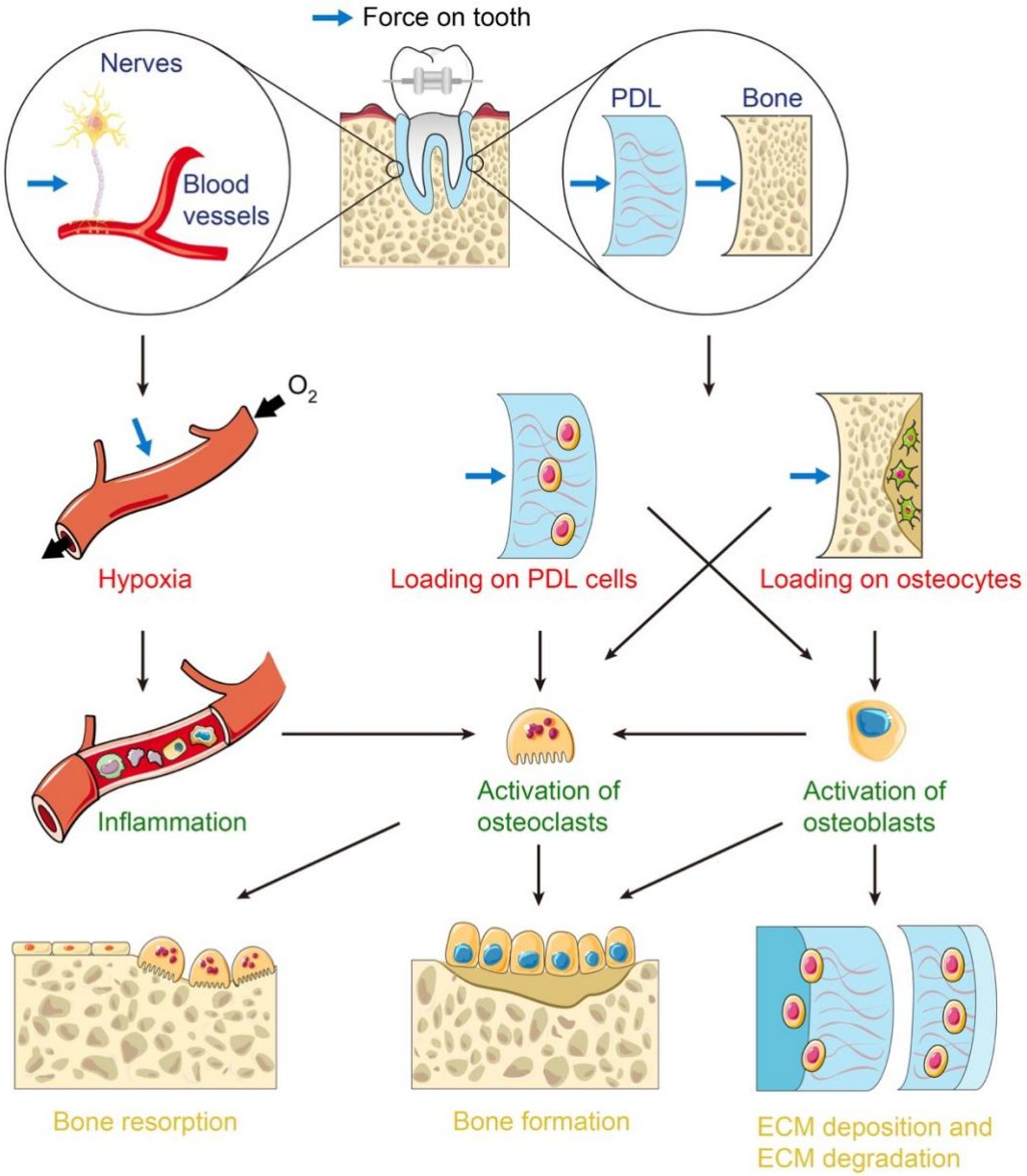

Figure 5. The course of biological and cellular events in periodontal tissues in response to orthodontic force. Step 1: extracellular mechanobiology of the periodontium (in blue text). Step 2: cell strains (in red text). Step 3: activation and differentiation of cells (in green text). Step 4: tissues remodeling (in yellow text). The figure is modified from Li et al. (129).

The rate of OTM can be impacted by a variety of internal or external factors including age (130), the magnitude of orthodontic force (131), surgical interventions (132, 133), light-emitting photobiomodulation therapy and low-level laser therapy (134, 135). In addition, local gene therapy could affect the rate of OTM either positively or negatively (136, 137). Lastly, chemical methods including hormones, drugs, and various synthetic molecules, whether administered locally or

systemically, may function as regulators of OTM (138). Reduced OTM rate has been observed with the treatments of non-steroidal anti-inflammatory drugs (139), adiponectin (140), bisphosphonates (141), exendin-4 (142), fluoride (143) and OPG (144). On the other hand, vitamin D (145), thyroid hormone (146), RANKL (147) and prostaglandin E_2 (148) represent the pharmacological agents capable of increasing the amount of OTM.

In the present thesis, the study on the potential role of irisin on PDL cells, periodontal tissue and OTM is of particular interest, as irisin has been shown to exert favorable effects on cells from periodontal and paradental tissues, though the research regarding this topic still remain largely unknown. Recombinant irisin may promote proliferation, migration, angiogenic potential, ECM deposition and osteogenic potential in hPDL cells cultured in 2D (149). Further, irisin treatment can rescue the *Porphyromonas gingivalis*-suppressed osteogenic/cementoblast differentiation in hPDL cells partially via p38 signaling pathway (150). Also, salivary irisin levels have been found to be increased in patients with chronic periodontitis and decreased in healthy patients with less plaque percentage, suggesting irisin could act as a biomarker for chronic periodontal disease (151). In addition, irisin has been identified as a novel cementoblast differentiation regulator. On one hand, irisin enhances cementoblast differentiation, mineralization and proliferation in an immortalized mouse cementoblast cell line OCCM-30 by p38 MAPK pathway (152), on the other hand, irisin stimulates cementoblast-mediated osteoclastogenesis by increasing the expression of RANKL and IL-6 at both transcriptional and protein level in OCCM-30 cells (153). Irisin also promotes odontogenic differentiation, mineralization and angiogenic potential through activation of MAPK and Akt signaling pathways in hDPCs (154). Moreover, the dental bud-derived MSCs respond to irisin stimulation with enhanced OCN expression and greater mineral matrix deposition (155). These findings together with the aforementioned beneficial effects of irisin on osteogenesis suggest that it may present as a possible novel agent for periodontal tissue regeneration, remodeling, and a potential chemical agent to study the effect on OTM.

5 AIMS AND HYPOTHESES OF THE THESIS

The overall aim of this thesis was to identify whether irisin could serve as a possible determining factor in OTM by affecting the tooth supporting tissues. And if so, to clarify the underlying mechanisms involved in irisin-mediated OTM using both *in vitro* and *in vivo* models.

The working hypothesis was that irisin administration will have an impact on periodontal tissues responsible for OTM outcome.

The specific research objectives were as follows:

A) The first objective was to study if FNDC5 was expressed and regulated in several dental and paradental cells and tissues. Focus was predominantly given upon PDL (paper I and II).

B) The second objective was to investigate the effects of local injection of recombinant irisin on tooth movement *in vivo* and evaluate the effect on bone remodeling near the injection site (paper II).

C) The third objective was to explore the potential cellular and molecular mechanisms by which irisin affects the PDL and thereby OTM. The biological changes after OTM at both molecular and structural levels in PDL were evaluated (paper II). The alterations in biological behaviors and molecular functions in the tissue-mimetic 3D hPDL cell spheroids in response to irisin treatment were examined (paper III).

6 OVERVIEW OF MATERIALS AND METHODS

In the present thesis, a series of *in vitro* and *in vivo* experiments has been conducted. The overview of applied materials, methods and analyses are presented below in the Table 1.

Table 1. Overview of cell lines, animal models, methods and analyses applied in this thesis.

Paper	Cell lines	Animal models	Methods and analyses
I	Human periodontal ligament cells Human dental pulp stem cells Human osteoblasts		Cell culture (monolayer and spheroids) Gene analyses (qPCR, electrophoresis, DNA sequencing) Immunodetection of FNDC5 (IF staining) Protein detection in culture medium (ELISA)
		Sprague-Dawley rats	Immunodetection of FNDC5 in dental and paradental tissues (IF staining)
II		Experimental OTM model on Wistar rats	Right first molar movement (feeler gauge, micro-CT) Plasma irisin levels (ELISA) Bone morphometric parameters (micro-CT) Morphology (Goldner's trichrome staining, H&E staining) Periodontal remodeling markers expression in PDL tissues after OTM (IF)
III	Human periodontal ligament cells		Cell culture (spheroids) Gene analyses (qPCR, Microarray, functional enrichment analysis, DEG analysis, IPA) Protein expression (IF staining) Morphology (Goldner's trichrome staining, IF staining) Mechanical properties (nanoindentation) Protein detection in culture medium (Luminex)

7 SUMMARY OF THE RESULTS

The research from this PhD body of work has culminated in three articles. The overview of the results is presented in this chapter.

Paper I

In this study, the objectives were to identify the expression and examine regulation of FNDC5 in the cells from dental and paradental tissues. FNDC5 was found to be expressed in periodontal tissues, dental pulp in an *in vivo* rat specimen as well as in hPDL cells, hDPCs and hOBs cultured in both 2D and 3D by immunofluorescence staining. The FNDC5 gene was further confirmed to be expressed in the cells by qPCR and electrophoresis, and Basic Local Alignment Search Tool (BLAST) analyses verified that the generated nucleotide alignments from hPDL cells matched with human FNDC5. The expression of FNDC5 was identified to be differently regulated in hPDL cells, hDPCs, and hOBs. Two dosages of irisin (10 ng/ml and 100 ng/ml, respectively) reduced, and administration of all-trans retinoic acid (ATRA) (1 μM and 10 μM, respectively) enhanced the expression of FNDC5 in hPDL cells. Similarly, administration of high-dose irisin reduced expression of FNDC5 in hDPCs, whereas low-dose irisin had no effect. On the other hand, low-dose ATRA enhanced FNDC5 expression in hDPCs, whereas high-dose ATRA had no effect. Finally, FNDC5 gene expression in hDPCs was enhanced during odontoblast-like differentiation induced by dexamethasone whereas the secretion of irisin was decreased compared to control.

Paper II

The aim was to evaluate whether submucosal injection of recombinant irisin would influence the rate of OTM in a rat model. To clarify this, male Wistar rats were subjected to irisin injections of 0.1 or 1 μg, or PBS (control group) every third day. The maxillary right first molar was mesially moved for 14 days. The 1 μg irisin administration significantly suppressed OTM at days 6, 9 and 12, and an inhibitory trend for OTM at day 14 in the 1 μg irisin group was observed but failed to be significant. On the other hand, no significant difference in OTM was observed between 0.1 μg irisin group and control group during the experiment, though there was an inhibitory trend between days 6 and 14. Further, the bone volume fraction, total porosity, root volume and plasma irisin levels were not influenced by the irisin injections.

The histological staining showed that the PDL on the compression side presented disorganized and sparse morphology in the control group, but denser and well-organized in the two irisin-treated groups. The control group also had more resorption lacunae and hyalinization area at the PDL-bone interface on the compression side, while these were scarce after irisin treatment. In addition, osteoblasts were found lining the PDL-bone interface on the compression side in the two irisin-treated groups. Immunofluorescence staining showed that collagen type I expression was significantly lower in the irisin groups on the tension side, but significantly enhanced on the compression side in the irisin groups. The expression of periostin and OCN was significantly enhanced on both tension and compression sides in the irisin groups compared to the control group. The levels of von Willebrand factor (vWF), however, were significantly decreased in the irisin groups on the tension side, while significantly increased in irisin groups on the compression side. Immunofluorescence detection of the non-secreted C-terminal region of FNDC5 demonstrated that irisin administration induced significantly enhanced levels of FNDC5 expression on both tension and compression sides compared to the control group.

Paper III

In this investigation, we generated tissue-mimetic 3D hPDL cell spheroids treated with 10 ng/mL irisin or plain PBS (control group). The effects of administrated irisin were evaluated by mechanical testing, qPCR for osteogenic markers and ECM markers, and bioinformatic analysis after microarray, with the intention to identify whether irisin affected the gene expression patterns directing the morphology, mechanical properties, osteogenic potential and ECM deposition in 3D hPDL cell spheroids. Bioinformatic data indicated that approximately 1000 genes were differentially expressed between control and irisin-treated 3D hPDL cell spheroids. Through Gene Ontology/Kyoto Encyclopedia of Genes and Genomes (GO/KEGG) analysis, we found that several biological processes and molecular functions were significantly altered: extracellular matrix organization, extracellular structure organization, negative regulation of nucleocytoplasmic transport and bitter taste receptor activity. Notably, some MMPs found to be regulated, including MMP-1, MMP-3, MMP-13 and MMP-17 are implicated in extracellular matrix organization and extracellular structure organization. These genes represent cellular and molecular mechanisms indicative of a role for irisin in PDL tissue remodeling. Interestingly, bitter taste-sensing type 2

receptor family subtypes (TAS2R) including TAS2R46, TAS2R10, TAS2R4, TAS2R20, TAS2R60 and TAS2R38, were also observed to be differentially expressed. In addition, the Ingenuity Pathway Analysis (IPA) showed that a total of 13 canonical signaling pathways were significantly associated with irisin treatment. Among these pathways, it was observed that coronavirus replication pathway, actin cytoskeleton signaling, integrin signaling, aldosterone signaling in epithelial cells, signaling by Rho family GTPases, and bladder cancer signaling were upregulated, while valine degradation I, GDNF family ligand-receptor interactions, thyroid cancer signaling, paxillin signaling, autophagy, apelin adipocyte signaling pathway, and tRNA charging were downregulated. Histological staining revealed that irisin induced a rim-like structure on the outer region of the 3D hPDL spheroids. The mechanical stiffness of the 3D hPDL spheroids, expressions of ECM-related proteins, osteogenic markers and angiogenic markers were all significantly enhanced by irisin treatment.

8 DISCUSSION

The completion of the present thesis involves a wide range of experimental methods, most of them have been well characterized, however, certain challenges and limitations exist. Prior to the discussion with regard to whether the results have fulfilled the aims and hypotheses described above, a systematic evaluation of the applied methods is presented as these highly influence the outcome of the research performed in this thesis.

8.1 Methodological considerations

The irisin used in the present thesis is an untagged recombinant protein produced through *Escherichia coli* (*E. coli*) by a commercial company AdipoGen (Liestal, Switzerland), with a molecular weight of 12 kDa.

Irisin may undergo post-translational modifications, including glycosylation, dimerization, glycosylated-dimer formation, or even complex binding with another protein (156, 157). It has been shown that *E. coli* is unable to produce recombinant proteins that require eukaryotic post-translational modifications due to incompatible expression systems (158, 159). Therefore, the recombinant irisin used in the thesis is most likely not modified and, if dimerization or complex binding is dependent on modifications, the recombinant protein used may not be dimerized. Thus, we cannot rule out the possibility that the results might not necessarily reflect the effects of endogenously and/or mammalian produced irisin, which is potentially modified. Therefore, this is a general limitation that exists throughout the present PhD thesis.

8.1.1 Cell culture techniques

Cell culturing allows us to understand cellular biology, tissue morphology, mechanisms of diseases, drug action, protein production and the development of tissue engineering, and it is widely applied in preclinical studies on drugs, cancers and research in gene functions (160). Generally, most cell types grow as a 2D monolayer in a culture flask or in a flat petri dish, but recently 3D culture has gained increasing attention (161). The 2D cell culture is cost-efficient and easy to perform, and 2D-cultured cells can withstand long-term culture (162-164). However, when cultured in 2D, the contact area is larger towards the plastic and culture media than with other cells, forcing them into a

polarization that does not reflect the complexity of cell-to-cell interactions and physiological conditions observed *in vivo* (165). By contrast, 3D-cultured cells possess diverse polarity and phenotype, moreover, the 3D setup helps cells assemble into a tissue-like structure, reflect the in vivo cellular structure and mirror cellular responses, which will enable greater cell-to-cell and cell-environment contacts and intercellular signaling. Similar to *in vivo* developmental processes, 3D cell assembly induces differentiation to form more complicated structures that mimic physiological microenvironment (160, 166, 167). Another important advantage of 3D cell culture is that its cellular topology, gene expression, cell signaling and metabolism are similar to cells growing *in vivo* (168-171). Throughout the present thesis, both 2D (paper I) and 3D (papers I and III) culture of hPDL cells have been used.

Figure 6. The CelVivo rotational 3D cell culture system used to generate 3D cell spheroids (172).

The transit from conventional 2D culture to 3D culture of PDL cells usually requires extracellular scaffolds or biomaterials (173-175). We did not use scaffolding materials because they have limitations which can negatively influence the cell stability and cell behavior during incubation (176). In this investigation, a rotating cell culture system (Figure 6) was adopted to establish the 3D hPDL cell spheroids. This culture method was selected because it has been used by a number of research groups that focus on the PDL research (177-179). The rotating cell culture system has a cell culture chamber screwed onto a rotator that slowly rotates the chamber around a horizontal axis.

The continual motion keeps the cells from attaching to the walls of chamber, and it is possible to adjust the rotational speed for optimal culture. As the culture chamber rotates, its contents rotate accordingly, leading to decreased shear stress experienced by the contents of the chamber, which is a major advantage of the rotating culture system (180, 181). The other advantages of this culture system are that it makes 3D culture on a large scale possible, enables long-term spheroid culture and its operation is relatively simple. Also, the ease in refreshing culture medium is also a claimed advantage for this method (181, 182). There is a common disadvantage for 3D spheroid culture, which is the limited supply of oxygen, nutrients and metabolites due to the lack of vasculature in the 3D-cultured cells (183). However, in the present thesis, the immunofluorescence staini and gene expression analysis revealed that the irisin-treated 3D hPDL cell spheroids exhibited increased angiogenic potential and osteogenic differentiation compared to control group (paper III).

8.1.2 Animal model

The laboratory rats are widely used in a plethora of research fields, because the use of humans and livestock in experiments is restricted for ethical and economic reasons, respectively (184). The laboratory rats are preferred in scientific research as the rat genome is similar to human, although the rat genome is smaller than the human genome, both of them encode similar amount of genes, and it is estimated that all human genes that are known to be related to diseases have orthologues in rat genome (185).

There are certain discrepancies in dentition and anatomy of tooth supporting tissues between rats and humans. The dentition of rats is characterized by being monophyodontic with continuously erupting incisors (186), but the rat molars including the pulp tissue are similar to human molars in terms of anatomy, histology, biology and physiology (187). The rat maxillary alveolar bone is generally denser than the corresponding human maxillary alveolar bone with lack of bone marrow spaces. Further, structural differences in PDL have also been reported, elastic fibers are not found in rat periodontal space while a moderate number of them are observed in the supra-alveolar tissue in human PDL. Moreover, tissue development during root formation and tissue changes in response to orthodontic treatment appear to be faster in rats than humans (188, 189). Finally, the alveolar bone of rats has a higher turnover rate compared to that of humans, making it a suitable model for

studies on bone modeling and remodeling (90). Despite the nuances, rats are generally considered as a good model to study OTM, because they are relatively inexpensive, easy to house and operate on. Besides, the histological preparation of rat specimens is less complicated than other animals. Additionally, most antibodies needed for cellular biological techniques and histological analysis are only available for rodents (189, 190).

The chosen OTM rat model (Figure 7) in the current thesis is a well-established method tested by a number of researchers, who have provided valuable research data and significant experience (140, 191-193). The recombinant irisin was injected submucosally, mesio-palatally to the maxillary right first molar, because anatomically palatal bone plate is thinner than the buccal bone plate (194), which may facilitate the diffusion of irisin. Two dosages of irisin (0.1 μg and 1 μg) were adopted because we wanted to test whether the effect of irisin on OTM rate depends on the concentration. The two dosages were determined based on Asadi *et al.* (195) who reported that injection of dosages starting from 0.5 μg/kg of irisin could induce substantial physiological changes in rats.

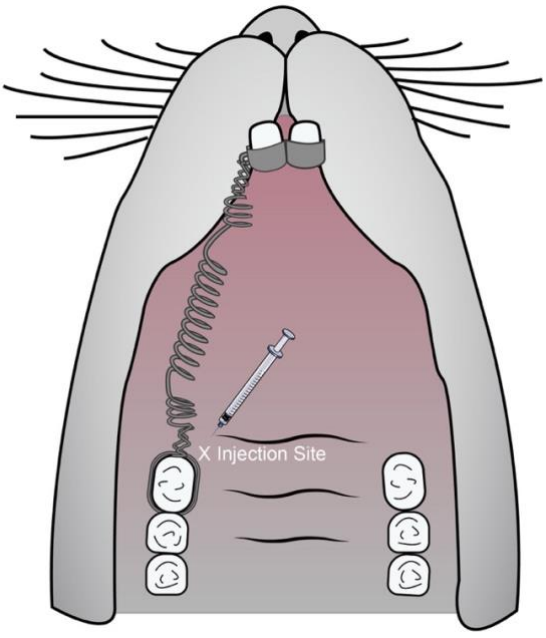

Figure 7. The schematic illustration of murine OTM model. The closed coil spring was ligated between the maxillary right first molar and the eyelet on the incisor band. An orthodontic force of approximately 0.5 N was exerted to induce a mesial movement of the first molar. Irisin was injected mesio-palatally to the first molar.

8.1.3 Measurement of tooth movement

Two measurement methods, feeler gauge and micro-CT were used in this thesis. The feeler gauge method represents a relatively simple, somewhat operator-dependent measurement technique, it allows the operator to quickly measure the tooth movement in rats under light anesthesia by isoflurane inhalation. However, it has a major disadvantage of low accuracy because its minimum measurable distance is only 0.05 mm (140). The tooth movement between maxillary right first molar and third molar, as well as between maxillary right first molar and second molar were measured by micro-CT. In short, the corner points of an enclosed rectangle covering the molar crowns were marked, and all the corner points were registered. Subsequently, the midpoints of the cuboids were acquired and the length of the vector between these midpoints was thus calculated (Figure 8). The micro-CT represents a more sophisticated, somewhat less operator-dependent measurement technique with relatively high accuracy. Additionally, more precise linear and angular measurements can be acquired by micro-CT, which display the teeth and the surrounding tissues without the interference from other structures (196).

The bone volume fraction (BVF), the porosity of maxillary alveolar bone and the mesial root volume of maxillary right first molar were measured by micro-CT. The micro-CT, which possesses a resolution as high as 9 μm per pixel, can be used to evaluate the microarchitecture of alveolar bone and root resorption craters (197). The average resolution of micro-CT is sufficient to evaluate structures such as rodent trabeculae as the width is estimated to range from approximately 30 μm to 50 μm according to histological data (198). In this study, the micro-CT scanning was conducted at a voxel size of 10 μm, which gave a relatively favorable quality within reasonable scanning time, however, the optimal 9 μm resolution was not chosen because it would increase the time needed for acquisition. No significant difference in bone volume fraction, porosity and root volume was observed between the two irisin-treated groups and the control group, which suggests that local injection of irisin did not affect the alveolar bones and roots during the entire 14-day OTM experiment. This lack of significance may be related to the selection of volume of interest (VOI), because it is challenging to define the most applicable site for quantification. We selected the mesial root of the right maxillary molar and the mesial alveolar ridge for micro-CT analysis because we wanted to assess the bone and root close to the injection site, which we believe may be more relevant

to a clinical situation.

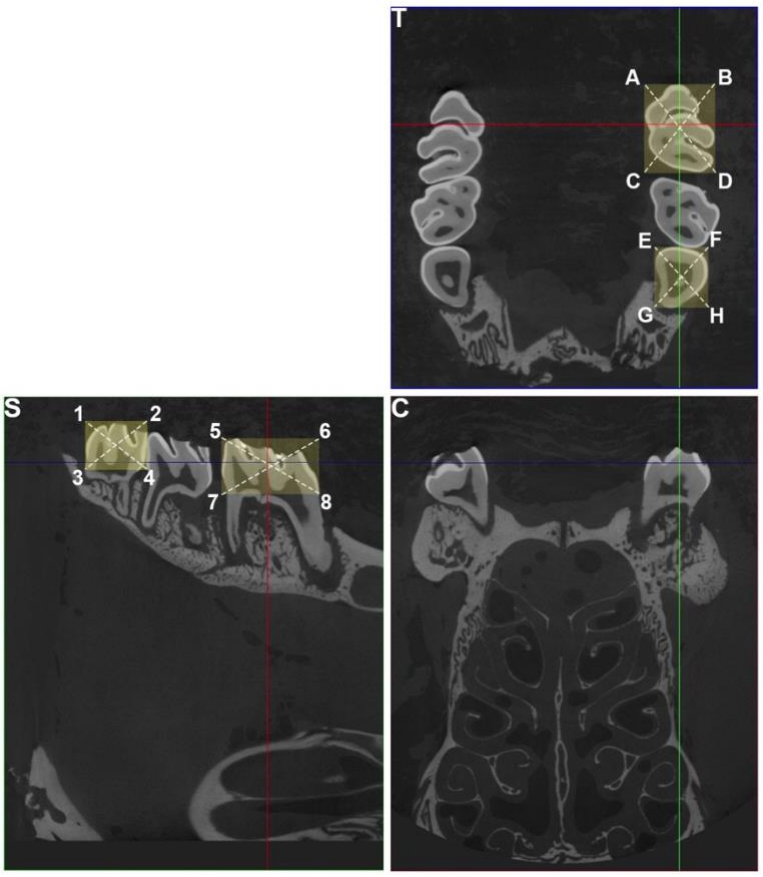

Figure 8. Tooth movement measured by micro-CT. The corner point coordinates of an enclosed rectangle covering the crown of both first and third molar were registered. According to these points the midpoints of cuboid around the molars were acquired. The length between the two midpoints was thus measured. In addition, shortest distance between distal surface of first molar and mesial surface of second molar was also measured using micro-CT. T: transversal, C: coronal, S: sagittal.

There are several limitations for the OTM experiment presented in the paper II. The general drawback may be that it is difficult to control the amount of orthodontic force and the type of tooth movement. During irisin injection, the needle might experience strong resistance from palatal mucosa, hence certain amount of irisin could be lost. Also, force decay may be a concern, since the spring coil was activated only in the beginning of the experiment and was not reactivated thereafter, thus the orthodontic force might decay over time. Similarly, the rat incisors, which acted as the anchorage teeth, kept erupting continuously, this might change the angle of orthodontic force from

almost horizontal to a steeper angle, and thereby lead to unstable anchorage and decrease the effective horizontal force (199). Although two dosages of irisin (0.1 μg and 1 μg) were chosen for the study, they may still be below the recommended optimum dosage of effect for irisin in mice and rats, which has been shown to be 500 μg/kg daily (200). These factors may interfere with the tooth movement and possibly explain why the suppressive effect of 1 μg irisin on OTM was not observed at day 14. Another limitation for this investigation is regarding the measurement methods. Both the feeler gauge technique and micro-CT measured OTM between the first and the second maxillary molars and resulted in similar trends, suggesting that the two methods are comparable. However, the micro-CT readings generally indicated smaller tooth movement compared to the feeler gauge method. This difference might be due to the flexibility of the periodontal ligament, which allows insertion of larger feeler gauge blades in-between first and second molars, hence leading to an overestimation of OTM reading. Therefore, the feeler gauge measurements should be carried out with meticulous care without applying excessive force to the blades. On the other hand, the OTM between the first and the third maxillary molars were also evaluated by the micro-CT. The group treated with 0.1 μg irisin exhibited a decreasing trend in OTM without significance between first and second molars by both feeler gauge and micro-CT, but the decreasing trend was not observed between first and third molars measured by micro-CT. It is possible that the measurements made by micro-CT at day 14 showed a higher OTM due to the gradual recommence of the natural distal drift of the maxillary third molars (201). Accordingly, the inhibitory effect on tooth movement induced by 0.1 μg irisin may have been masked. Finally, the orthodontic treatment is a rather long course (202), in contrast with the 14-day experimental OTM in this investigation, hence the research data presented in the paper II can only be considered preliminary and care must be taken to extrapolate the findings to a clinical setting due to the limitations in a rodent model.

8.1.4 Analytical methods

8.1.4.1 Gene expression analyses

For gene expression analyses, both qPCR (papers I and III) and microarray (paper III) were utilized in this thesis. In order to make sure the qPCR data are reliable, a normalization strategy is required (203). One common strategy is to compare the target gene with an endogenous control (reference gene) in the same sample. Currently, the so-called housekeeping genes such as glyceraldehyde-3-

phosphate dehydrogenase (GAPDH), actin, ubiquitin and ribosomal genes are universally used as reference genes, because they are considered to be constitutively and stably expressed under different physiological and experimental conditions (204, 205). In papers I and III, only one housekeeping gene GAPDH was used as reference gene, although it has been advised that more than one housekeeping gene should be used to avoid misinterpretation of gene expression data (206). However, normalization of qPCR data to a single housekeeping gene is a very common practice in majority of studies by far (207).

Microarray technique was used to compare the differential gene expression patterns between 3D hPDL cell spheroids treated with or without irisin. This technology is widely used in a large number of biomedical research fields for quantitative and highly parallel measurements of gene expression (208). Affymetrix GeneChip microarray (Affymetrix, Santa Clara, CA, USA) was used in the present study. The differentially expressed genes (DEGs) were analyzed using the R package: limma (version 3.52.4). Functional enrichment analysis was subsequently performed on the factors obtained from DEGs analysis using the clusterProfiler package (version 3.14.3). To classify genes into signaling pathways that were altered upon irisin exposure, the gene expression data were analyzed using a software Ingenuity Pathway Analysis (IPA, http://www.ingenuity.com/, Redwood City, CA, USA). Since we intended to exhibit the discrepancies between the control and irisin-treated 3D hPDL cell spheroids, we presented lists of biological functions and most up- and down-regulated genes, as well as a histogram showing activated and inhibited signaling pathways (paper III). A clear strength for the microarray analysis in this study is that we adopted diverse software packages to process the data, which provided substantial and abundant informatic data that may possibly stimulate more research on irisin and periodontal ligament cells in the future. The limitations are that only a single dosage of irisin (10 ng/mL) and only one time point (14 days) were applied to the 3D hPDL cell spheroids in the experimental setting, and that the most up- and down-regulated genes were not validated via other experimental methods such as qPCR or immunodetection.

8.1.4.2 Detection of secreted proteins in culture medium

The cellular biological functions are regulated by secreted proteins such as cytokines, growth factors

and enzymes. These proteins are secreted or released into culture medium by cells. A variety of methods for detection and quantification of protein secreted to cell culture media exist. In this study, ELISA (paper I and II) and Luminex multiplex system (paper III) were selected.

ELISA has been extensively used for detection and quantification of biological agents in biomedical research. It is generally considered to be a highly reproducible, reliable, sensitive and specific method because of the antibody-antigen coupling approach (209). When compared with other immunoassays in terms of blood serum and plasma samples, ELISA is proved to be superior due to the availability of the reagents, robust performance and great accessibility in many labs (210). These are also the main reasons why we chose ELISA to quantify irisin levels in rat plasma, moreover, ELISA was the only available test at that time (paper II). However, ELISA suffers from certain general shortcomings such as labor-intensive operation, high possibility of false positive/negative results, and the possibility to measure only one target, hence quantification of multiple targets is time-consuming and expensive (211). Although a great number of studies have reported irisin levels in response to different physiological conditions (7, 212, 213), but the results may be compromised by flawed quantitative assays (4). Irisin detection in biological fluids is largely dependent on commercial ELISA kits based on polyclonal antibodies not necessarily previously tested for cross-reacting proteins in plasma, serum *etc.* (157). It is advised to use recombinant irisin, both glycosylated and non-glycosylated, as positive controls in the evaluation of false signals from cross-reacting proteins of polyclonal antibodies in irisin detection by ELISA (214). By contrast, the Luminex multi-analyte-profiling technology provides quantitative measurements of multiple factors concurrently in a small volume of medium and is therefore considered efficient and cost-saving. The employment of different target capture techniques has distinguished the Luminex assays from ELISA. The Luminex assays collect targets on spherical beads in suspension, whereas ELISA normally captures targets on flat surfaces in multi-well plates (215). A major challenge for Luminex assays is cross-reactivity, which prevents expansion of multiplexing, limits the assay performance, and leads to inaccurate readings, and hence wrong conclusions (216). In paper III, only 3 (osteonectin, LIF and IL-6) out of 15 myokines were detectable by the human myokine magnetic bead panel. This is probably due to the fact that as the 3D-cultured cells developed, the molecules secreted by the cells may be accumulated within the ECM and hence limiting the diffusion of those

secreted molecules into the culture medium (217), therefore, future Luminex assay can be performed in the mixture of cell lysis and culture medium rather than only culture medium. Moreover, it has been suggested that secretome detection should be performed using serum-free medium, since serum may mask the low abundant secreted proteins and interferes with the interpretation of data. However, the serum-containing medium was still used in the present thesis (paper III), because serum-free medium limits the cell growth and thus can induce distorted results in the landscape of secretome (218).

8.1.4.3 Mechanical testing

In order to compare the mechanical stiffness of 3D hPDL cell spheroids exposed to irisin and PBS (control), the so-called nanoindentation was introduced in paper III. Nanoindentation is a technique frequently used to detect the mechanical properties of small volumes of materials, elastic modulus and hardness of the materials can be measured using this technique. This method is broadly applied in material research regarding biological tissues, films and other cement-based materials (219). The mechanical properties of spheroidal samples were normally evaluated by nanoindentation with a sharp tip. However, this conventional nanoindentation was challenging for mechanical characterization because of the complicated geometry and large deformation of samples. To overcome this shortcoming, a nanoindentation-based flat punch method (220) was adopted for compression test of 3D hPDL cell spheroids (paper III). Briefly, the 3D hPDL cell spheroids were placed on a silicon substrate and then compressed by a specially designed square diamond flat punch, and the stress-strain curves of the tested spheroids were recorded during the indentation (Figure 9).

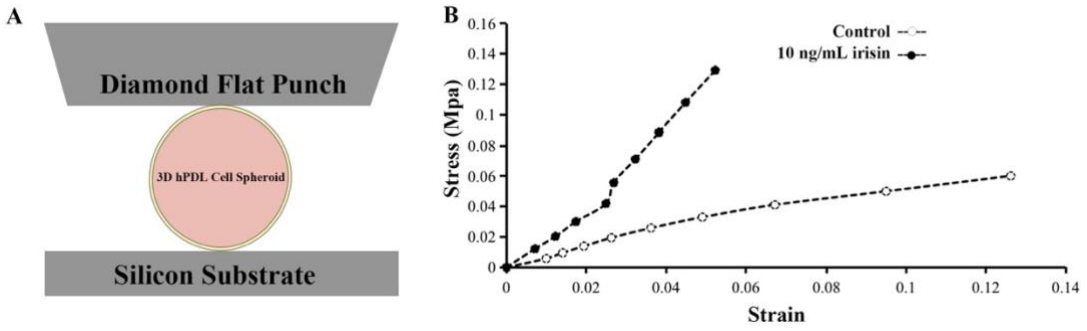

Figure 9. A. The schematic illustration of the flat punch method for nanoindentation test of 3D hPDL cell spheroids. B. The stress-strain relationship from 3D hPDL cell spheroids treated with and without 10 ng/ mL irisin.

A challenge with the nanoindentation in this study is that a sharp turning point at around strain 0.025/stress 0.04 for the 10 ng/mL irisin-treated sample was observed on the stress-strain curve, we believe this turning point was not caused by the treatment of irisin, instead it was possibly due to the liquid within the spheroids being suddenly squeezed out during nanoindentation. It is therefore advised that biological tissues or cell spheroids cultured in 3D should be properly dehydrated before the mechanical testing for future investigations. Another challenge is related to the size of the 3D hPDL cell spheroids as the size could not be maintained completely the same during the 3D cell culture, hence it might have interfered with the final compression test data, since smaller the sample diameter, the harder the material becomes (220).

8.1.4.4 Histological and microscopic analysis

Two histological preparation and sectioning techniques, cryo-sectioning (paper I and III) and paraffin sectioning (paper II) are employed in the thesis. In paper I and III, the 3D-cultured spheroids of hPDL cells, hDPCs and hOBs were fixed and embedded in optimal cutting temperature compound (Leica, Werzlar, Germany), 7 µm-thickness serial sections of the spheroids were acquired with the CryoStarTM NX70 Cryostat (Thermo Fisher Scientific, Kalamazoo, MI, USA). The cryo-sectioning method was chosen because its procedure is quick and simple and can be finished within one day. This procedure is highly suitable for soft cell spheroids, which do not require lengthy preparations such as decalcification of hard tissues before embedding. Further, labeling efficiency with antibodies is improved throughout the immunolabeling procedure as there is no need for

dehydration (221). Moreover, the tissue shrinkage and deformation, which happen frequently in other embedding techniques such as plastic and paraffin embedding, can be largely minimized (222). Nevertheless, several limitations with cryosection exist, the general problems are sample folding, smudging and crumbling during sectioning, which are normally associated with the temperature in Cryostat chamber and section blade. In order to solve these problems, repeated fine tuning of the temperature is often required. In addition, thinner sections usually have superior morphology and less background noise, however, in practice, it is very difficult to produce intact 5 μm-thick 3D hPDL cell sections with Cryostat sectioning system. This difficulty is possibly related to the type of tissue, as it has been reported that samples rich in connective tissues tend to be more difficult for cryo-sectioning (223), therefore, the minimum thickness was finally set as 7 μm.

In paper II, the paraffin embedding technique was chosen for the rat maxillae specimen, and decalcification was performed prior to the embedding and sectioning. Decalcification technique is often needed for samples containing hard tissues such as bone and teeth before histological preparations, as hard tissues may damage the cutting blade and crumble during sectioning. Hence decalcification is often necessary to remove calcium salt from the tissues without damaging the morphology to facilitate the sectioning procedure (224). An array of agents are available for decalcification, and ethylenediaminetetraacetic acid (EDTA) was used in the thesis, because it preserves the tissue integrity better than other methods, and is generally accepted as a reliable decalcification agent for histological preparations (225). A major weakness of EDTA decalcification is that the process is time-consuming. In the present study, the rat maxillae specimens were decalcified for 3 months. Also, EDTA solution needs to be frequently refreshed (every second day) and pH must be carefully checked and kept at 7 every time the old solution is replaced by the new solution, which accounts for extra laboratory work. Another limitation with EDTA is that it may cause the degradation of cells and ECM components in tissues, which undermines the stainability of the tissue sections (226).

Several histological analysis techniques including Goldner's trichrome staining (paper II and III), H&E staining (paper III), and immunofluorescence staining (paper I, II and III) were applied throughout the entire PhD thesis. The Goldner's trichrome staining technique is a specifically

designed method for morphological examination of specimens rich in collagens such as connective tissues and bones. By use of combination of three dyes with different molecule sizes, collagen fibers, fibrin, erythrocytes, muscles and keratin can be thus selectively and visualized by different colors (227). H&E staining is the most widely used method in histology, it presents great morphology and provides excellent contrast between cellular components, enabling identification of normal and pathological structures. The rat maxillae samples were generally stained weak for nuclei by both H&E and Goldner's trichrome staining. Attempts such as lengthening the hematoxylin incubation time and permeabilizing the nuclei with Triton X-100 were made, however, the nuclear staining results were still not improved. We believe the weak nuclear staining is probably due to the long decalcification time, which might have caused potential loss of nuclear details (228). To overcome the challenge, it is thus suggested to embedded the specimens containing hard tissues in methyl methacrylate, as this embedding agent does not require decalcification procedure (229). Immunofluorescence (IF) staining was used for immunodetection of FNDC5 in hPDL cells, hDPCs, hOBs, as well as in rat paradental tissues (paper I). In addition, it was deployed to compare the expression levels of several ECM markers and osteogenic markers between 3D hPDL cell spheroids and rat PDL tissues subjected to experimental OTM with or without recombinant irisin (paper II and III). It is a common technique that allows detection of localization and comparison of expression levels of a wide variety of antigens in different tissues and various cells. This broad ability is fulfilled via combinations of specific antibodies tagged with fluorophores. Moreover, IF possesses excellent sensitivity and amplification of signals in comparison with immunohistochemistry (230). General limitations for IF staining include non-specific staining, high background staining and weak staining, which can be solved by adjusting antibody concentration, increasing blocking serum incubation time or change of antibody. Another major challenge with the IF procedure in the present thesis was about the heat-mediated epitope retrieval (HIER). Despite the fact that HIER is usually effective in unmasking antigens and can give excellent staining results, it is destructive to skeletal tissues (231), hence the rat maxillae sections detached from the glass slides very often during the procedure, which caused unwanted waste of considerable samples. Therefore, alternative antigen retrieval methods such as enzyme digestion may be considered in future investigations.

8.2 General discussion of the results

It is widely accepted that high levels of bone mass and strong bone structure can be achieved by physical activity, by contrast, lack of physical activity or disuse of skeletal muscles results in severe bone loss (45, 232). In a similar context as for muscle load, the periodontal tissues are also constantly exposed to mechanical loading generated by various biological processes such as mastication (233), tongue movements (234), and under specific therapeutic conditions such as orthodontic treatment (235). Additionally, healthy PDL helps to maintain the bone mass of the tooth-supporting alveolar bone, while diseased periodontal tissues or loss of teeth will cause loss of load, thus resulting in destructive bone resorption (236-238). Obviously, PDL is situated in an environment that is very similar to that of skeletal muscles. Based on this evidence, it is thus speculated that the FNDC5 mRNA is likely to be expressed and regulated in dental and paradental cells and tissues.

8.2.1 Expression and regulation of FNDC5 in PDL cells and tissues

Irisin, which is produced by the cleavage of FNDC5, has been considered as a myokine and adipokine that plays a crucial role in regulating metabolism through various biological functions, as well as in a large number of other physiological processes (239). Previous research has indicated that FNDC5 is highly expressed in tissues with high energy demands, including the skeletal muscle, brain, and heart (240). Moreover, FNDC5 has also been found to be expressed in multiple other tissues including pericardium, intracranial artery, rectum, kidney, lung and liver (241). Irisin has been shown to play an important role in several processes in cementoblasts and PDL cells such as osteogenesis (149), cementoblast differentiation (152), osteoclastogenesis (242) and periodontitis (243). Based on these findings, we aimed to assess the expression and regulation of FNDC5 in cells from different oral tissues, especially the PDL. Our results show that FNDC5 is expressed in several dental and paradental tissues and cells, including rodent PDL, dental pulp and alveolar bone, as well as in hPDL cells, hDPCs and hOBs (paper I and II). Further, the autoregulation of FNDC5 expression was investigated by administration of recombinant irisin, while extrinsic regulation was tested by administration of ATRA, which has been documented to induce FNDC5 expression in skeletal muscle cells (244).

A discordance in FNDC5 expression was observed in all treated cells, the differential regulation of FNDC5 expression has been previously documented in other tissues under different physiological conditions. In obesity, adipose tissue may overexpress FNDC5 and oversecrete irisin in an attempt to counterbalance the metabolic deregulation (245). Another study demonstrated that FNDC5 expression is different depending on the WAT depot, moreover, a considerable decrease in visceral and epididymal adipose tissue depots is correlated with enhanced FNDC5 expression due to a possible compensatory effect. Additionally, hypothalamic FNDC5 expression was not affected by diets but was increased with leptin, insulin and metformin treatments, indicating that the regulation of central and peripheral FNDC5 expression are different (246). On the other hand, the complexity in higher eukaryotes gives rise to a large number of highly specialized cell types and tissues, some genes exhibit ubiquitous patterns of expression, while some others may display tissue-specific activity (247). Based on the results presented in the present thesis, FNDC5 expression pattern appears to be more tissue-specific than ubiquitous.

The regulation of FNDC5 expression is rather complex and autoregulation by irisin is reported in a few studies. Irisin administration has been found to positively regulate FNDC5 expression in human WAT (248), similarly, positive regulation of FNDC5 expression induced by irisin is confirmed in C2C12 myoblasts (48). On the other hand, a study conducted in human skeletal muscle cells revealed that irisin treatment resulted in an upregulation of FNDC5 2 hours after treatment, whereas more long-term treatment (6 and 24 hours after irisin treatment) resulted in downregulation of FNDC5 expression levels, suggesting that exogenous irisin stimulation may cause a negative feedback loop to decrease endogenous expression of FNDC5 (249). In addition to autoregulation by irisin, FNDC5 expression can also be modulated by multiple other factors such as exercise (250), diet and hormones (246), pathological conditions (251), as well as pharmaceutical chemicals (252). However, FNDC5 expression and its regulation in cells and tissues of oral origin have been rarely studied by far.

In addition to regulation of FNDC5 expression in cells, it was also noticed that irisin local injection enhanced FNDC5 expression in the rat PDL on both orthodontic tension and compression sides (paper II). These *in vivo* findings contradict the results from PDL cells, which showed a reduced

FNDC5 expression upon irisin administration (paper I). This discrepancy of FNDC5 expression in PDL cells and PDL tissue is probably due to the complex components in the structure of PDL. The PDL contains not only PDL cells, but also many other components like epithelial cell rest of Malassez, blood and lymph vessels, as well as those surrounding hard tissues including cementum and alveolar bone (253), hence the overall FNDC5 expression pattern in the intact PDL tissue may be largely impacted by the gene expression in the cells from these components. Additionally, the regulation of FNDC5 expression in PDL tissue was examined in the presence of mechanical loading, we cannot rule out the possibility that mechanical stimulation may have affected the FNDC5 expression, and this is a limitation in the present thesis. Our results imply that irisin may have a pleiotropic effect on dental and paradental cells and tissues, moreover, the regulation of FNDC5 expression might be dependent on cell and tissue type, *in vitro* and *in vivo* environment, and perhaps different receptor density or sensitivity. Afterall, no universal irisin receptor (254) or related pathway (255) have been discovered by far. In addition, as mentioned above, the dimerization of irisin implies that it may bind to more than one particular receptor to exert its functions (9).

8.2.2 Irisin and experimental tooth movement

Previous studies have demonstrated that irisin administration can boost the growth, migration, and osteogenic activity of hPDL cells (149). Irisin's role in regulating mechano-transduction in bone has been documented as well (45). Moreover, irisin injection has been shown to increase cortical bone mineral density and positively modify bone geometry in rodents (256). These findings suggest that irisin can probably serve as a potential agent affecting OTM. Hence, we further aimed to explore the effects of irisin on OTM, with particular focus on structural and molecular changes in PDL tissue. The orthodontic forces create strain in periodontal cells and their surrounding ECM, triggering a series of mechanical, chemical, and cellular events, which lead to structural alterations and eventually tooth movement (257). Certain chemicals may affect this process by interacting with local cells, thus working in concert with orthodontic forces and exerting additive, inhibitory or synergistic effects on OTM (258, 259). In paper II, we demonstrated that submucosal injection of 1 μg irisin reduced tooth movement in an experimental murine orthodontic model during a 14-day experimental OTM setting without causing systemic or local negative effects. However, the inhibitory effect of irisin on OTM seemed to be only local and effective for a short period. The

explanations to the unsustainable reduction in OTM, as stated above, might be related to the different OTM measurement techniques, natural distal drift of maxillary third molars, orthodontic force decay, as well as frequency and dosages of irisin application.

In the process of orthodontic treatment, an inflammatory response occurs simultaneously along with the initial phase because of the vascular compression and blood flow alteration induced by sustained pressure, leading to cellular activation and secretion of proinflammatory factors in PDL, such as cytokines and prostaglandins (260-262). It has been previously suggested that prostaglandins could induce bone resorption activity in PDL cells and increase OTM rate (262). While the use of nonsteroidal anti-inflammatory drugs (NSAIDs) including aspirin, acetaminophen, ibuprofen, *etc.* has been confirmed to be capable of suppressing OTM by inhibition of osteoclast activity, possibly through decreasing the production of prostaglandins (263). The therapeutic potential of irisin against inflammation-related diseases has been confirmed in recent years and has received a great deal of attention. It has been shown to downregulate the expression and secretion of multiple proinflammatory factors in a variety of cell types and several animal models (264, 265). In PDL with inflammation, salivary irisin levels have been observed to be enhanced, while reduced along with decreasing dental plaque percentage in healthy individuals (151). In addition, irisin has been shown to rescue the suppressed osteogenic potential in hPDL cells subjected to inflammatory stimulation (150). Hence, the anti-inflammatory properties of irisin may possibly help to explain the reduced OTM observed after local irisin injection, however, future investigations are needed to verify this.

The OTM rate is mainly based on the remodeling of alveolar bone, which is mediated by the activity of osteoblasts and osteoclasts. Active bone formation on the tension side and bone resorption on the compression side can lead to rapid OTM (266). In other words, OTM may be inhibited through interfering with the osteoclast activity or stimulating the osteoblast activity in the alveolar bone remodeling. It is widely accepted that the osteoclastogenesis is highly active in PDL with inflammation or subjected to compression (267, 268). In the current thesis, though the osteoclast numbers were not quantified, obvious bone resorption lacunae were observed at the PDL-bone surface on the compression side in the control group, while the resorption lacunae were scarce in

the groups given recombinant irisin, indicating an inhibitory role of irisin on bone resorption activity. However, local injection of both dosages of irisin did not induce significant changes in bone volume fraction and bone porosity of alveolar bone compared with the control group. A previous study has shown that irisin administration increases bone mineral density in rodents with osteoporosis, while it has no effect on the bone of healthy animals (269). The implications from these findings possibly indicate that on one hand, the anti-osteoporosis effect of irisin suggests that it may serve as a potential agent mitigating periodontal disease and alveolar bone loss. On the other hand, more consequential anabolic alveolar bone effect of irisin during OTM might be expected in periodontally compromised teeth, nevertheless, more research studying the effect of irisin on the alveolar bone is required to clarify its therapeutic viability.

The tooth mobility is also associated with mechanical properties of PDL, the teeth tend to be more immobile with stiffer PDL, whereas more mobile with mechanically weak and disorganized PDL (270). As a result, expression of two crucial ECM markers collagen type I and periostin, which can bind to each other to enhance collagen fibrillogenesis and therefore the mechanical properties of connective tissues, was evaluated. The elevated expression of collagen type I and periostin on the compression side and elevated expression of periostin on the tension side by 1 μg irisin reflect increased ECM deposition and stiffness in PDL in the presence of irisin. Moreover, the denser and well-organized PDL on the compression side visualized by histological analysis in the two irisin-treated groups further supports this finding. In the paper III, the mechanical stiffness of 3D hPDL cell spheroids, evaluated by nanoindentation, was increased by irisin. Moreover, irisin treatment increased the protein expression of several important ECM markers including collagen type I, periostin and fibronectin. It is hence inferred from these findings that irisin might also grant the PDL tissues stiffer mechanical properties by promoting the deposition of ECM to hinder the mobility of the teeth. It is worth pointing out that local injection of another biomarker for insulin sensitivity, adiponectin, has been reported to block OTM in rats (140). In previous research, it was discovered that irisin is capable of enhancing adiponectin protein levels (271). Based on the results from these studies, we cannot exclude the possibility that local injection of irisin might enhance adiponectin production in the periodontal tissues of the rats, thus contributing to the reduced tooth movement in the present thesis, and further studies are deserved to validate this speculation.

8.2.3 Effects of irisin on rodent PDL tissue and 3D-cultured hPDL cells

Mechanical forces may regulate the differentiation of the PDL cells and thus affect the OTM rate (272). Based on this, we firstly evaluated the expression of osteogenic marker OCN, the most abundant non-collagenous protein expressed in periodontal tissues reflecting the osteogenic differentiation activity during bone formation (273), and angiogenic marker vWF, as angiogenesis is essential for osteogenesis to take place (274). Irisin induced significant increase in the osteogenic marker OCN and angiogenic marker vWF in the PDL on the compression side, while on tension side, only 0.1 μg irisin increased OCN expression. In addition, hPDL cells have been shown to respond to irisin administration with enhanced cell growth, migration and osteogenic behavior *in vitro* (149). Thus, the decreased OTM in our study may be attributed to the enhanced osteoblast activity by irisin application.

To obtain further understanding of the cellular mechanisms that may impact the OTM rate, we sought to examine whether the observations acquired in rodent tissues could be replicated in tissue-mimetic 3D hPDL cell spheroids (paper III). Interestingly, the expression levels of ECM markers including collagen type I, periostin, fibronectin and angiogenic marker vWF were all enhanced by irisin exposure, which is in line with the results in paper II. Moreover, by carrying out microarray and GO/KEGG analysis, some important biological processes related to ECM remodeling were screened out, notably, several MMPs (MMP-1, MMP-3, MMP-13 and MMP-17) family genes were implicated. Periodontal disease is characterized by inflammatory destruction of the periodontal attachment apparatus, and it is believed that degradation of collagen type I in periodontal tissues is a pivotal step in periodontal attachment loss (72). The overexpression of MMPs has been significantly identified in resident cells in the PDL in response to inflammatory stimulation, they can collaboratively degrade almost all ECM components including collagen fibers and their activities are strictly regulated at different levels, thus any abnormal alterations of MMPs may lead to deterioration of periodontal disease (275, 276). The most prevalent kind of MMPs associated with tissue breakdown in periodontal tissue are MMP-8 and MMP-13, with significant contribution from MMP-9 and MMP-14, while other types of MMPs have been shown to play less role in periodontal destruction (277, 278). According to GO/KEGG analysis, MMP-1, MMP-3 and MMP-13 were all downregulated in irisin-treated 3D hPDL cell spheroids, which complies with a previous

study demonstrating that irisin decreased MMP-1 and MMP-13 expression in osteoarthritic chondrocytes (279) and suggests that irisin may also serve as a potential therapeutic agent against periodontal disease, however, effect of irisin on MMP-3 and MMP-17 expression has not been reported to date. These findings together with the enhanced ECM deposition induced by irisin observed in both rat PDL and 3D hPDL cell spheroids (paper II and III) indicate an anti-catabolic effect of irisin on ECM organization of PDL by inhibiting the degradation of collagen fibers in the PDL and alleviating inflammation.

Furthermore, we observed that TAS2Rs were differentially expressed between 3D hPDL cell spheroids treated with or without irisin. TAS2Rs are mainly expressed in taste bud regions and play vital roles in perception of bitterness and are expressed throughout body tissues including periodontal ligament, and hence termed as non-lingual receptors (280, 281). By far, the effect of TAS2Rs family in PDL cells has not been evaluated yet, however, it was recently demonstrated that TAS2Rs were related to odontoblastic differentiation in an inflammatory microenvironment in hDPCs (282), which may imply that in the 3D hPDL culture model irisin administration regulates cell differentiation. In addition, activation of TAS2Rs by their agonists has been shown to either enhance or inhibit the deposition of ECM in airway smooth muscle cells (283, 284), moreover, TAS2Rs activation inhibited secretion of several proinflammatory cytokines and eicosanoids in the whole blood from adults (285, 286). Therefore, it could be inferred that TAS2Rs may be involved in ECM remodeling and regulation of inflammatory reaction in PDL cells as well.

By using the IPA tool, several signaling pathways were involved upon irisin exposure. The actin cytoskeleton is a complex system of actin filaments. It primarily functions as a force-generating machinery producing pushing and pulling forces, thus affecting cell migration, interaction with the environment, morphology and mechanical properties of the cell surface (287). The disassembly of actin cytoskeleton has been shown to lead to down regulation of collagen type I production (288), while the activation of actin cytoskeleton signaling upon irisin treatment may indicate enhanced ECM deposition in 3D hPDL cell spheroids, which corresponds to the results in a previous study performed in 2D cell culture (149). Rho-family GTPases are of vital importance in integration of intracellular signals acting downstream of mechano-sensors, therefore playing a central role in

regulating assembly and disassembly of the actin cytoskeleton, which is necessary for some important cellular functions such as cell-shape alterations and eventually migration (289). In addition, the Rho-family GTPases also regulate the formation of cell-matrix adhesion sites called focal adhesions, which are closely associated with actin structures (290). Both actin cytoskeleton signaling and Rho-family GTPases signaling have been activated in the presence of irisin according to IPA. The observation thus leads us to a speculation that irisin may be a potential upstream activator of Rho-family GTPases-actin cytoskeleton signaling, and further influences an array of cellular functions in hPDL cells. Therefore, future investigations are advised to focus on the validation of this putative irisin-Rho-family GTPases-actin cytoskeleton signaling pathway, moreover, it would be interesting to explore the potential effectors acting downstream the signaling pathway.

A rim-like tissue around irisin-treated 3D hPDL cell spheroids was observed, the mechanism for the formation of this rim-like tissue was not examined in this thesis. However, the possible explanation might be related to the enhanced fibronectin expression. Fibronectin is the main component of basement membrane, which possesses a more compact and less porous structure compared with other elements in ECM (291), the upregulation of fibronectin expression upon irisin treatment may indicate that irisin induced a less porous, more organized structure in the spheroids, which could possibly help to explain the formation of this rim-like tissue. In addition, the regulatory role of irisin on cellular morphology, which was described above, may be associated with the formation of rim-like tissue.

9 CONCLUSIONS

The overall hypothesis was verified as local irisin injection reduced OTM in a rat model, though the effect appeared to be transient. On the other hand, molecular and cellular changes were observed in both PDL tissues and 3D hPDL cell spheroids upon irisin administration (paper II and III).

The following main conclusions can be drawn in response to the research objectives:

A) FNDC5 gene is expressed in a number of dental and paradental cells and tissues including hPDL cells, hDPCs, hOBs, rat PDL tissue, rat dental pulp tissue and rat alveolar bone. Furthermore, FNDC5/irisin expression and/or secretion from hPDL cells, hDPCs and hOBs is discordantly regulated, indicating that regulation of FNDC5/irisin expression and/or secretion is probably dependent on the type of tissues and cells. Moreover, FNDC5/irisin may have pleiotropic effects in cells and tissues from oral origin.

B) Local submucosal injection of recombinant irisin may exert inhibitory effect on OTM rate in rats on short term, without causing any local or systemic negative effects. The potential mechanisms involved are possibly attributed to the inhibited osteoclast activity at PDL-bone interface, enhanced ECM deposition, osteogenic potential and angiogenic potential, as well as increased mechanical properties in PDL. These effects of irisin appear to be more potent on the OTM compression side. The inhibitory effect of irisin on OTM was temporary and this may be related to various factors, including irisin dosage, application frequency and orthodontic appliance force decay.

C) Administration of irisin may serve as a clear switch, which induces differential expression of a large number of genes and mediates several signaling pathways in 3D hPDL cell spheroids. These genes and pathways are associated with a variety of biological functions such as proliferation, differentiation and ECM metabolism. To be more specific, irisin mainly plays a role in maintaining the ECM integrity of 3D hPDL cell spheroids by inhibiting the ECM catabolic process. Additionally, irisin may be able to alleviate inflammation in 3D hPDL cell spheroids. These findings together suggest that irisin has a potential role in PDL remodeling

and repair, thus it may be considered as a promising therapeutic agent to restore the structures and functions of periodontal tissues under pathological conditions.

10 FUTURE PERSPECTIVES

The present PhD thesis investigated several questions including FNDC5 expression in several dental and paradental tissues, irisin effects on OTM and hPDL cells cultured in 3D. However, there are several limitations that should be addressed in future investigations.

To improve the study of experimental OTM, future studies should consider performing micro-CT scanning both before and after the experiment to compare the data. Additionally, structural changes in gingiva and dental pulp tissue after OTM with irisin administration should be examined. Also, improvement of irisin injection methodology with irisin action time/period and dosages must be taken into serious consideration for future investigations. Since irisin has an inhibitory effect on OTM, studying the role of irisin in an orthodontic relapse model or in a biological tooth anchorage reinforcement model would also be of interest.

As irisin has been verified to be mediated through mechanical stress induced by physical activity, and PDL is constantly exposed to mechanical loading, further studies can be performed to evaluate how irisin may affect PDL cells subjected to stretch or compression force *in vitro*. It would also be interesting to compare the secretion of irisin in gingival crevicular fluid in multiple different time points between OTM rats and rats without treatment. This could provide practical information about the optimal dosages for irisin application for future investigations. In addition, gain- and loss-of-function *in vitro* and *in vivo* models for FNDC5 gene overexpression or knockdown could be established in the future. In combination with signaling pathway studies, these studies may provide a deeper understanding of the cellular mechanisms by which FNDC5/irisin regulates the biological behavior of PDL tissue and cells and make contribution to elucidating the role of FNDC5/irisin on mechano-transduction in periodontal tissues during OTM.

According to the bioinformatic analyses, irisin has been suggested to play an important role in protecting the ECM from degradation induced by MMPs, future investigations should focus on validating and assessing the effects of irisin in periodontitis and identifying the underlying mechanisms involved. Furthermore, it would also be necessary to verify the most up- and down-regulated genes screened by microarray analysis in the present study using qPCR or Western blot.

REFERENCES

1. Ferrer-Martínez, A., Ruiz-Lozano, P., Chien, K.R. (2002) Mouse pep: A novel peroxisomal protein linked to myoblast differentiation and development. *Developmental dynamics: an official publication of the American Association of Anatomists*, 224(2),154-167.
2. Teufel, A., Malik, N., Mukhopadhyay, M., Westphal, H. (2002) Frcp1 and frcp2, two novel fibronectin type iii repeat containing genes. *Gene*, 297(1-2),79-83.
3. Boström, P.*, et al.* (2012) A pgc1-α-dependent myokine that drives brown-fat-like development of white fat and thermogenesis. *Nature*, 481(7382),463-468.
4. Maak, S., Norheim, F., Drevon, C.A., Erickson, H.P. (2021) Progress and challenges in the biology of fndc5 and irisin. *Endocrine reviews*, 42(4),436-456.
5. Flori, L., Testai, L., Calderone, V. (2021) The "irisin system": From biological roles to pharmacological and nutraceutical perspectives. *Life Sciences*, 267,118954.
6. Kim, H.K., Jeong, Y.J., Song, I.-S., Noh, Y.H., Seo, K.W., Kim, M., Han, J. (2017) Glucocorticoid receptor positively regulates transcription of fndc5 in the liver. *Scientific Reports*, 7(1),43296.
7. Young, M.F., Valaris, S., Wrann, C.D. (2019) A role for fndc5/irisin in the beneficial effects of exercise on the brain and in neurodegenerative diseases. *Progress in Cardiovascular Diseases*, 62(2),172-178.
8. Panati, K., Suneetha, Y., Narala, V. (2016) Irisin/fndc5-an updated review. *Eur Rev Med Pharmacol Sci*, 20(4),689-697.
9. Pinkowska, A., Podhorska-Okołów, M., Dzięgiel, P., Nowińska, K. (2021) The role of irisin in cancer disease. *Cells*, 10(6),1479.
10. Kim, P.-J., Lee, D.-Y., Jeong, H. (2009) Centralized modularity of n-linked glycosylation pathways in mammalian cells. *PLoS One*, 4(10),e7317.
11. Varki, A. (2017) Biological roles of glycans. *Glycobiology*, 27(1),3-49.
12. Nie, Y., Liu, D. (2017) N-glycosylation is required for fdnc5 stabilization and irisin secretion. *Biochemical Journal*, 474(18),3167-3177.
13. Waseem, R., Shamsi, A., Shahbaz, M., Khan, T., Kazim, S.N., Ahmad, F., Hassan, M.I., Islam, A. (2022) Effect of ph on the structure and stability of irisin, a multifunctional protein: Multispectroscopic and molecular dynamics simulation approach. *Journal of Molecular Structure*, 1252,132141.
14. Schumacher, M.A., Chinnam, N., Ohashi, T., Shah, R.S., Erickson, H.P. (2013) The structure of irisin reveals a novel intersubunit β-sheet fibronectin type iii (fniii) dimer: Implications for receptor activation. *Journal of Biological Chemistry*, 288(47),33738-33744.
15. Kim, H.*, et al.* (2018) Irisin mediates effects on bone and fat via αv integrin receptors. *Cell*, 175(7),1756-1768.e1717.
16. Anastasilakis, A.D., Polyzos, S.A., Makras, P., Douni, E., Mantzoros, C.S. (2019) Irisin: Good or bad for the bone? A new path forward after the reported discovery of irisin receptor? *Metabolism*, 93,100-102.
17. Oguri, Y.*, et al.* (2020) Cd81 controls beige fat progenitor cell growth and energy balance via fak signaling. *Cell*, 182(3),563-577. e520.
18. Estell, E.G.*, et al.* (2020) Irisin directly stimulates osteoclastogenesis and bone resorption in vitro and in vivo. *Elife*, 9,e58172.
19. Duong, L.T., Lakkakorpi, P., Nakamura, I., Rodan, G.A. (2000) Integrins and signaling in osteoclast function. *Matrix Biology*, 19(2),97-105.
20. Yavropoulou, M., Yovos, J. (2008) Osteoclastogenesis--current knowledge and future perspectives.

J Musculoskelet Neuronal Interact, 8(3),204-216.
21. Chen, N., Li, Q., Liu, J., Jia, S. (2016) Irisin, an exercise-induced myokine as a metabolic regulator: An updated narrative review. *Diabetes/Metabolism Research and Reviews*, 32(1),51-59.
22. Wu, J.*, et al.* (2012) Beige adipocytes are a distinct type of thermogenic fat cell in mouse and human. *Cell*, 150(2),366-376.
23. Spiegelman, B.M. (2013) Banting lecture 2012: Regulation of adipogenesis: Toward new therapeutics for metabolic disease. *Diabetes*, 62(6),1774-1782.
24. Boström, P.*, et al.* (2012) A pgc1-α-dependent myokine that drives brown-fat-like development of white fat and thermogenesis. *Nature*, 481(7382),463-468.
25. Perakakis, N., Triantafyllou, G.A., Fernández-Real, J.M., Huh, J.Y., Park, K.H., Seufert, J., Mantzoros, C.S. (2017) Physiology and role of irisin in glucose homeostasis. *Nature reviews endocrinology*, 13(6),324-337.
26. Castillo-Quan, J.I. (2012) From white to brown fat through the pgc-1α-dependent myokine irisin: Implications for diabetes and obesity. *Disease Models & Mechanisms*, 5(3),293-295.
27. Puigserver, P., Wu, Z., Park, C.W., Graves, R., Wright, M., Spiegelman, B.M. (1998) A cold-inducible coactivator of nuclear receptors linked to adaptive thermogenesis. *Cell*, 92(6),829-839.
28. Polyzos, S.A., Anastasilakis, A.D., Efstathiadou, Z.A., Makras, P., Perakakis, N., Kountouras, J., Mantzoros, C.S. (2018) Irisin in metabolic diseases. *Endocrine*, 59(2),260-274.
29. Tu, T., Peng, J., Jiang, Y. (2020) Fndc5/irisin: A new protagonist in acute brain injury. *Stem cells and development*, 29(9),533-543.
30. Wrann, C.D. (2015) Fndc5/irisin–their role in the nervous system and as a mediator for beneficial effects of exercise on the brain. *Brain plasticity*, 1(1),55-61.
31. Forouzanfar, M., Rabiee, F., Ghaedi, K., Beheshti, S., Tanhaei, S., Shoaraye Nejati, A., Jodeiri Farshbaf, M., Baharvand, H., Nasr-Esfahani, M.H. (2015) Fndc5 overexpression facilitated neural differentiation of mouse embryonic stem cells. *Cell biology international*, 39(5),629-637.
32. Hashemi, M.S., Ghaedi, K., Salamian, A., Karbalaie, K., Emadi-Baygi, M., Tanhaei, S., Nasr-Esfahani, M.H., Baharvand, H. (2013) Fndc5 knockdown significantly decreased neural differentiation rate of mouse embryonic stem cells. *Neuroscience*, 231,296-304.
33. HUANG, Y.S., Wu, C.Y. (2019) Mechanisms of exercise protein fndc5/irisin in vasculature during zebrafish development. *The FASEB Journal*, 33(S1),643.642-643.642.
34. Wu, F.*, et al.* (2015) Irisin induces angiogenesis in human umbilical vein endothelial cells in vitro and in zebrafish embryos in vivo via activation of the erk signaling pathway. *PLoS One*, 10(8),e0134662.
35. Kan, T.*, et al.* (2022) Irisin promotes fracture healing by improving osteogenesis and angiogenesis. *Journal of Orthopaedic Translation*, 37,37-45.
36. Zhang, D., Tan, X., Tang, N., Huang, F., Chen, Z., Shi, G. (2020) Review of research on the role of irisin in tumors. *OncoTargets and therapy*, 13,4423.
37. Altay, D.U., Keha, E.E., Karagüzel, E., Menteşe, A., Yaman, S.O., Alver, A. (2018) The diagnostic value of fndc5/irisin in renal cell cancer. *International braz j urol*, 44,734-739.
38. Nowinska, K.*, et al.* (2019) Expression of irisin/fndc5 in cancer cells and stromal fibroblasts of non-small cell lung cancer. *Cancers*, 11(10),1538.
39. Zhang, Z.-p., Zhang, X.-f., Li, H., Liu, T.-j., Zhao, Q.-p., Huang, L.-h., Cao, Z.-j., He, L.-m., Hao, D.-j. (2018) Serum irisin associates with breast cancer to spinal metastasis. *Medicine*, 97(17).
40. Xiong, X.-Q.*, et al.* (2018) Fndc5 attenuates adipose tissue inflammation and insulin resistance via ampk-mediated macrophage polarization in obesity. *Metabolism*, 83,31-41.

41. Li, Q., Tan, Y., Chen, S., Xiao, X., Zhang, M., Wu, Q., Dong, M. (2021) Irisin alleviates lps-induced liver injury and inflammation through inhibition of nlrp3 inflammasome and nf-κb signaling. *Journal of Receptors and Signal Transduction*, 41(3),294-303.
42. Wang, K., Song, F., Xu, K., Liu, Z., Han, S., Li, F., Sun, Y. (2019) Irisin attenuates neuroinflammation and prevents the memory and cognitive deterioration in streptozotocin-induced diabetic mice. *Mediators of inflammation*, 2019.
43. Mazur-Bialy, A.I. (2017) Irisin acts as a regulator of macrophages host defense. *Life Sciences*, 176,21-25.
44. Peng, J.*, et al.* (2017) Irisin protects against neuronal injury induced by oxygen-glucose deprivation in part depends on the inhibition of ros-nlrp3 inflammatory signaling pathway. *Molecular Immunology*, 91,185-194.
45. Colaianni, G., Cuscito, C., Mongelli, T., Oranger, A., Mori, G., Brunetti, G., Colucci, S., Cinti, S., Grano, M. (2014) Irisin enhances osteoblast differentiation in vitro. *International Journal of Endocrinology*, 2014.
46. Qiao, X., Nie, Y., Ma, Y., Chen, Y., Cheng, R., Yin, W., Hu, Y., Xu, W., Xu, L. (2016) Irisin promotes osteoblast proliferation and differentiation via activating the map kinase signaling pathways. *Scientific Reports*, 6(1),1-12.
47. Chen, Z.*, et al.* (2020) Recombinant irisin prevents the reduction of osteoblast differentiation induced by stimulated microgravity through increasing β-catenin expression. *International journal of molecular sciences*, 21(4),1259.
48. Colaianni, G.*, et al.* (2015) The myokine irisin increases cortical bone mass. *Proceedings of the National Academy of Sciences*, 112(39),12157-12162.
49. Aydin, S.*, et al.* (2014) Cardiac, skeletal muscle and serum irisin responses to with or without water exercise in young and old male rats: Cardiac muscle produces more irisin than skeletal muscle. *Peptides*, 52,68-73.
50. Aydin, S.*, et al.* (2014) A comprehensive immunohistochemical examination of the distribution of the fat-burning protein irisin in biological tissues. *Peptides*, 61,130-136.
51. Gençer Tarakçı, B., Girgin, A., Timurkaan, S., Yalçın, M., Gür, F., Karan, M. (2016) Immunohistochemical localization of irisin in skin, eye, and thyroid and pineal glands of the crested porcupine (hystrix cristata). *Biotechnic & Histochemistry*, 91(6),423-427.
52. Dun, S.L., Lyu, R.-M., Chen, Y.-H., Chang, J.-K., Luo, J.J., Dun, N.J. (2013) Irisin-immunoreactivity in neural and non-neural cells of the rodent. *Neuroscience*, 240,155-162.
53. Aydin, S., Ogeturk, M., Kuloglu, T., Kavakli, A., Aydin, S. (2015) Effect of carnosine supplementation on apoptosis and irisin, total oxidant and antioxidants levels in the serum, liver and lung tissues in rats exposed to formaldehyde inhalation. *Peptides*, 64,14-23.
54. Moreno-Navarrete, J.M., Ortega, F., Serrano, M., Guerra, E., Pardo, G., Tinahones, F., Ricart, W., Fernández-Real, J.M. (2013) Irisin is expressed and produced by human muscle and adipose tissue in association with obesity and insulin resistance. *The Journal of Clinical Endocrinology & Metabolism*, 98(4),E769-E778.
55. Piya, M.K.*, et al.* (2014) The identification of irisin in human cerebrospinal fluid: Influence of adiposity, metabolic markers, and gestational diabetes. *American Journal of Physiology-Endocrinology and Metabolism*, 306(5),E512-E518.
56. Bakal, U., Aydin, S., Sarac, M., Kuloglu, T., Kalayci, M., Artas, G., Yardim, M., Kazez, A. (2016) Serum, saliva, and urine irisin with and without acute appendicitis and abdominal pain. *Biochemistry*

Insights, 9,BCI. S39671.
57. Aydin, S.*, et al.* (2014) Decreased saliva/serum irisin concentrations in the acute myocardial infarction promising for being a new candidate biomarker for diagnosis of this pathology. *Peptides*, 56,141-145.
58. Yang, Y., Pullisaar, H., Landin, M.A., Heyward, C.A., Schröder, M., Geng, T., Grano, M., Reseland, J.E. (2021) Fndc5/irisin is expressed and regulated differently in human periodontal ligament cells, dental pulp stem cells and osteoblasts. *Archives of Oral Biology*, 124,105061.
59. Madukwe, I. (2014) Anatomy of the periodontium: A biological basis for radiographic evaluation of periradicular pathology. *Journal of dentistry and oral hygiene*, 6(7),70-76.
60. Iwata, T., Yamato, M., Ishikawa, I., Ando, T., Okano, T. (2014) Tissue engineering in periodontal tissue. *The Anatomical Record*, 297(1),16-25.
61. Buduneli, N., Buduneli, N. (2020) Anatomy of periodontal tissues. *Biomarkers in Periodontal Health and Disease: Rationale, Benefits, and Future Directions*,1-7.
62. De Jong, T., Bakker, A., Everts, V., Smit, T. (2017) The intricate anatomy of the periodontal ligament and its development: Lessons for periodontal regeneration. *Journal of Periodontal Research*, 52(6),965-974.
63. Beertsen, W., McCulloch, C.A., Sodek, J. (1997) The periodontal ligament: A unique, multifunctional connective tissue. *Periodontology 2000*, 13(1),20-40.
64. Connizzo, B., Sun, L., Lacin, N., Gendelman, A., Solomonov, I., Sagi, I., Grodzinsky, A., Naveh, G. (2021) Nonuniformity in periodontal ligament: Mechanics and matrix composition. *Journal of Dental Research*, 100(2),179-186.
65. Najafidoust, M., Hashemi, A., Oskui, I.Z. (2020) Dynamic viscoelastic behavior of bovine periodontal ligament in compression. *Journal of Periodontal Research*, 55(5),651-659.
66. Bergomi, M., Cugnoni, J., Botsis, J., Belser, U.C., Wiskott, H.A. (2010) The role of the fluid phase in the viscous response of bovine periodontal ligament. *Journal of biomechanics*, 43(6),1146-1152.
67. Dangaria, S.J., Ito, Y., Walker, C., Druzinsky, R., Luan, X., Diekwisch, T.G. (2009) Extracellular matrix-mediated differentiation of periodontal progenitor cells. *Differentiation*, 78(2-3),79-90.
68. Waddington, R., Embery, G. (2001) Proteoglycans and orthodontic tooth movement. *Journal of orthodontics*, 28(4),281-290.
69. Watanabe, T., Kubota, T. (1998) Characterization of fibromodulin isolated from bovine periodontal ligament. *Journal of Periodontal Research*, 33(1),1-7.
70. Matsuura, M., Herr, Y., Han, K.Y., Lin, W.L., Genco, R.J., Cho, M.I. (1995) Immunohistochemical expression of extracellular matrix components of normal and healing periodontal tissues in the beagle dog. *Journal of Periodontology*, 66(7),579-593.
71. Rios, H.*, et al.* (2005) Periostin null mice exhibit dwarfism, incisor enamel defects, and an early-onset periodontal disease-like phenotype. *Molecular and Cellular Biology*, 25(24),11131-11144.
72. Sapna, G., Gokul, S., Bagri-Manjrekar, K. (2014) Matrix metalloproteinases and periodontal diseases. *Oral Diseases*, 20(6),538-550.
73. Mcculloch, C.A., Lekic, P., Mckee, M.D. (2000) Role of physical forces in regulating the form and function of the periodontal ligament. *Periodontology 2000*, 24(1),56-72.
74. Liu, S.H., Yang, R.-S., Al-Shaikh, R., Lane, J.M. (1995) Collagen in tendon, ligament, and bone healing. A current review. *Clinical orthopaedics and related research*, (318),265-278.
75. Kihara, T., Hirose, M., Oshima, A., Ohgushi, H. (2006) Exogenous type i collagen facilitates osteogenic differentiation and acts as a substrate for mineralization of rat marrow mesenchymal stem

cells in vitro. *Biochemical and Biophysical Research Communications*, 341(4),1029-1035.
76. Scanlon, C.S., Marchesan, J.T., Soehren, S., Matsuo, M., Kapila, Y. (2011) Capturing the regenerative potential of periodontal ligament fibroblasts. *Journal of stem cells & regenerative medicine*, 7(1),54.
77. McCulloch, C.A., Bordin, S. (1991) Role of fibroblast subpopulations in periodontal physiology and pathology. *Journal of Periodontal Research*, 26(3),144-154.
78. Nanci, A., Bosshardt, D.D. (2006) Structure of periodontal tissues in health and disease. *Periodontology 2000*, 40(1),11-28.
79. Gould, T., Melcher, A., Brunette, D. (1980) Migration and division of progenitor cell populations in periodontal ligament after wounding. *Journal of Periodontal Research*, 15(1),20-42.
80. McCulloch, C., Melcher, A. (1983) Cell density and cell generation in the periodontal ligament of mice. *American Journal of Anatomy*, 167(1),43-58.
81. Wang, H.L., Greenwell, H., Fiorellini, J., Giannobile, W., Offenbacher, S., Salkin, L., Townsend, C., Sheridan, P., Genco, R.J. (2005) Periodontal regeneration. *Journal of Periodontology*, 76(9),1601-1622.
82. Liu, H.W., Yacobi, R., Savion, N., Narayanan, A.S., Pitaru, S. (1997) A collagenous cementum-derived attachment protein is a marker for progenitors of the mineralized tissue-forming cell lineage of the periodontal ligament. *Journal of Bone and Mineral Research*, 12(10),1691-1699.
83. Seo, B.-M.*, et al.* (2004) Investigation of multipotent postnatal stem cells from human periodontal ligament. *The Lancet*, 364(9429),149-155.
84. Xu, J., Wang, W., Kapila, Y., Lotz, J., Kapila, S. (2009) Multiple differentiation capacity of stro-1+/cd146+ pdl mesenchymal progenitor cells. *Stem cells and development*, 18(3),487-496.
85. Kuru, L., Parkar, M., Griffiths, G., Newman, H., Olsen, I. (1998) Flow cytometry analysis of gingival and periodontal ligament cells. *Journal of Dental Research*, 77(4),555-564.
86. HASSELL, T.M. (1993) Tissues and cells of the periodontium. *Periodontology 2000*, 3(1),9-38.
87. CHO, M.I., Garant, P.R. (2000) Development and general structure of the periodontium. *Periodontology 2000*, 24(1),9-27.
88. Omi, M., Mishina, Y. (2022) Roles of osteoclasts in alveolar bone remodeling. *genesis*, 60(8-9),e23490.
89. Huang, X., Xie, M., Xie, Y., Mei, F., Lu, X., Li, X., Chen, L. (2020) The roles of osteocytes in alveolar bone destruction in periodontitis. *Journal of Translational Medicine*, 18(1),1-15.
90. Vignery, A., Baron, R. (1980) Dynamic histomorphometry of alveolar bone remodeling in the adult rat. *The Anatomical Record*, 196(2),191-200.
91. Xu, F., Teitelbaum, S.L. (2013) Osteoclasts: New insights. *Bone Research*, 1(1),11-26.
92. Feng, X., McDonald, J.M. (2011) Disorders of bone remodeling. *Annual review of pathology*, 6,121.
93. Lerner, U.H., editor Osteoblasts, osteoclasts, and osteocytes: Unveiling their intimate-associated responses to applied orthodontic forces. Seminars in Orthodontics; 2012: Elsevier.
94. Servier Medical Art. Available from: https://smart.servier.com.
95. Jiang, N.*, et al.* (2016) Periodontal ligament and alveolar bone in health and adaptation: Tooth movement. *Tooth movement*, 18,1-8.
96. Seita, J., Weissman, I.L. (2010) Hematopoietic stem cell: Self-renewal versus differentiation. *Wiley Interdisciplinary Reviews: Systems Biology and Medicine*, 2(6),640-653.
97. Udagawa, N., Takahashi, N., Akatsu, T., Tanaka, H., Sasaki, T., Nishihara, T., Koga, T., Martin, T.J., Suda, T. (1990) Origin of osteoclasts: Mature monocytes and macrophages are capable of differentiating

into osteoclasts under a suitable microenvironment prepared by bone marrow-derived stromal cells. *Proceedings of the National Academy of Sciences*, 87(18),7260-7264.

98. Aliprantis, A.O., Ueki, Y., Sulyanto, R., Park, A., Sigrist, K.S., Sharma, S.M., Ostrowski, M.C., Olsen, B.R., Glimcher, L.H. (2008) Nfatc1 in mice represses osteoprotegerin during osteoclastogenesis and dissociates systemic osteopenia from inflammation in cherubism. *The Journal of clinical investigation*, 118(11),3775-3789.

99. Grigoriadis, A.E., Wang, Z.-Q., Cecchini, M.G., Hofstetter, W., Felix, R., Fleisch, H.A., Wagner, E.F. (1994) C-fos: A key regulator of osteoclast-macrophage lineage determination and bone remodeling. *Science*, 266(5184),443-448.

100. Teitelbaum, S.L. (2000) Bone resorption by osteoclasts. *Science*, 289(5484),1504-1508.

101. Kim, T., Handa, A., Iida, J., Yoshida, S. (2007) Rankl expression in rat periodontal ligament subjected to a continuous orthodontic force. *Archives of Oral Biology*, 52(3),244-250.

102. Shiotani, A., Shibasaki, Y., Sasaki, T. (2001) Localization of receptor activator of nfκb ligand, rankl, in periodontal tissues during experimental movement of rat molars. *Journal of electron microscopy*, 50(4),365-369.

103. Karsenty, G., Kronenberg, H.M., Settembre, C. (2009) Genetic control of bone formation. *Annual Review of Cell and Developmental*, 25,629-648.

104. Ottewell, P.D. (2016) The role of osteoblasts in bone metastasis. *Journal of bone oncology*, 5(3),124-127.

105. Caetano-Lopes, J., Canhao, H., Fonseca, J.E. (2007) Osteoblasts and bone formation. *Acta reumatológica portuguesa*, 32(2),103-110.

106. Mizoguchi, T., Ono, N. (2021) The diverse origin of bone-forming osteoblasts. *Journal of Bone and Mineral Research*, 36(8),1432-1447.

107. Algate, K., Haynes, D., Bartold, P., Crotti, T., Cantley, M. (2016) The effects of tumour necrosis factor-α on bone cells involved in periodontal alveolar bone loss; osteoclasts, osteoblasts and osteocytes. *Journal of Periodontal Research*, 51(5),549-566.

108. Nakashima, T*., et al.* (2011) Evidence for osteocyte regulation of bone homeostasis through rankl expression. *Nature medicine*, 17(10),1231-1234.

109. Martin, T.J., Sims, N.A. (2015) Rankl/opg; critical role in bone physiology. *Reviews in Endocrine and Metabolic Disorders*, 16(2),131-139.

110. Kogianni, G., Mann, V., Noble, B.S. (2008) Apoptotic bodies convey activity capable of initiating osteoclastogenesis and localized bone destruction. *Journal of Bone and Mineral Research*, 23(6),915-927.

111. Uda, Y., Azab, E., Sun, N., Shi, C., Pajevic, P.D. (2017) Osteocyte mechanobiology. *Current Osteoporosis Reports*, 15(4),318-325.

112. Matsuo, K. (2009) Cross-talk among bone cells. *Current opinion in nephrology and hypertension*, 18(4),292-297.

113. Vansant, L., De Llano-Pérula, M.C., Verdonck, A., Willems, G. (2018) Expression of biological mediators during orthodontic tooth movement: A systematic review. *Archives of Oral Biology*, 95,170-186.

114. Jin, Y., Li, J., Wang, Y., Ye, R., Feng, X., Jing, Z., Zhao, Z. (2015) Functional role of mechanosensitive ion channel piezo1 in human periodontal ligament cells. *The Angle Orthodontist*, 85(1),87-94.

115. von Böhl, M., Kuijpers-Jagtman, A.M. (2009) Hyalinization during orthodontic tooth movement:

A systematic review on tissue reactions. *The European Journal of Orthodontics*, 31(1),30-36.
116. Militi, A.*, et al.* (2019) An immunofluorescence study on vegf and extracellular matrix proteins in human periodontal ligament during tooth movement. *Heliyon*, 5(10),e02572.
117. Reitan, K. (1947) Continuous bodily tooth movement and its histological significance. *Acta Odontologica Scandinavica*, 7(2),115-144.
118. Pilon, J.J., Kuijpers-Jagtman, A.M., Maltha, J.C. (1996) Magnitude of orthodontic forces and rate of bodily tooth movement. An experimental study. *American Journal of Orthodontics and Dentofacial Orthopedics*, 110(1),16-23.
119. Kashyap, S. (2016) Current concepts in the biology of orthodontic tooth movement: A brief overview. *NJDSR*, 1(4),28-31.
120. Van Leeuwen, E.J., Maltha, J.C., Kuijpers-Jagtman, A.M. (1999) Tooth movement with light continuous and discontinuous forces in beagle dogs. *European journal of oral sciences*, 107(6),468-474.
121. Patil, A., Jayade, V. (2006) Advances in biology of orthodontic tooth movement. A review. *Journal of Indian Orthodontic Society*, 39,155-164.
122. Zainal Ariffin, S.H., Yamamoto, Z., Abidin, Z., Megat Abdul Wahab, R., Zainal Ariffin, Z. (2011) Cellular and molecular changes in orthodontic tooth movement. *The Scientific World Journal*, 11,1788-1803.
123. Di Domenico, M.*, et al.* (2012) Cytokines and vegf induction in orthodontic movement in animal models. *Journal of Biomedicine and Biotechnology*, 2012.
124. Krishnan, V., Davidovitch, Z.e. (2006) Cellular, molecular, and tissue-level reactions to orthodontic force. *American Journal of Orthodontics and Dentofacial Orthopedics*, 129(4),469. e461-469. e432.
125. Feller, L., Khammissa, R., Schechter, I., Moodley, A., Thomadakis, G., Lemmer, J. (2015) Periodontal biological events associated with orthodontic tooth movement: The biomechanics of the cytoskeleton and the extracellular matrix. *The Scientific World Journal*, 2015.
126. Garlet, T.P., Coelho, U., Silva, J.S., Garlet, G.P. (2007) Cytokine expression pattern in compression and tension sides of the periodontal ligament during orthodontic tooth movement in humans. *European journal of oral sciences*, 115(5),355-362.
127. d'Apuzzo, F., Cappabianca, S., Ciavarella, D., Monsurrò, A., Silvestrini-Biavati, A., Perillo, L. (2013) Biomarkers of periodontal tissue remodeling during orthodontic tooth movement in mice and men: Overview and clinical relevance. *The Scientific World Journal*, 2013.
128. Brooks, P.J., Nilforoushan, D., Manolson, M.F., Simmons, C.A., Gong, S.-G. (2009) Molecular markers of early orthodontic tooth movement. *The Angle Orthodontist*, 79(6),1108-1113.
129. Li, Y., Zhan, Q., Bao, M., Yi, J., Li, Y. (2021) Biomechanical and biological responses of periodontium in orthodontic tooth movement: Up-date in a new decade. *International journal of oral science*, 13(1),1-19.
130. Dudic, A., Giannopoulou, C., Kiliaridis, S. (2013) Factors related to the rate of orthodontically induced tooth movement. *American Journal of Orthodontics and Dentofacial Orthopedics*, 143(5),616-621.
131. Kılıç, N., Oktay, H., Ersöz, M. (2010) Effects of force magnitude on tooth movement: An experimental study in rabbits. *The European Journal of Orthodontics*, 32(2),154-158.
132. Lee, W. (2018) Corticotomy for orthodontic tooth movement. *Journal of the Korean Association of Oral and Maxillofacial Surgeons*, 44(6),251-258.
133. AlGhamdi, A.S.T. (2010) Corticotomy facilitated orthodontics: Review of a technique. *The Saudi Dental Journal*, 22(1),1-5.

134. Genc, G., Kocadereli, I., Tasar, F., Kilinc, K., El, S., Sarkarati, B. (2013) Effect of low-level laser therapy (lllt) on orthodontic tooth movement. *Lasers in medical science*, 28(1),41-47.
135. Seifi, M., Shafeei, H.A., Daneshdoost, S., Mir, M. (2007) Effects of two types of low-level laser wave lengths (850 and 630 nm) on the orthodontic tooth movements in rabbits. *Lasers in medical science*, 22(4),261-264.
136. Kanzaki, H., Chiba, M., Takahashi, I., Haruyama, N., Nishimura, M., Mitani, H. (2004) Local opg gene transfer to periodontal tissue inhibits orthodontic tooth movement. *Journal of Dental Research*, 83(12),920-925.
137. Iglesias-Linares, A., Moreno-Fernandez, A., Yañez-Vico, R., Mendoza-Mendoza, A., Gonzalez-Moles, M., Solano-Reina, E. (2011) The use of gene therapy vs. Corticotomy surgery in accelerating orthodontic tooth movement. *Orthodontics & Craniofacial Research*, 14(3),138-148.
138. Bartzela, T., Türp, J.C., Motschall, E., Maltha, J.C. (2009) Medication effects on the rate of orthodontic tooth movement: A systematic literature review. *American Journal of Orthodontics and Dentofacial Orthopedics*, 135(1),16-26.
139. Walker, J.B., Buring, S.M. (2001) Nsaid impairment of orthodontic tooth movement. *Annals of Pharmacotherapy*, 35(1),113-115.
140. Haugen, S., Aasarød, K.M., Stunes, A.K., Mosti, M.P., Franzen, T., Vandevska-Radunovic, V., Syversen, U., Reseland, J.E. (2017) Adiponectin prevents orthodontic tooth movement in rats. *Archives of Oral Biology*, 83,304-311.
141. Krishnan, S., Pandian, S., Kumar, A. (2015) Effect of bisphosphonates on orthodontic tooth movement—an update. *Journal of clinical and diagnostic research: JCDR*, 9(4),ZE01.
142. Shen, W.-R.*, et al.* (2021) Local administration of high-dose diabetes medicine exendin-4 inhibits orthodontic tooth movement in mice. *The Angle Orthodontist*, 91(1),111-118.
143. Gonzales, C., Hotokezaka, H., Karadeniz, E.I., Miyazaki, T., Kobayashi, E., Darendeliler, M.A., Yoshida, N. (2011) Effects of fluoride intake on orthodontic tooth movement and orthodontically induced root resorption. *American Journal of Orthodontics and Dentofacial Orthopedics*, 139(2),196-205.
144. Dunn, M.D., Park, C.H., Kostenuik, P.J., Kapila, S., Giannobile, W.V. (2007) Local delivery of osteoprotegerin inhibits mechanically mediated bone modeling in orthodontic tooth movement. *Bone*, 41(3),446-455.
145. Collins, M.K., Sinclair, P.M. (1988) The local use of vitamin d to increase the rate of orthodontic tooth movement. *American Journal of Orthodontics and Dentofacial Orthopedics*, 94(4),278-284.
146. Shirazi, M., Dehpour, A., Jafari, F. (1999) The effect of thyroid hormone on orthodontic tooth movement in rats. *The Journal of clinical pediatric dentistry*, 23(3),259-264.
147. Chang, J.H., Chen, P.-J., Arul, M.R., Dutra, E.H., Nanda, R., Kumbar, S.G., Yadav, S. (2020) Injectable rankl sustained release formulations to accelerate orthodontic tooth movement. *European Journal of Orthodontics*, 42(3),317-325.
148. Leiker, B.J., Nanda, R.S., Currier, G.F., Howes, R.I., Sinha, P.K. (1995) The effects of exogenous prostaglandins on orthodontic tooth movement in rats. *American Journal of Orthodontics and Dentofacial Orthopedics*, 108(4),380-388.
149. Pullisaar, H., Colaianni, G., Lian, A.-M., Vandevska-Radunovic, V., Grano, M., Reseland, J.E. (2020) Irisin promotes growth, migration and matrix formation in human periodontal ligament cells. *Archives of Oral Biology*, 111,104635.
150. Huang, X., Xiao, J., Wang, X., Cao, Z. (2022) Irisin attenuates p. Gingivalis-suppressed osteogenic/cementogenic differentiation of periodontal ligament cells via p38 signaling pathway.

Biochemical and Biophysical Research Communications, 618, 100-106.
151. Khan, S.U., Ghafoor, S., Khaliq, S., Syed, A.R. (2022) Salivary irisin and periodontal clinical parameters in patients of chronic periodontitis and healthy individuals: A novel salivary myokine for periodontal disease. *Journal of the Pakistan Medical Association*, 72(01),27-32.
152. Zhu, J., Wang, Y., Cao, Z., Du, M., Hao, Y., Pan, J., He, H. (2020) Irisin promotes cementoblast differentiation via p38 mapk pathway. *Oral Diseases*, 26(5),974-982.
153. Zhao, C., Wang, Y., Cao, Z., Zhu, J., He, H. (2022) Effect of irisin on the expression of osteoclast-related genes in cementoblasts. *European Journal of Orthodontics*, 44(4), 420-426.
154. Son, J., Choi, S., Jang, J., Koh, J., Oh, W., Hwang, Y., Lee, B. (2021) Irisin promotes odontogenic differentiation and angiogenic potential in human dental pulp cells. *International Endodontic Journal*, 54(3),399-412.
155. Posa, F., Colaianni, G., Di Cosola, M., Dicarlo, M., Gaccione, F., Colucci, S., Grano, M., Mori, G. (2021) The myokine irisin promotes osteogenic differentiation of dental bud-derived mscs. *Biology*, 10(4),295.
156. Montes-Nieto, R., Martínez-García, M.Á., Luque-Ramírez, M., Escobar-Morreale, H.F. (2016) Differences in analytical and biological results between older and newer lots of a widely used irisin immunoassay question the validity of previous studies. *Clinical Chemistry and Laboratory Medicine (CCLM)*, 54(7),e199-e201.
157. Sanchis-Gomar, F., Alis, R., Lippi, G. (2015) Circulating irisin detection: Does it really work? *Trends in Endocrinology & Metabolism*, 26(7),335-336.
158. Choi, J., Lee, S. (2004) Secretory and extracellular production of recombinant proteins using escherichia coli. *Applied microbiology and biotechnology*, 64,625-635.
159. Rosano, G.L., Ceccarelli, E.A. (2014) Recombinant protein expression in escherichia coli: Advances and challenges. *Frontiers in microbiology*, 5,172.
160. Kapałczyńska, M.*, et al.* (2018) 2d and 3d cell cultures–a comparison of different types of cancer cell cultures. *Archives of Medical Science*, 14(4),910-919.
161. Pampaloni, F., Reynaud, E.G., Stelzer, E.H. (2007) The third dimension bridges the gap between cell culture and live tissue. *Nature reviews Molecular cell biology*, 8(10),839-845.
162. Baker, B.M., Chen, C.S. (2012) Deconstructing the third dimension–how 3d culture microenvironments alter cellular cues. *Journal of cell science*, 125(13),3015-3024.
163. Aggarwal, B.B., Danda, D., Gupta, S., Gehlot, P. (2009) Models for prevention and treatment of cancer: Problems vs promises. *Biochemical pharmacology*, 78(9),1083-1094.
164. Bissell, M.J., Rizki, A., Mian, I.S. (2003) Tissue architecture: The ultimate regulator of breast epithelial function. *Current opinion in cell biology*, 15(6),753.
165. Fontoura, J.C., Viezzer, C., Dos Santos, F.G., Ligabue, R.A., Weinlich, R., Puga, R.D., Antonow, D., Severino, P., Bonorino, C. (2020) Comparison of 2d and 3d cell culture models for cell growth, gene expression and drug resistance. *Materials Science and Engineering: C*, 107,110264.
166. Edmondson, R., Broglie, J.J., Adcock, A.F., Yang, L. (2014) Three-dimensional cell culture systems and their applications in drug discovery and cell-based biosensors. *ASSAY and Drug Development Technologies*, 12(4),207-218.
167. Knight, E., Przyborski, S. (2015) Advances in 3d cell culture technologies enabling tissue-like structures to be created in vitro. *Journal of Anatomy*, 227(6),746-756.
168. Ghosh, S., Spagnoli, G.C., Martin, I., Ploegert, S., Demougin, P., Heberer, M., Reschner, A. (2005) Three-dimensional culture of melanoma cells profoundly affects gene expression profile: A high density

oligonucleotide array study. *Journal of Cellular Physiology*, 204(2),522-531.
169. Berthiaume, F., Moghe, P.V., Toner, M., Yarmush, M.L. (1996) Effect of extracellular matrix topology on cell structure, function, and physiological responsiveness: Hepatocytes cultured in a sandwich configuration. *The FASEB Journal*, 10(13),1471-1484.
170. Semino, C.E., Merok, J.R., Crane, G.G., Panagiotakos, G., Zhang, S. (2003) Functional differentiation of hepatocyte-like spheroid structures from putative liver progenitor cells in three-dimensional peptide scaffolds. *Differentiation*, 71(4-5),262-270.
171. Powers, M.J., Janigian, D.M., Wack, K.E., Baker, C.S., Stolz, D.B., Griffith, L.G. (2002) Functional behavior of primary rat liver cells in a three-dimensional perfused microarray bioreactor. *Tissue Engineering*, 8(3),499-513.
172. Celvivo. Available from: https://celvivo.com/products/clinostar/.
173. Inanc, B., Elcin, A.E., Elcin, Y.M. (2006) Osteogenic induction of human periodontal ligament fibroblasts under two-and three-dimensional culture conditions. *Tissue Engineering*, 12(2),257-266.
174. Li, M., Yi, J., Yang, Y., Zheng, W., Li, Y., Zhao, Z. (2016) Investigation of optimal orthodontic force at the cellular level through three-dimensionally cultured periodontal ligament cells. *European Journal of Orthodontics*, 38(4),366-372.
175. Moritani, Y.*, et al.* (2018) Spheroid culture enhances osteogenic potential of periodontal ligament mesenchymal stem cells. *Journal of Periodontal Research*, 53(5),870-882.
176. Jeong, Y.Y., Kim, M.S., Lee, K.E., Nam, O.H., Jang, J.-H., Choi, S.-C., Lee, H.-S. (2021) Comparison of 2-and 3-dimensional cultured periodontal ligament stem cells; a pilot study. *Applied Sciences*, 11(3),1083.
177. Hoz, L., Romo, E., Zeichner-David, M., Sanz, M., Nuñez, J., Gaitán, L., Mercado, G., Arzate, H. (2012) Cementum protein 1 (cemp1) induces differentiation by human periodontal ligament cells under three-dimensional culture conditions. *Cell biology international*, 36(2),129-136.
178. Li, S., Ma, Z., Niu, Z., Qian, H., Xuan, D., Hou, R., Ni, L. (2009) Nasa-approved rotary bioreactor enhances proliferation and osteogenesis of human periodontal ligament stem cells. *Stem cells and development*, 18(9),1273-1282.
179. Inanç, B., Eser Elçin, A., Koç, A., Baloş, K., Parlar, A., Murat Elcin, Y. (2007) Encapsulation and osteoinduction of human periodontal ligament fibroblasts in chitosan–hydroxyapatite microspheres. *Journal of Biomedical Materials Research Part A: An Official Journal of The Society for Biomaterials, The Japanese Society for Biomaterials, and The Australian Society for Biomaterials and the Korean Society for Biomaterials*, 82(4),917-926.
180. Goodwin, T., Prewett, T., Wolf, D.A., Spaulding, G. (1993) Reduced shear stress: A major component in the ability of mammalian tissues to form three-dimensional assemblies in simulated microgravity. *Journal of Cellular Biochemistry*, 51(3),301-311.
181. Breslin, S., O'Driscoll, L. (2013) Three-dimensional cell culture: The missing link in drug discovery. *Drug discovery today*, 18(5-6),240-249.
182. Barrila, J., Radtke, A.L., Crabbé, A., Sarker, S.F., Herbst-Kralovetz, M.M., Ott, C.M., Nickerson, C.A. (2010) Organotypic 3d cell culture models: Using the rotating wall vessel to study host–pathogen interactions. *Nature Reviews Microbiology*, 8(11),791-801.
183. Verjans, E.T., Doijen, J., Luyten, W., Landuyt, B., Schoofs, L. (2018) Three-dimensional cell culture models for anticancer drug screening: Worth the effort? *Journal of Cellular Physiology*, 233(4),2993-3003.
184. Huda, Y.H., Md, Z.A.B.Z. (2013) Reproductive characteristics of the female laboratory rat. *African*

journal of biotechnology, 12(19),2510-2514.
185. 14, U.o.U.W.R.B.D.D.M., NISC Comparative Sequencing Program, N.G.E.D.B.R.W.B.G.G., de Jong, P.J., Osoegawa, K., Zhu, B., Marra, M., Schein, J., Bosdet, I., Fjell, C. (2004) Genome sequence of the brown norway rat yields insights into mammalian evolution. *Nature*, 428(6982),493-521.
186. GREVSTAD, H.J., SELVIG, K.A. (1982) Presence of enamel on the lingual surface of rabbit permanent incisors. *European journal of oral sciences*, 90(3),173-181.
187. Dammaschke, T. (2010) Rat molar teeth as a study model for direct pulp capping research in dentistry. *Laboratory Animals*, 44(1),1-6.
188. REITAN, K., KVAM, E. (1971) Comparative behavior of human and animal tissue during experimental tooth movement. *The Angle Orthodontist*, 41(1),1-14.
189. Ren, Y., Maltha, J.C., Kuijpers-Jagtman, A.M. (2004) The rat as a model for orthodontic tooth movement—a critical review and a proposed solution. *The European Journal of Orthodontics*, 26(5),483-490.
190. Khajuria, D.K., Razdan, R., Mahapatra, D.R. (2012) Description of a new method of ovariectomy in female rats. *Revista brasileira de reumatologia*, 52,466-470.
191. Franzen, T.J., Brudvik, P., Vandevska-Radunovic, V. (2013) Periodontal tissue reaction during orthodontic relapse in rat molars. *The European Journal of Orthodontics*, 35(2),152-159.
192. Franzen, T., Monjo, M., Rubert, M., Vandevska-Radunovic, V. (2014) Expression of bone markers and micro-ct analysis of alveolar bone during orthodontic relapse. *Orthodontics & Craniofacial Research*, 17(4),249-258.
193. Franzen, T.J., Zahra, S.E., El-Kadi, A., Vandevska-Radunovic, V. (2015) The influence of low-level laser on orthodontic relapse in rats. *European Journal of Orthodontics*, 37(1),111-117.
194. Matsuda, H., Borzabadi-Farahani, A., Le, B.T. (2016) Three-dimensional alveolar bone anatomy of the maxillary first molars: A cone-beam computed tomography study with implications for immediate implant placement. *Implant dentistry*, 25(3),367-372.
195. Asadi, Y., Gorjipour, F., Behrouzifar, S., Vakili, A. (2018) Irisin peptide protects brain against ischemic injury through reducing apoptosis and enhancing bdnf in a rodent model of stroke. *Neurochemical Research*, 43(8),1549-1560.
196. Wang, C., Cao, L., Yang, C., Fan, Y. (2018) A novel method to quantify longitudinal orthodontic bone changes with in vivo micro-ct data. *Journal of healthcare engineering*, 2018.
197. Ru, N., Liu, S.S.-Y., Zhuang, L., Li, S., Bai, Y. (2013) In vivo microcomputed tomography evaluation of rat alveolar bone and root resorption during orthodontic tooth movement. *The Angle Orthodontist*, 83(3),402-409.
198. Martín-Badosa, E., Amblard, D., Nuzzo, S., Elmoutaouakkil, A., Vico, L., Peyrin, F. (2003) Excised bone structures in mice: Imaging at three-dimensional synchrotron radiation micro ct. *Radiology*, 229(3),921-928.
199. Kirschneck, C., Proff, P., Fanghaenel, J., Behr, M., Wahlmann, U., Roemer, P. (2013) Differentiated analysis of orthodontic tooth movement in rats with an improved rat model and three-dimensional imaging. *Annals of Anatomy - Anatomischer Anzeiger*, 195(6),539-553.
200. Alzoughool, F., Al-Zghoul, M.B., Al-Nassan, S., Alanagreh, L.a., Mufleh, D., Atoum, M. (2020) The optimal therapeutic irisin dose intervention in animal model: A systematic review. *Veterinary World*, 13(10),2191.
201. King, G.J., Keeling, S.D., McCoy, E.A., Ward, T.H. (1991) Measuring dental drift and orthodontic tooth movement in response to various initial forces in adult rats. *American Journal of Orthodontics and*

Dentofacial Orthopedics, 99(5),456-465.
202. Shah, R., AlQuraini, N., Cunningham, S.J. (2019) Parents' perceptions of outcomes of orthodontic treatment in adolescent patients: A qualitative study. *European Journal of Orthodontics*, 41(3),301-307.
203. Jacob, F., Guertler, R., Naim, S., Nixdorf, S., Fedier, A., Hacker, N.F., Heinzelmann-Schwarz, V. (2013) Careful selection of reference genes is required for reliable performance of rt-qpcr in human normal and cancer cell lines. *PLoS One*, 8(3),e59180.
204. Piazza, V.G., Bartke, A., Miquet, J.G., Sotelo, A.I. (2017) Analysis of different approaches for the selection of reference genes in rt-qpcr experiments: A case study in skeletal muscle of growing mice. *International journal of molecular sciences*, 18(5),1060.
205. Panina, Y., Germond, A., Masui, S., Watanabe, T.M. (2018) Validation of common housekeeping genes as reference for qpcr gene expression analysis during ips reprogramming process. *Scientific Reports*, 8(1),1-8.
206. Cai, J., Li, T., Huang, B., Cheng, H., Ding, H., Dong, W., Xiao, M., Liu, L., Wang, Z. (2014) The use of laser microdissection in the identification of suitable reference genes for normalization of quantitative real-time pcr in human ffpe epithelial ovarian tissue samples. *PLoS One*, 9(4),e95974.
207. Aithal, M.G., Rajeswari, N. (2015) Validation of housekeeping genes for gene expression analysis in glioblastoma using quantitative real-time polymerase chain reaction. *Brain tumor research and treatment*, 3(1),24-29.
208. Irizarry, R.A., Bolstad, B.M., Collin, F., Cope, L.M., Hobbs, B., Speed, T.P. (2003) Summaries of affymetrix genechip probe level data. *Nucleic acids research*, 31(4),e15-e15.
209. Hosseini, S., Vázquez-Villegas, P., Rito-Palomares, M., Martinez-Chapa, S.O. (2018) Advantages, disadvantages and modifications of conventional elisa. *Enzyme-linked immunosorbent assay (ELISA): From A to Z*, 67-115.
210. Mikulskis, A., Yeung, D., Subramanyam, M., Amaravadi, L. (2011) Solution elisa as a platform of choice for development of robust, drug tolerant immunogenicity assays in support of drug development. *Journal of immunological methods*, 365(1-2),38-49.
211. Sakamoto, S., Putalun, W., Vimolmangkang, S., Phoolcharoen, W., Shoyama, Y., Tanaka, H., Morimoto, S. (2018) Enzyme-linked immunosorbent assay for the quantitative/qualitative analysis of plant secondary metabolites. *Journal of natural medicines*, 72(1),32-42.
212. Korta, P., Pocheć, E., Mazur-Biały, A. (2019) Irisin as a multifunctional protein: Implications for health and certain diseases. *Medicina*, 55(8),485.
213. Colaianni, G., Storlino, G., Sanesi, L., Colucci, S., Grano, M. (2020) Myokines and osteokines in the pathogenesis of muscle and bone diseases. *Current Osteoporosis Reports*, 18,401-407.
214. Albrecht, E*., et al.* (2015) Irisin–a myth rather than an exercise-inducible myokine. *Scientific Reports*, 5(1),8889.
215. Mountjoy, K.G. (2021) Elisa versus luminex assay for measuring mouse metabolic hormones and cytokines: Sharing the lessons i have learned. *Journal of Immunoassay and Immunochemistry*, 42(2),154-173.
216. Juncker, D., Bergeron, S., Laforte, V., Li, H. (2014) Cross-reactivity in antibody microarrays and multiplexed sandwich assays: Shedding light on the dark side of multiplexing. *Current opinion in chemical biology*, 18,29-37.
217. Centeno, E.G., Cimarosti, H., Bithell, A. (2018) 2d versus 3d human induced pluripotent stem cell-derived cultures for neurodegenerative disease modelling. *Molecular neurodegeneration*, 13(1),1-15.
218. Shin, J., Rhim, J., Kwon, Y., Choi, S.Y., Shin, S., Ha, C.-W., Lee, C. (2019) Comparative analysis

of differentially secreted proteins in serum-free and serum-containing media by using boncat and pulsed silac. *Scientific Reports*, 9(1),1-12.
219. Liu, K., Ostadhassan, M., Bubach, B. (2016) Applications of nano-indentation methods to estimate nanoscale mechanical properties of shale reservoir rocks. *Journal of Natural Gas Science and Engineering*, 35,1310-1319.
220. He, J., Zhang, Z., Kristiansen, H. (2009) Nanomechanical characterization of single micron-sized polymer particles. *Journal of Applied Polymer Science*, 113(3),1398-1405.
221. Webster, P., Webster, A. (2007) Cryosectioning fixed and cryoprotected biological material for immunocytochemistry. *Electron microscopy: Methods and Protocols*, 257-289.
222. Tran, H., Jan, N.-J., Hu, D., Voorhees, A., Schuman, J.S., Smith, M.A., Wollstein, G., Sigal, I.A. (2017) Formalin fixation and cryosectioning cause only minimal changes in shape or size of ocular tissues. *Scientific Reports*, 7(1),1-11.
223. Hira, V.V., de Jong, A.L., Ferro, K., Khurshed, M., Molenaar, R.J., Van Noorden, C.J. (2019) Comparison of different methodologies and cryostat versus paraffin sections for chromogenic immunohistochemistry. *Acta Histochemica*, 121(2),125-134.
224. Dey, P. (2022) Decalcification of bony and hard tissue for histopathology processing. *Basic and Advanced Laboratory Techniques in Histopathology and Cytology*, 35-40.
225. Savi, F.M., Brierly, G.I., Baldwin, J., Theodoropoulos, C., Woodruff, M.A. (2017) Comparison of different decalcification methods using rat mandibles as a model. *Journal of Histochemistry & Cytochemistry*, 65(12),705-722.
226. Mattuella, L.G., Bento, L.W., Vier-Pelisser, F.V., Araujo, F.B., Fossati, A.C.M. (2007) Comparative analysis of two fixating and two decalcifying solutions for processing of human primary teeth with inactive dentin carious lesion.
227. Bloch, W., Korkmaz, Y. (2005) Classical histological staining procedures in cardiovascular research. *Practical Methods in Cardiovascular Research*, 485-499.
228. GUSSEN, R., DONAHUE, D. (1965) Decalcification of temporal bones with tetrasodium edetate. *Archives of Otolaryngology*, 82(2),110-114.
229. Akkiraju, H., Bonor, J., Nohe, A. (2016) An improved immunostaining and imaging methodology to determine cell and protein distributions within the bone environment. *Journal of Histochemistry & Cytochemistry*, 64(3),168-178.
230. Im, K., Mareninov, S., Diaz, M., Yong, W.H. (2019) An introduction to performing immunofluorescence staining. *Biobanking*, 299-311.
231. Roelofs, A.J., De Bari, C. (2019) Immunostaining of skeletal tissues. *Bone Research Protocols*, 437-450.
232. Chestnut III, C. (1993) Bone mass and exercise. *The American Journal of Medicine*, 95(5),S34-S36.
233. Bosma, J. (1963) Oral and pharyngeal development and function. *Journal of Dental Research*, 42(1), 375-380.
234. Hiiemae, K.M., Palmer, J.B. (2003) Tongue movements in feeding and speech. *Critical Reviews in Oral Biology & Medicine*, 14(6), 413-429.
235. Meeran, N.A. (2012) Biological response at the cellular level within the periodontal ligament on application of orthodontic force–an update. *Journal of Orthodontic Science*, 1(1), 2.
236. Berkovitz, B.K. (2004) Periodontal ligament: Structural and clinical correlates. *Dental Update*, 31(1), 46-54.
237. Bodic, F., Hamel, L., Lerouxel, E., Baslé, M.F., Chappard, D. (2005) Bone loss and teeth. *Joint*

Bone Spine, 72(3), 215-221.
238. Di Benedetto, A., Gigante, I., Colucci, S., Grano, M. (2013) Periodontal disease: Linking the primary inflammation to bone loss. *Clinical and Developmental Immunology*, 2013.
239. Tanhaei, S., Nikpour, P., Ghaedi, K., Rabiee, F., Homayouni Moghadam, F., Nasr-Esfahani, M.H. (2018) Rna/protein discordant expression of fndc5 in central nervous system is likely to be mediated through micrornas. *DNA and Cell Biology*, 37(4), 373-380.
240. Kelly, D.P. (2012) Irisin, light my fire. *Science*, 336(6077), 42-43.
241. Huh, J.Y., Panagiotou, G., Mougios, V., Brinkoetter, M., Vamvini, M.T., Schneider, B.E., Mantzoros, C.S. (2012) Fndc5 and irisin in humans: I. Predictors of circulating concentrations in serum and plasma and ii. Mrna expression and circulating concentrations in response to weight loss and exercise. *Metabolism*, 61(12), 1725-1738.
242. Zhao, C., Wang, Y., Cao, Z., Zhu, J., He, H. (2022) Effect of irisin on the expression of osteoclast-related genes in cementoblasts. *European Journal of Orthodontics*, 44(4), 420-426.
243. Turkmen, E., Uzun, E.V., Bozaba, F., Balci, N., Toygar, H. (2023) Salivary irisin level is higher and related with interleukin-6 in generalized periodontitis. *Clinical Oral Investigations*, 1-8.
244. Amengual, J., García-Carrizo, F.J., Arreguín, A., Mušinović, H., Granados, N., Palou, A., Bonet, M.L., Ribot, J. (2018) Retinoic acid increases fatty acid oxidation and irisin expression in skeletal muscle cells and impacts irisin in vivo. *Cellular physiology and biochemistry*, 46(1), 187-202.
245. Pérez-Sotelo, D., Roca-Rivada, A., Baamonde, I., Baltar, J., Castro, A., Domínguez, E., Collado, M., Casanueva, F., Pardo, M. (2017) Lack of adipocyte-fndc5/irisin expression and secretion reduces thermogenesis and enhances adipogenesis. *Scientific Reports*, 7(1), 1-15.
246. Varela-Rodríguez, B.M., Pena-Bello, L., Juiz-Valiña, P., Vidal-Bretal, B., Cordido, F., Sangiao-Alvarellos, S. (2016) Fndc5 expression and circulating irisin levels are modified by diet and hormonal conditions in hypothalamus, adipose tissue and muscle. *Scientific Reports*, 6(1), 1-13.
247. Dimas, A.S.*, et al.* (2009) Common regulatory variation impacts gene expression in a cell type–dependent manner. *Science*, 325(5945), 1246-1250.
248. Zhang, Y.*, et al.* (2016) Irisin exerts dual effects on browning and adipogenesis of human white adipocytes. *American Journal of Physiology-Endocrinology and Metabolism*, 311(2), E530-E541.
249. Huh, J., Dincer, F., Mesfum, E., Mantzoros, C. (2014) Irisin stimulates muscle growth-related genes and regulates adipocyte differentiation and metabolism in humans. *International Journal of Obesity*, 38(12), 1538-1544.
250. Norheim, F.*, et al.* (2014) The effects of acute and chronic exercise on pgc-1α, irisin and browning of subcutaneous adipose tissue in humans. *The FEBS journal*, 281(3), 739-749.
251. Kurdiova, T.*, et al.* (2014) Effects of obesity, diabetes and exercise on fndc5 gene expression and irisin release in human skeletal muscle and adipose tissue: In vivo and in vitro studies. *The Journal of Physiology*, 592(5), 1091-1107.
252. Chen, S.-Q., Ding, L.-N., Zeng, N.-X., Liu, H.-M., Zheng, S.-H., Xu, J.-W., Li, R.-M. (2019) Icariin induces irisin/fndc5 expression in c2c12 cells via the ampk pathway. *Biomedicine & Pharmacotherapy*, 115, 108930.
253. Hosiriluck, N., Kashio, H., Takada, A., Mizuguchi, I., Arakawa, T. (2022) The profiling and analysis of gene expression in human periodontal ligament tissue and fibroblasts. *Clinical and Experimental Dental Research*, 8(3), 658-672.
254. Mahgoub, M.O., D'Souza, C., Al Darmaki, R.S., Baniyas, M.M., Adeghate, E. (2018) An update on the role of irisin in the regulation of endocrine and metabolic functions. *Peptides*, 104, 15-23.

255. Sumsuzzman, D.M., Jin, Y., Choi, J., Yu, J.-H., Lee, T.H., Hong, Y. (2019) Pathophysiological role of endogenous irisin against tumorigenesis and metastasis: Is it a potential biomarker and therapeutic? *Tumor Biology*, 41(12), 1010428319892790.
256. Colaianni, G., Grano, M. (2015) Role of irisin on the bone–muscle functional unit. *Bone Key Reports*, 4.
257. Krishnan, V., Davidovitch, Z. (2009) On a path to unfolding the biological mechanisms of orthodontic tooth movement. *Journal of Dental Research*, 88(7), 597-608.
258. Almpani, K., Kantarci, A. (2016) Nonsurgical methods for the acceleration of the orthodontic tooth movement. *Tooth Movement*, 18, 80-91.
259. Diravidamani, K., Sivalingam, S.K., Agarwal, V. (2012) Drugs influencing orthodontic tooth movement: An overall review. *Journal of pharmacy & bioallied sciences*, 4(Suppl 2), S299-S303.
260. Rygh, P., Bowling, K., Hovlandsdal, L., Williams, S. (1986) Activation of the vascular system: A main mediator of periodontal fiber remodeling in orthodontic tooth movement. *American Journal of Orthodontics*, 89(6), 453-468.
261. Saito, M., Saito, S., Ngan, P.W., Shanfeld, J., Davidovitch, Z. (1991) Interleukin 1 beta and prostaglandin e are involved in the response of periodontal cells to mechanical stress in vivo and in vitro. *American Journal of Orthodontics and Dentofacial Orthopedics*, 99(3), 226-240.
262. Kyrkanides, S., O'Banion, M.K., Subtelny, J.D. (2000) Nonsteroidal anti-inflammatory drugs in orthodontic tooth movement: Metalloproteinase activity and collagen synthesis by endothelial cells. *American Journal of Orthodontics and Dentofacial Orthopedics*, 118(2), 203-209.
263. Arias, O.R., Marquez-Orozco, M.C. (2006) Aspirin, acetaminophen, and ibuprofen: Their effects on orthodontic tooth movement. *American Journal of Orthodontics and Dentofacial Orthopedics*, 130(3), 364-370.
264. Askari, H., Rajani, S.F., Poorebrahim, M., Haghi-Aminjan, H., Raeis-Abdollahi, E., Abdollahi, M. (2018) A glance at the therapeutic potential of irisin against diseases involving inflammation, oxidative stress, and apoptosis: An introductory review. *Pharmacological Research*, 129, 44-55.
265. Mazur-Bialy, A.I., Pocheć, E., Zarawski, M. (2017) Anti-inflammatory properties of irisin, mediator of physical activity, are connected with tlr4/myd88 signaling pathway activation. *International Journal of Molecular Sciences*, 18(4), 701.
266. Ren, A., Lv, T., Kang, N., Zhao, B., Chen, Y., Bai, D. (2007) Rapid orthodontic tooth movement aided by alveolar surgery in beagles. *American Journal of Orthodontics and Dentofacial Orthopedics*, 131(2),160. e161-160. e110.
267. Kitaura, H., Kimura, K., Ishida, M., Sugisawa, H., Kohara, H., Yoshimatsu, M., Takano-Yamamoto, T. (2014) Effect of cytokines on osteoclast formation and bone resorption during mechanical force loading of the periodontal membrane. *The Scientific World Journal*, 2014.
268. Wiebe, S., Hafezi, M., Sandhu, H., Sims, S., Dixon, S. (1996) Osteoclast activation in inflammatory periodontal diseases. *Oral Diseases*, 2(2), 167-180.
269. Pereira, L.J., Andrade, E.F., Barroso, L.C., Lima, R.R.d., Macari, S., Paiva, S.M., Silva, T.A. (2022) Irisin effects on bone: Systematic review with meta-analysis of preclinical studies and prospects for oral health. *Brazilian Oral Research*, 36.
270. Madan, M.S., Liu, Z.J., Gu, G.M., King, G.J. (2007) Effects of human relaxin on orthodontic tooth movement and periodontal ligaments in rats. *American Journal of Orthodontics and Dentofacial Orthopedics*, 131(1),8. e1-8. e10.
271. Hou, N., Du, G., Han, F., Zhang, J., Jiao, X., Sun, X. (2017) Irisin regulates heme oxygenase-

1/adiponectin axis in perivascular adipose tissue and improves endothelial dysfunction in diet-induced obese mice. *Cellular Physiology and Biochemistry*, 42(2), 603-614.
272. Huang, H., Yang, R., Zhou, Y.-h. (2018) Mechanobiology of periodontal ligament stem cells in orthodontic tooth movement. *Stem Cells International*, 2018.
273. Brito, M.V., Pérez, M.A.Á., Rodríguez, F.J.M. (2013) Osteocalcin expression in periodontal ligament when inducing orthodontic forces. *Revista Odontológica Mexicana*, 17(3), 152-155.
274. Fang, T.D*., et al.* (2005) Angiogenesis is required for successful bone induction during distraction osteogenesis. *Journal of Bone and Mineral Research*, 20(7), 1114-1124.
275. Khuda, F., Anuar, N.N.M., Baharin, B., Nasruddin, N.S., Khuda, F., Anuar, N., Baharin, B., Nasruddin, N. (2021) A mini review on the associations of matrix metalloproteinases (mmps)-1,-8,-13 with periodontal disease. *AIMS Molecular Science*, 8, 13-31.
276. Sorsa, T., Tjäderhane, L., Konttinen, Y.T., Lauhio, A., Salo, T., Lee, H.M., Golub, L.M., Brown, D.L., Mäntylä, P. (2006) Matrix metalloproteinases: Contribution to pathogenesis, diagnosis and treatment of periodontal inflammation. *Annals of Medicine*, 38(5), 306-321.
277. Franco, C., Patricia, H.-R., Timo, S., Claudia, B., Marcela, H. (2017) Matrix metalloproteinases as regulators of periodontal inflammation. *International Journal of Molecular Sciences*, 18(2), 440.
278. Checchi, V., Maravic, T., Bellini, P., Generali, L., Consolo, U., Breschi, L., Mazzoni, A. (2020) The role of matrix metalloproteinases in periodontal disease. *International Journal of Environmental Research and Public Health*, 17(14), 4923.
279. Vadalà, G., Di Giacomo, G., Ambrosio, L., Cannata, F., Cicione, C., Papalia, R., Denaro, V. (2020) Irisin recovers osteoarthritic chondrocytes in vitro. *Cells*, 9(6).
280. Xi, R., Zheng, X., Tizzano, M. (2022) Role of taste receptors in innate immunity and oral health. *Journal of Dental Research*, 101(7), 759-768.
281. Chen, J.-G., Ping, N.-N., Liang, D., Li, M.-Y., Mi, Y.-N., Li, S., Cao, L., Cai, Y., Cao, Y.-X. (2017) The expression of bitter taste receptors in mesenteric, cerebral and omental arteries. *Life Sciences*, 170,16-24.
282. Kang, W., Wang, Y., Li, J., Xie, W., Zhao, D., Wu, L., Wang, H., Xie, S. (2022) Tas2r supports odontoblastic differentiation of human dental pulp stem cells in the inflammatory microenvironment. *Stem Cell Research & Therapy*, 13(1), 374.
283. Sharma, P., Yi, R., Nayak, A.P., Wang, N., Tang, F., Knight, M.J., Pan, S., Oliver, B., Deshpande, D.A. (2017) Bitter taste receptor agonists mitigate features of allergic asthma in mice. *Scientific Reports*, 7(1), 1-14.
284. Zhou, Y.-W*., et al.* (2022) Tas2r activation relaxes airway smooth muscle by release of gαt targeting on achr signaling. *Proceedings of the National Academy of Sciences*, 119(26), e2121513119.
285. Orsmark-Pietras, C*., et al.* (2013) Transcriptome analysis reveals upregulation of bitter taste receptors in severe asthmatics. *European Respiratory Journal*, 42(1), 65-78.
286. Grassin-Delyle, S., Salvator, H., Mantov, N., Abrial, C., Brollo, M., Faisy, C., Naline, E., Couderc, L.-J., Devillier, P. (2019) Bitter taste receptors (tas2rs) in human lung macrophages: Receptor expression and inhibitory effects of tas2r agonists. *Frontiers in Physiology*, 10, 1267.
287. Svitkina, T.M. (2018) Ultrastructure of the actin cytoskeleton. *Current Opinion in Cell Biology*, 54, 1-8.
288. Qin, Z., Fisher, G.J., Voorhees, J.J., Quan, T. (2018) Actin cytoskeleton assembly regulates collagen production via tgf-β type ii receptor in human skin fibroblasts. *Journal of Cellular and Molecular Medicine*, 22(9), 4085-4096.

289. Sadok, A., Marshall, C.J. (2014) Rho gtpases: Masters of cell migration. *Small GTPases*, 5, e29710-e29710.
290. Hall, A., Nobes, C.D. (2000) Rho gtpases: Molecular switches that control the organization and dynamics of the actin cytoskeleton. *Philosophical Transactions of the Royal Society of London Series B: Biological Sciences*, 355(1399), 965-970.
291. Kular, J.K., Basu, S., Sharma, R.I. (2014) The extracellular matrix: Structure, composition, age-related differences, tools for analysis and applications for tissue engineering. *Journal of Tissue Engineering*, 5, 2041731414557112.

I

Archives of Oral Biology 124 (2021) 105061

Contents lists available at ScienceDirect

Archives of Oral Biology

journal homepage: www.elsevier.com/locate/archoralbio

FNDC5/irisin is expressed and regulated differently in human periodontal ligament cells, dental pulp stem cells and osteoblasts

Yang Yang [a], Helen Pullisaar [b], Maria A. Landin [a], Catherine Anne Heyward [c], Maria Schröder [a], Tianxiang Geng [a], Maria Grano [d], Janne Elin Reseland [a,*]

[a] Department of Biomaterials, Faculty of Dentistry, University of Oslo, Oslo, Norway
[b] Department of Orthodontics, Faculty of Dentistry, University of Oslo, Oslo, Norway
[c] Oral Research Laboratory, Faculty of Dentistry, University of Oslo, Oslo, Norway
[d] Department of Emergency and Organ Transplantation, University of Bari, Bari, Italy

ARTICLE INFO

Keywords:
FNDC5
Irisin
Human periodontal ligament cell
Human dental pulp stem cell
Human osteoblast

ABSTRACT

Objective: To examine the expression and regulation of fibronectin type III domain-containing protein 5/irisin (FNDC5/irisin) in primary human periodontal ligament (hPDL) cells, dental pulp stem cells (hDPCs) and osteoblasts (hOBs).

Methods: FNDC5/irisin was identified in sections of paraffin embedded rat maxillae, cryo-sections of 3D cultured spheroids hPDL cells, hDPCs and hOBs, 2D cultured hPDL cells, hDPCs and hOBs by immunohistochemistry. The expression of FNDC5/irisin was identified by qPCR, followed by sequencing of the qPCR product. Regulation of FNDC5/irisin expression in hPDL cells, hDPCs and hOBs were evaluated after administration of different concentrations of irisin and all-trans retinoic acid (ATRA). qPCR and ELISA were used to identify expression and secretion of FNDC5/irisin in odontoblast-like differentiation of hDPCs.

Results: FNDC5/irisin was confirmed to be present in rat periodontium and dental pulp regions, as well as in 2D and 3D cultured hPDL cells, hDPCs and hOBs. BLAST analyses verified the generated nucleotide alignments matched human FNDC5/irisin. FNDC5/irisin gene expression was enhanced during odontoblast-like differentiation of hDPCs whereas the secretion of the protein was decreased compared to control. The protein signals in rat periodontal and pulpal tissues were higher than that of alveolar bone, and the expression of FNDC5/irisin was differently regulated by recombinant irisin and ATRA in hPDL cells and hDPCs compared to hOBs.

Conclusions: FNDC5/irisin expression was verified in rodent periodontium and dental pulp, and in hPDL cells, hDPCs and hOBs. The FNDC5/irisin expression was regulated by recombinant irisin and ATRA. Finally, expression and secretion of FNDC5/irisin were affected during odontoblast-like differentiation of hDPCs.

1. Introduction

Irisin is a newly identified polypeptide hormone that is proteolytically cleaved from its precursor fibronectin type III domain-containing protein 5 (FNDC5), released into circulation in response to physical activity, and identified to be present in skeletal muscle and blood plasma (Boström et al., 2012). The systematic location and expression of FNDC5/irisin in other human tissues was first comprehensively examined by Aydin et al., who identified FNDC5/irisin to be expressed in perimysium, endomysium, testis, pancreas, spleen, liver, brain, stomach and cardiac tissues. They also defined the nerve sheaths spreading within human skeletal muscles to be the main producers of FNDC5/irisin (Aydin, Kuloglu et al., 2014). Nonetheless, the expression of FNDC5/irisin within oral tissues has only been ascertained in 3 main salivary glands, which are parotid, sublingual and submandibular glands (Aydin, Aydin et al., 2014, 2013). The role of FNC5/irisin in these oral tissues remains unclear, however, *in vitro* studies have demonstrated that administration of recombinant irisin enhanced cell growth, migration and extracellular matrix deposition in both primary human periodontal ligament cells and osteoblasts (Pullisaar et al., 2019),

Abbreviations: hPDL cells, human periodontal ligament cells; hDPCs, human dental pulp stem cells; hOBs, human osteoblasts; FNDC5, fibronectin type III domain-containing protein 5; ATRA, all-trans retinoic acid.

* Corresponding author.
E-mail address: j.e.reseland@odont.uio.no (J.E. Reseland).

https://doi.org/10.1016/j.archoralbio.2021.105061
Received 31 July 2020; Received in revised form 2 January 2021; Accepted 10 January 2021
Available online 23 January 2021

whereas recombinant irisin was found to reduce proliferation and promote mineral deposition and differentiation of an immortalized mouse cementoblast cell line (Zhu et al., 2020). Hence, it would be of interest to investigate if FNDC5/irisin is expressed in oral tissues and cells supporting tooth attachment.

Periodontium is a sophisticated tooth-supporting apparatus composed of four important tissues - gingiva, cementum, alveolar bone and periodontal ligament (PDL) (Bartold, 1991). PDL is a connective tissue situated between tooth root cementum and alveolar bone, and is constantly exposed to mechanical stimuli from surrounding tissues and physiological functions such as mastication and speech (Ozaki, Kaneko, Podyma-Inoue, Yanagishita, & Soma, 2005). PDL together with cementum and alveolar bone form a dynamic and biomechanically active fibrous joint called bone-PDL-tooth complex, which comprises two adaptive functional interfaces, namely PDL-bone and PDL-cementum. When loaded, the mechanical load can stimulate PDL cells residing at the multiple sites of the complex to induce an array of biological events such as osteogenesis, osteoclastogenesis and inflammation (Feller et al., 2015; Lin et al., 2017). Based on the fact that FNDC5/irisin is activated in response to mechanical loading, we thus hypothesize that FNDC5/irisin is likely to be expressed in PDL cells because PDL is frequently subject to mechanical stimuli.

Dental pulp is a soft connective tissue located in a hard chamber consisting of dentine, enamel and cementum, and contains blood vessels, nerves and mesenchymal tissue, and is essential in tooth development and maintenance (Chalisserry, Nam, Park, & Anil, 2017). The dental pulp possesses a mesenchymal stem cell population, which is referred to as dental pulp stem cells (DPCs) (Nuti, Corallo, Chan, Ferrari, & Gerami-Naini, 2016). They have multi-lineage differentiation potential, and can differentiate towards osteoblasts, odontoblasts, adipocytes, chondrocytes and neural-like cells, which grant the DPCs a pivotal role in dental tissue regeneration (Nuti et al., 2016). Since FNDC5/irisin has been reported to be involved in neural and cardiomyocyte differentiation of mouse embryonic stem cells (Forouzanfar et al., 2015; Rabiee et al., 2014), we also speculate that FNDC5/irisin may be expressed in DPCs and involved in their differentiation.

Therefore, the primary aim of the present research is to study possible expression of FNDC5/irisin within rat periodontal ligament, dental pulp, alveolar bone, commercially available hPDL cells, hDPCs and hOBs. Further, to examine the regulation of FNDC5/irisin expression within these cells and clarify if odontoblast-like differentiation could affect FNDC5/irisin expression and secretion in hDPCs.

2. Materials and methods

2.1. Histology of oral tissues from rats

In order to verify the expression of irisin in rats' periodontal and dental pulp tissues, sections of the dental tissues around upper first molars of 3 male, 12-week-old Sprague-Dawley rats were used. The rat samples were acquired from a previous study and the preparation and embedding of the tissues are described elsewhere (Villa et al., 2015). The experiment was approved by the National Animal Research Authority, in accordance with the Animal Welfare Act of January 1, 2010, Section 13 and the Regulation on Animal Experimentation of January 15, 1996.

Tissues were sectioned into 5 μm-thickness bucco-lingual cross-section cuts parallel to the long axis of upper first molars and mounted onto glass slides. Tissue sections were deparaffinized, rehydrated and antigen-retrieved by heating in Tris-EDTA buffer (10 mM Tris base, 1 mM EDTA solution, 0.05 % Tween 20, PH 9.0) in a microwave oven for 10 min prior to immunofluorescence staining.

2.2. 2D cell culture

hPDL cells (Lonza, Walkersville, MD, USA) and hDPCs (Lonza, Walkersville, MD, USA) were cultured in Dulbecco's modified Eagle's medium (Sigma-Aldrich, Saint-Louis, Missouri, USA) supplemented with 200 mM GlutaMAX (Gibco, Thermo Fisher Scientific, Waltham, MA, USA), 10 % fetal bovine serum and 100 μg/mL penicillin/100 IU μg/mL streptomycin (Lonza, Allendale, NJ, USA) at 37 °C in a humid atmosphere of 5 % CO_2. The cells were used in passages 4–8.

Human osteoblasts (hOBs) (Lonza, Walkersville, MD, USA) were cultured in osteoblast culture medium supplemented with 10 % fetal bovine serum, 0.1 % gentamicin sulfate, amphotericin-B and ascorbic acid (Lonza, Walkersville, MD, USA) at 37 °C in a humid atmosphere of 5 % CO_2. The hOBs in passages 4–8 were used.

To test whether the expression of FNDC/irisin was regulated. hPDL cells, hDPCs and hOBs were seeded in 12-well culture plates at the density of 5×10^3 cells/cm^2, 3.5×10^3 cells/cm^2 and 6.0×10^3 cells/cm^2, respectively. At 80 % confluence, 10 ng/mL and 100 ng/mL of recombinant irisin (Adipogen, Liestal, Switzerland), or 1 μM and 10 μM of all-trans retinoic acid (ATRA) (Sigma-Aldrich, Saint-Louis, Missouri, USA) (Amengual et al., 2018) were administrated, respectively. The control groups for each of the treatment were incubated with equal volumes of sterile milliQ water (control for recombinant irisin) or DMSO (control for ATRA). The cells were maintained in a humidified incubator supplemented with 5 % CO_2 at 37 °C for 3 days prior to harvest and further analyses.

For immunofluorescence analysis, hPDL cells, hDPCs and hOBs were fixed in 4 % paraformaldehyde (PFA) for 15 min and preserved in PBS at 4 °C until use.

Dexamethasone (10^{-8} M; Sigma-Aldrich, Saint-Louis, Missouri, USA) was administrated to confluent hDPCs to induce differentiation towards odontoblast-like cells. The corresponding control cells received equal amounts of the diluent 0.1 % ethanol, without dexamethasone. Cells were cultured for 14 days, culture medium were refreshed 24 h before harvest and both mRNA and cell culture medium were collected at each time point (1, 3, 7 and 14 days) and stored at -80 °C prior to qPCR and ELISA analyses, respectively.

2.3. 3D cell culture

Spheroids were generated from approximately 6.5×10^6 hPDL cells, 4.6×10^6 hDPCs and 7.8×10^6 hOBs in individual disposable 10 mL vessel using the rotational 3D cell culture system from CelVivo (Blommenslyst, Denmark). The culture media was replaced every 3 days. After 14 days of 3D culture, spheroids of different sizes were generated, and the largest spheroids (diameter between 0.5–1 mm) were fixed in 4 % PFA for 30 min, transferred to PBS and stored at 4 °C prior to further analyses.

The fixed spheroids were embedded in optimal cutting temperature (OCT) compound (Leica, Buffalo Grove, IL, USA), and frozen at −20 °C. Serial sections of the spheroids (7 μm) were obtained using a CryoStar™ NX70 Cryostat (Thermo Fisher Scientific, Kalamazoo, MI, USA) and mounted onto glass slides and stored at −20 °C.

2.4. mRNA extraction

Dynabeads™ mRNA DIRECT™ Purification Kit (Thermo Fisher Scientific, Carlsbad, CA, USA) was used for mRNA extraction. Briefly, 2D cultured hPDL cells, hDPCs and hOBs were washed in cold PBS and lysed, and the mRNA was isolated using magnetic beads according to manufacturer's instructions. mRNA was separated from the beads by heat treatment (80 °C for 2 min) and quantified using a nano-drop spectrophotometer (ND-1000, Thermo Scientific, Wilmington, DE, USA, with software version 3.3.1.).

2.5. cDNA synthesis and qPCR

cDNA was synthesized using 2 μg of mRNA with first strand cDNA synthesis kit (Thermo Fisher Scientific, Waltham, MA, USA) according to

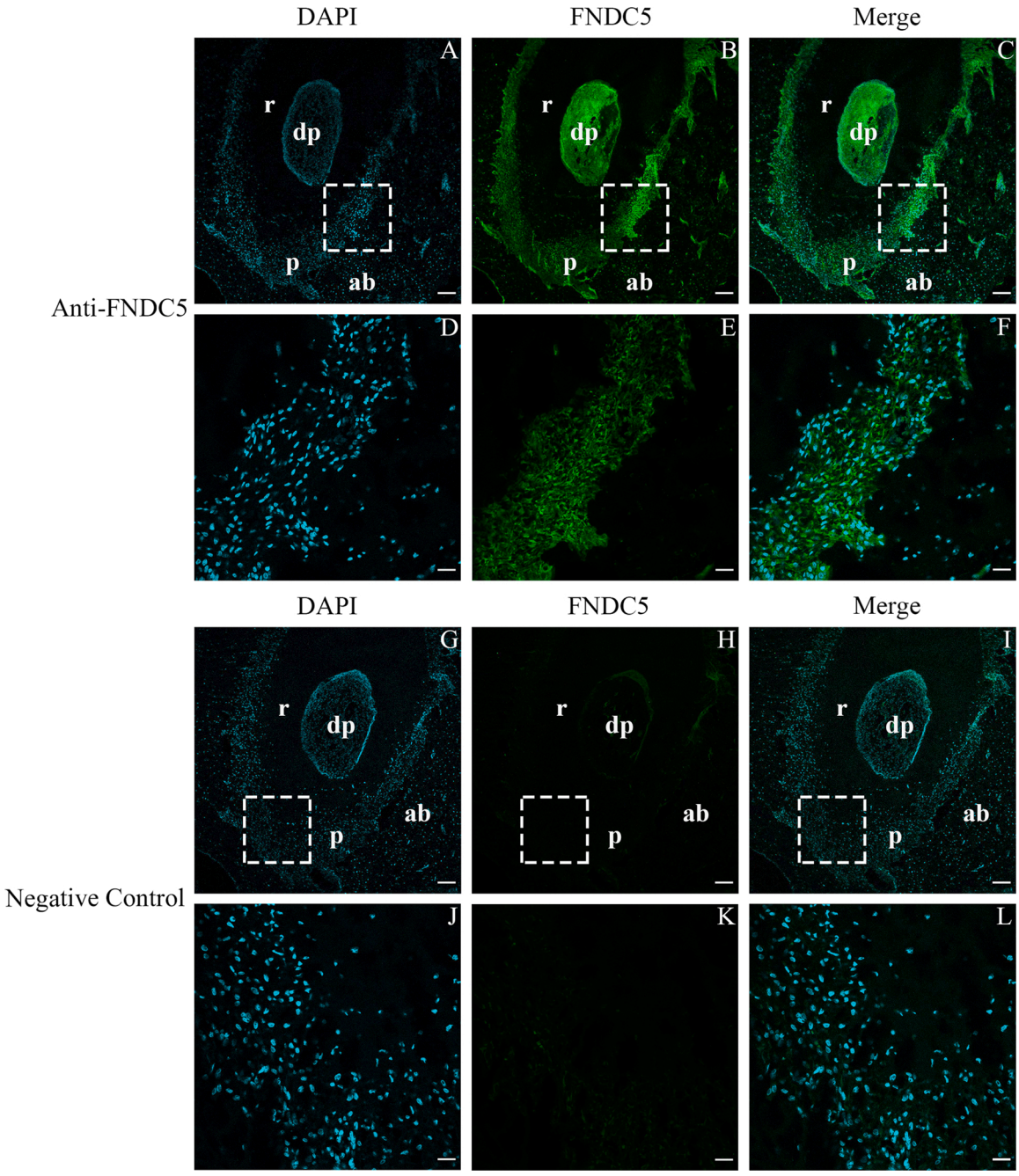

Fig. 1. Immunofluorescence detection of FNDC5 in rats' oral tissues. Histological sections of periodontium and dental pulp of upper first molars were analyzed by immunofluorescence staining for FNDC5 (B, C, E and F). Negative control was not treated with anti-FNDC5 primary antibody (H, I, K and L). Nuclei were counterstained with DAPI (A, C, D, F, G, I, J and L). Merged images of DAPI and FNDC5 are shown in C, F, I and L. The white boxed areas are shown at a higher magnification (D, E, F, J, K and L). The images are representative of the respective groups. Abbreviations: r for root, dp for dental pulp, p for periodontium, ab for alveolar bone. Scale bars in A, B, C, G, H and I represent 100 μm, scale bars in D, E, F, J, K and L represent 25 μm.

manufacturer's instructions. qPCR was conducted in a CFX384 TouchReal-Time PCR Detection System (Bio Rad, Hercules, California, USA) using IQ SYBR Green Supermix (Bio Rad, Hercules, California, USA) in a total volume of 20 μL (1 ng cDNA). The $^{\Delta\Delta}$Ct method (Livak & Schmittgen, 2001) was utilized to calculate the relative mRNA levels of the genes that were normalized to glyceraldehyde-3-phosphate dehydrogenase (GAPDH). The primers used for qPCR were synthesized by Invitrogen (Thermo Fisher Scientific, Carlsbad, CA, USA), and are as follows: GAPDH, forward 5′-CTCTGCTCCTCCTGTTCGAC-3′, reverse 5′-ACGACCAAATCCGTTGACTC-3′; FNDC5, forward 5′-CTCTCCACTG CCCCTTTCTG-3′, reverse 5′-GCAGATGTCCACCTCTTCCC-3′.

2.6. DNA -electrophoresis

DNA electrophoresis of the qPCR products were performed using the FlashGel System (Lonza, Allendale, NJ, USA) according to the producers' instructions. A mixture of 5 μL of DNA marker, 5 μL of qPCR products from 2D cultured hPDL cells, hDPCs and hOBs, and 1 μL of 6 X DNA loading dye (Thermo Fisher Scientific, Waltham, MA, USA) were loaded on a 2 % agarose Tris-acetate-EDTA (TAE) gel containing 0.01 % SYBR safe DNA gel stain (Thermo Fisher Scientific, Waltham, MA, USA). Images of the bands in the gels were captured through the built-in camera within the FlashGel System.

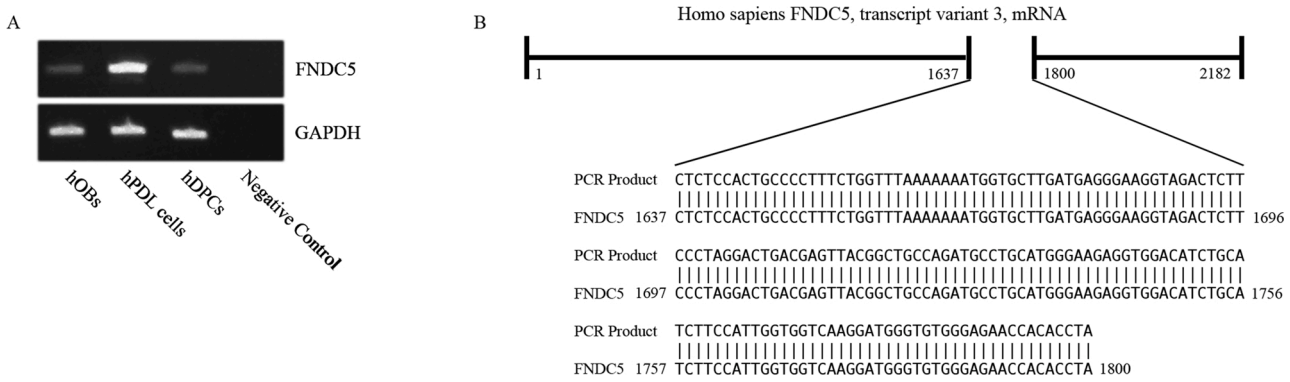

Fig. 2. Expression of FNDC5 in hPDL cells, hDPCs and hOBs. The images are representative of the respective groups. H_2O was used as negative control (A). The BLAST search and DNA sequencing analysis. The alignments of deduced amino acid sequences from hPDL cells qPCR products matched Homo sapiens FNDC5, transcript variant 3, mRNA sequence GenBank ID: NM_001171940.2, length: 2182, range: 1637 to 1800 (B).

2.7. Sequencing of PCR products

Aliquots (5 μl) of PCR product from 2D cultured hPDL cells were purified with 2 μl ExoSAP-IT Express PCR Cleanup Reagents (Thermo Fisher Scientific, Waltham, MA, USA), and diluted with DNAse-free water (1:5). The samples were sequenced at the MRC Protein Phosphorylation and Ubiquitylation Unit (MRC PPU) (School of Life Sciences, University of Dundee, Dundee, United Kingdom).

Analysis and identification of the matches were performed using a Basic Local Alignment Search Tool (BLAST) (https://blast.ncbi.nlm.nih.gov/Blast.cgi) (Altschul, Gish, Miller, Myers, & Lipman, 1990) in the National Center for Biotechnology Information nucleotide database (NCBI) (Coordinators, 2016)

2.8. Immunohistochemistry identification of FNDC5/irisin

The tissue sections around rats' upper molars, hPDL cells spheroids, hDPCs spheroids, hOBs spheroids, 2D cultured hPDL cells, hDPCs and hOBs were permeabilized with 0.1 % Triton X-100 (Sigma-Aldrich, Saint-Louis, Missouri, USA) in PBS for 5 min at room temperature. The samples were washed in PBS, blocked with 10 % normal goat serum (Abcam, Cambridge, United Kingdom) for 1 h prior to incubation with 1:200 diluted rabbit polyclonal anti-FNDC5 C-terminal antibody (ab181884; Abcam, Cambridge, United Kingdom) in 2 % normal goat serum overnight at 4 °C. For exclusion of the non-specific staining signals, negative control groups were incubated in 2 % normal goat serum without anti-FNDC5 antibody. On the following day, samples were washed 3 times in PBS and incubated with 1:500 diluted Alexa 488-conjugated goat anti-rabbit antibody (Invitrogen, Thermo Fisher Scientific, Carlsbad, CA, USA) in 4 % normal goat serum for 1 h in a humidified dark chamber at room temperature. The samples were washed 3 times in PBS, incubated with 300 nM 4′,6-diamidino-2-phenylindole (DAPI) (Sigma-Aldrich, Saint-Louis, Missouri, USA) for 20 min at room temperature, and covered by glass slips with Mowiol mounting medium made from Mowiol 4–88 (Sigma-Aldrich, Saint-Louis, Missouri, USA). Samples on the glass slides were kept in a dark chamber at room temperature until microscopic analysis.

FNDC5-expressing cells were imaged with Leica SP8 confocal microscope (Leica Microsystems CMS GmbH, Mannheim, Germany) using 405 nm and 488 nm excitation, and 420−480 nm and 500−550 nm emission filters for DAPI and Alexa Fluor 488, respectively. 3 images were captured for each group, the imaging settings were kept constant during individual assays.

2.9. ELISA assay

FNDC5/irisin secretion in hDPCs was quantified in culture media obtained after 1, 3, 7 and 14 days of culture by an FNDC5 ELISA Kit (Human): 96 Wells (Aviva Systems Biology, San Diego, CA, USA) following manufacturer's instructions. The plates were read at the wavelength of 450 nm using a spectrophotometer (BioTek, Winooski, USA), and the concentrations of FNDC5/irisin were determined by comparing the optical density (OD) values of the tested samples to that of the standard curve.

2.10. Statistics

All data obtained from qPCR and ELISA are presented as the mean ± standard deviation (SD). Statistical comparison between groups (control groups and treatment groups) was performed using unpaired Student's *t* tests as both normality tests and equality tests passed (SigmaPlot 14.0; Systat Software, San Jose, CA, USA). A probability of ≤ 0.05 was considered statistically significant. All experiments were performed in triplicates.

3. Results

3.1. FNDC5/irisin is expressed in rats' periodontium and dental pulp tissues and in hPDL cells, hDPCs and hOBs

A strong FNDC5/irisin immunofluorescence signal was detected both in rats' PDL (Fig. 1B, E, C, F) and dental pulp (Fig. 1B, C). However, only weak immunofluorescent signal was observed in the alveolar bone (Fig. 1B, C). The FNDC5/irisin immunofluorescent signal was found to be specific, as there was virtually no signal detectable from the negative control sample which lacked the primary antibody (Fig. 1H, I, K, L).

The PCR product corresponding to FNDC5/irisin was confirmed to be present in all tested cell types by DNA electrophoresis (Fig. 2A). Sequencing of the PCR product from hPDL cells revealed that the deduced sequence was identical to Homo sapiens fibronectin type III domain containing 5 (FNDC5), transcript variant 3 in GenBank (Accession number NM_001171940.2) (Fig. 2B).

The FNDC5/irisin protein was correspondingly identified in spheroids of hPDL cells (Fig. 3B, C, E, F), spheroids of hDPCs (Fig. 4B, C, E, F), spheroids of hOBs (Fig. 5B, C, E, F), 2D cultured hPDL cells (Fig. 6B and C), 2 D cultured hDPCs (Fig. 6H and I) and 2D cultured hOBs (Fig. 6N and O). Moreover, the intensity of the immunostained protein appeared to be localized in the cytoplasm of hPDL cells (Fig. 6B and C), hDPCs (Fig. 6H and I) and hOBs (Fig. 6N and O).

3.2. FNDC5/irisin expression is regulated in hPDL cells, hDPCs and hOBs

The potential autoregulation of the FNDC5/irisin expression was investigated by administration of recombinant human irisin, while

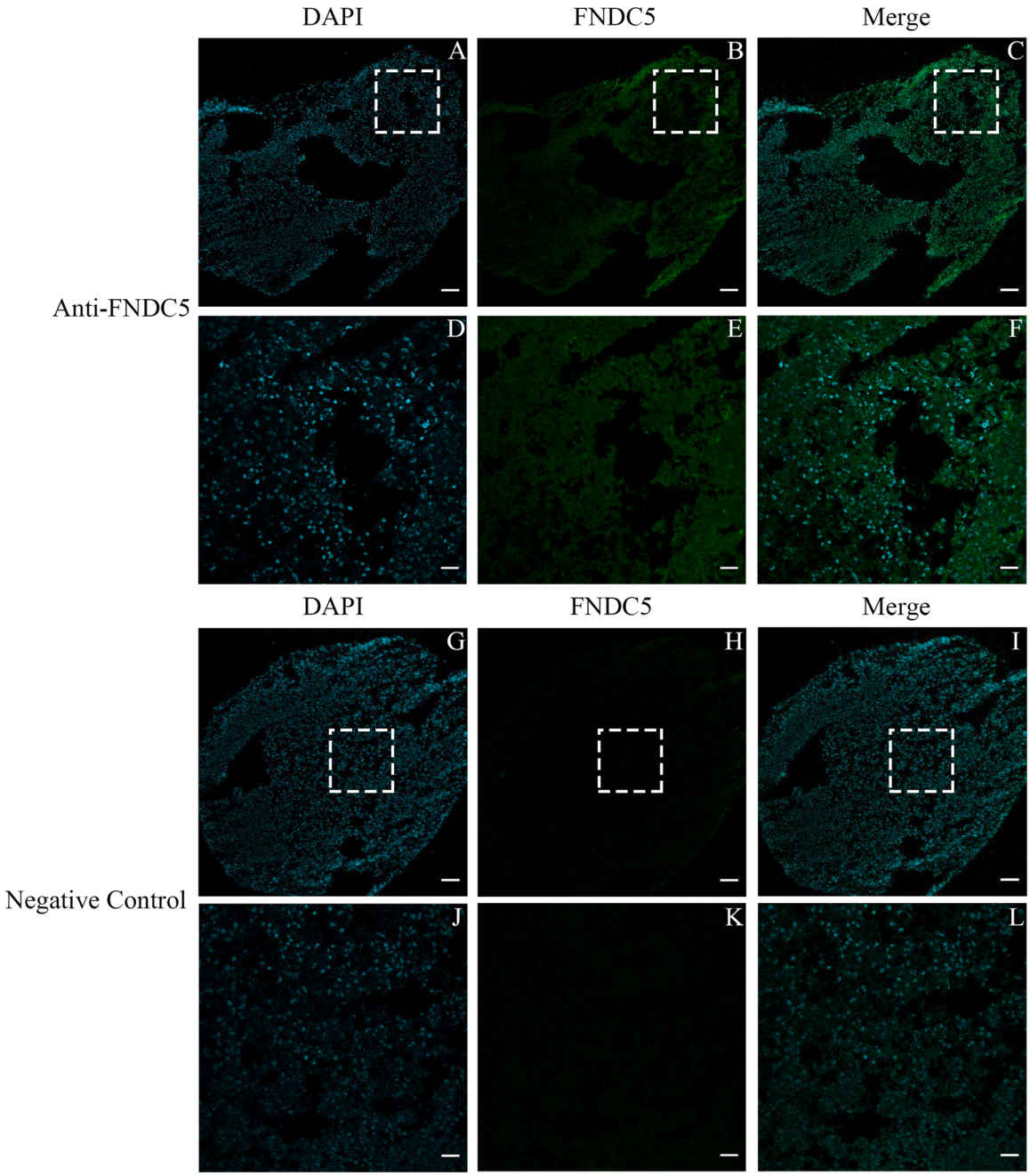

Fig. 3. Immunofluorescence detection of FNDC5/irisin in hPDL cell spheroids. Cryopreserved sections of spheroids were analyzed by immunofluorescence staining for FNDC5 (B, C, E and F), while negative control was not treated with anti-FNDC5 primary antibody (H, I, K and L). Nuclei were counterstained with DAPI (A, C, D, F, G, I, J and L). Merged images of DAPI and FNDC5 are shown in C, F, I and L. The white boxed areas are shown at a higher magnification (D, E, F, J, K and L). The images are representative of the respective groups. Scale bars in A, B, C, G, H and I represent 100 μm, scale bars in D, E, F, J, K and L represent 25 μm.

regulation was tested by administration of ATRA (Amengual et al., 2018) for 3 days. Both low and high concentrations of recombinant irisin significantly reduced FNDC5/irisin mRNA expression by 0.79 and 0.76 fold in hPDL cells compared to untreated control ($P = 0.008$ for 10 ng/mL, and $P = 0.014$ for 100 ng/mL) (Fig. 7A). Administration of ATRA significantly enhanced expression of FNDC5/irisin in hPDL cells by 2.8 ($P = 0.0003$ for 1 μM) and 1.7 fold ($P = 0.0002$ for 10 μM) compared to control (Fig. 7B).

Administration of the high dosage of recombinant irisin (100 ng/mL) significantly reduced expression of FNDC5/irisin ($P = 0.01$) by 0.5 fold in hDPCs compared to control, whereas the low dosage (10 ng/mL) had no effect ($P = 0.15$) (Fig. 7C). On the other hand, 1 μM ATRA enhanced FNDC5/irisin expression by approximately 3.1 fold ($P = 0.0004$) but the high dosage (10 μM) had no significant effect compared with control ($P = 0.25$) (Fig. 7D).

An inverse dose-dependent relationship was also observed in hOBs, where administration of 10 ng/mL recombinant irisin significantly enhanced the expression of FNDC5/irisin by nearly 4 fold in comparison to untreated control cells ($P = 0.01$), but 100 ng/mL did not affect the FNDC5/irisin mRNA expression ($P = 0.15$) (Fig. 7E). Both low and high concentrations of ATRA significantly decreased the FNDC5/irisin expression by 0.6 and 0.5n fold in hOBs ($P = 0.0008$ for 1 μM, and $P = 0.017$ for 10 μM) compared to control (Fig. 7F).

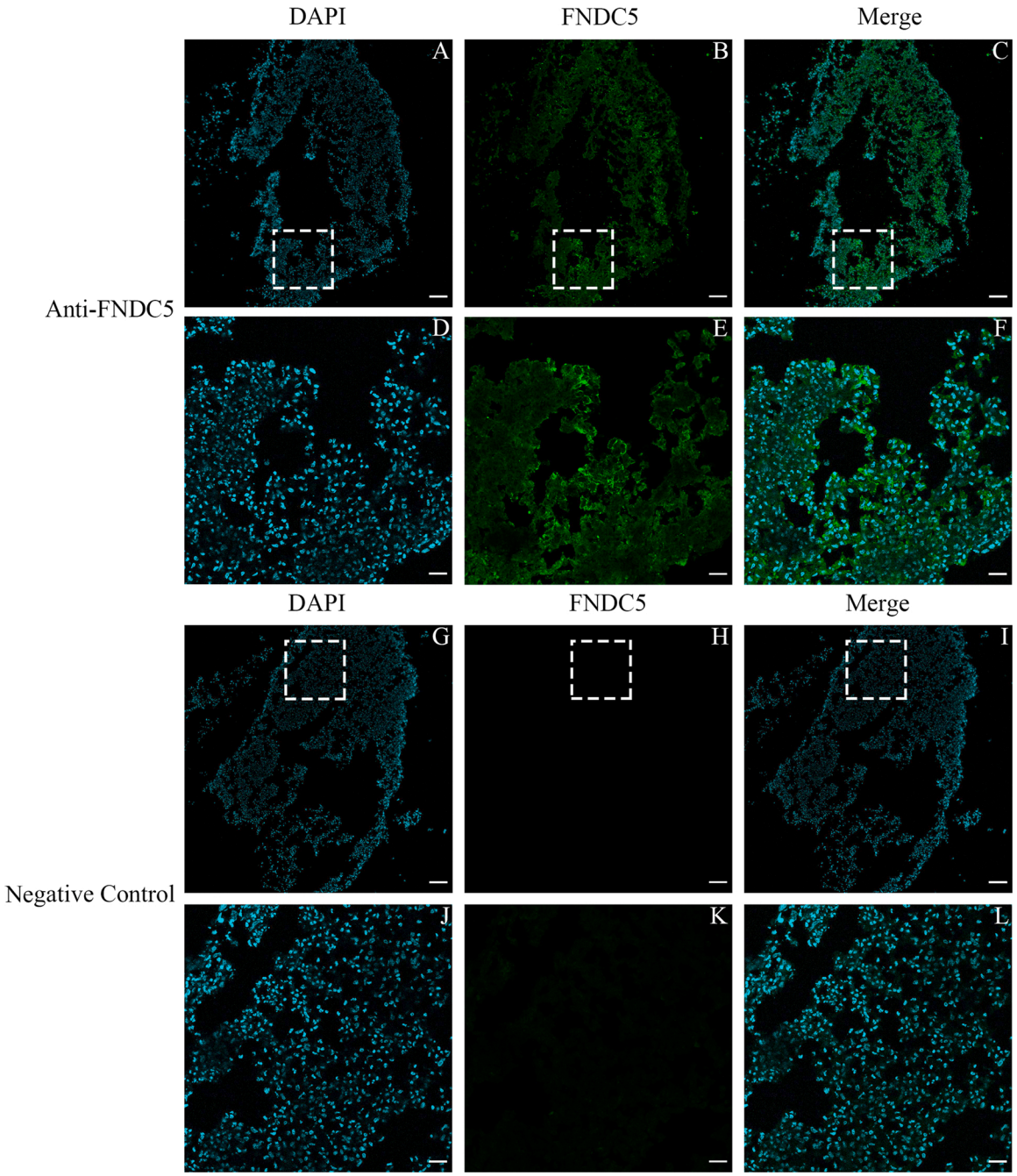

Fig. 4. Immunofluorescence detection of FNDC5/irisin in hDPCs spheroids. Cryopreserved sections of spheroids were analyzed by immunofluorescence staining for FNDC5 (B, E, C and F), while negative control was not treated with anti-FNDC5 primary antibody (H, I, K and L). Nuclei were counterstained with DAPI (A, C, D, F, G, I, J and L). Merged images of DAPI and FNDC5 are shown in C, F, I and L. The white boxed areas are shown at a higher magnification (D, E, F, J, K and L). The images are representative of the respective groups. Scale bars in A, B, C, G, H and I represent 100 μm, scale bars in D, E, F, J, K and L represent 25 μm.

3.3. The expression and secretion of FNDC5/irisin was affected by differentiation of hDPCs to odontoblast-like cells

The expression of FNDC5/irisin in hDPCs cultured with dexamethasone was significantly reduced by 0.22 fold at day 1 ($P = 0.007$) compared to control. At day 3, the expression of FNDC5/irisin was not different from control ($P = 0.17$), whereas the expression was significantly enhanced by 1.5 fold ($P = 0.0001$) at day 7 and 2.1 fold ($P = 0.0002$) at day14 compared to control (Fig. 8A). However, this enhancement of mRNA expression was not reflected in the levels of FNDC5/irisin secreted to cell culture medium over the same time period (Fig. 8B). No significant differences were observed at days 1, 3 and 7 ($P = 0.54$, $P = 0.15$, and $P = 0.69$, respectively), but at day 14 dexamethasone induced approximately 11 % decrease ($P = 0.017$) in the secretion of FNDC5/irisin compared to control (Fig. 8B).

4. Discussion

To the authors' best knowledge, the present research is the first to confirm that FNDC5/irisin is expressed in hPDL cells, hDPCs and hOBs. Moreover, a regulatory role of recombinant irisin and ATRA on FNDC5/irisin expression in hPDL cells and hDPCs was demonstrated. Finally, odontoblast-like differentiation of hDPCs might have an effect on the expression and secretion of FNDC5/irisin.

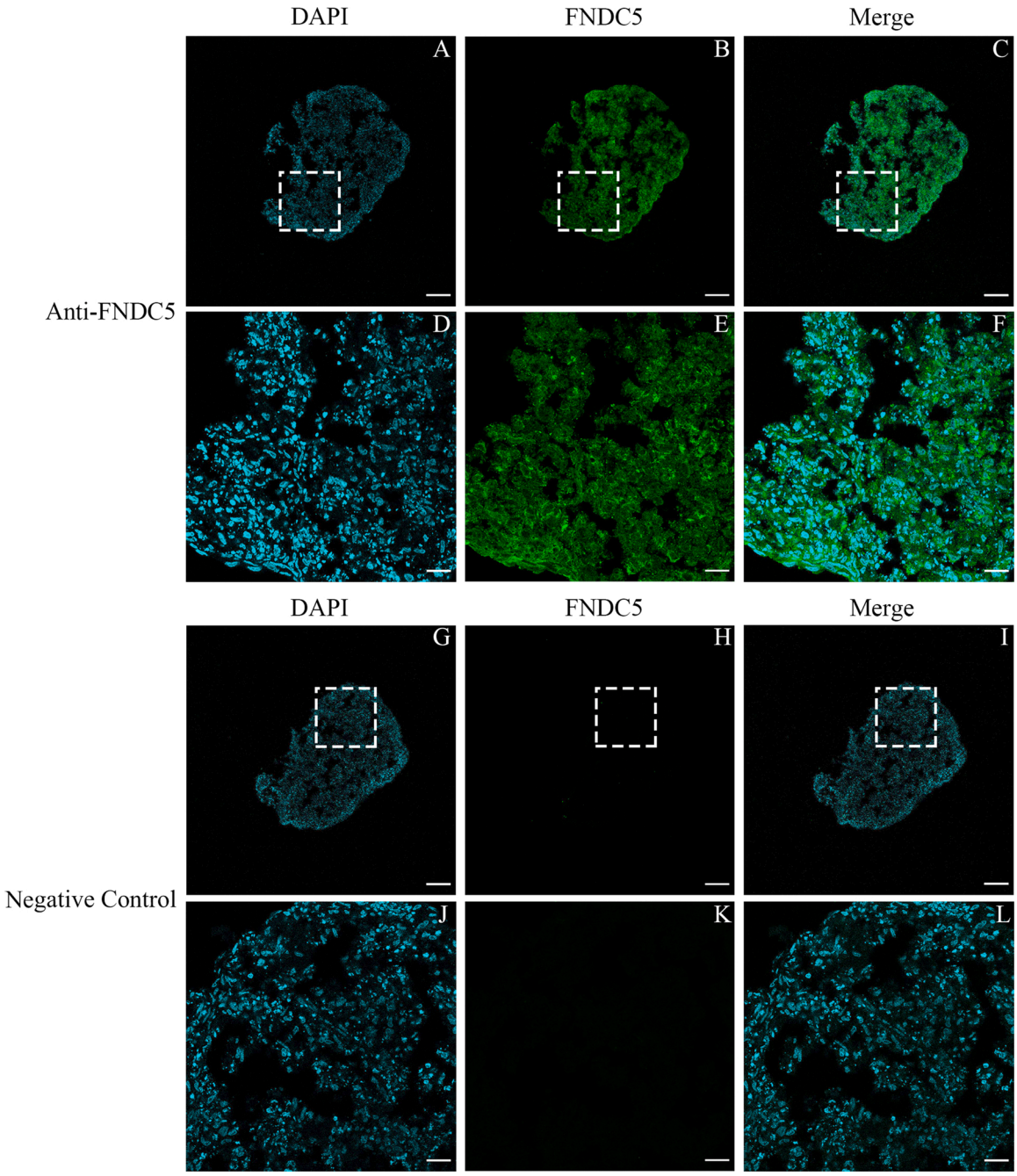

Fig. 5. Immunofluorescence detection of FNDC5/irisin in hOBs spheroids. Cryopreserved sections of spheroids were analyzed by immunofluorescence staining for FNDC5 (B, C, E and F), while negative control was not treated with anti-FNDC5 primary antibody (H, I, K and L). Nuclei were counterstained with DAPI (A, C, D, F, G, I, J and L). Merged images of DAPI and FNDC5 are shown in C, F, I and L. The white boxed areas are shown at a higher magnification (D, E, F, J, K and L). The images are representative of the respective groups. Scale bars in A, B, C, G, H and I represent 100 μm, scale bars in D, E, F, J, K and L represent 25 μm.

A FNDC5/irisin immunofluorescent signal was found in PDL tissues of rats. The sequence alignment of the amplified irisin product from hPDL cells matched with the human FNDC5 gene, which serves as evidence to confirm the expression of FNDC5/irisin in hPDL cells. According to Böstrom's study, FNDC5 comprises of a signal peptide, two fibronectin domains and one hydrophobic domain in structure (Boström et al., 2012). They found that the C-terminal region FNDC5 accumulated in cytoplasm, while the N-terminal region of FNDC5, which is termed as irisin, was proteolytically cleaved and released into circulation (Boström et al., 2012). Anti-FNDC5-C-terminal antibodies stained mainly the cytoplasm of 2D cultured hPDL cells, hDPCs and hOBs, which is in accordance with Boström et al.'s observations. Together with our previous findings suggesting that treatment with recombinant irisin enhanced both hPDL cells' and hOBs' growth, migration and osteogenic behavior (Pullisaar et al., 2019), the present findings could indicate that the FNDC5/irisin may play a role in periodontal regeneration.

Irisin is the first myokine that has been reported to be involved in mechano-transduction and could be regulated by mechanical stress (Boström et al., 2012; Kawao, Moritake, Tatsumi, & Kaji, 2018). In addition, irisin is released into blood in response to physical exercise and may have peripheral effects on various tissues (Varela-Rodríguez et al., 2016) as well as autocrine effect on skeletal muscles (Colaianni, Brunetti, Colucci, & Grano, 2018). It is widely accepted that high bone mass and strengthened bones can be achieved by physical activities, on the

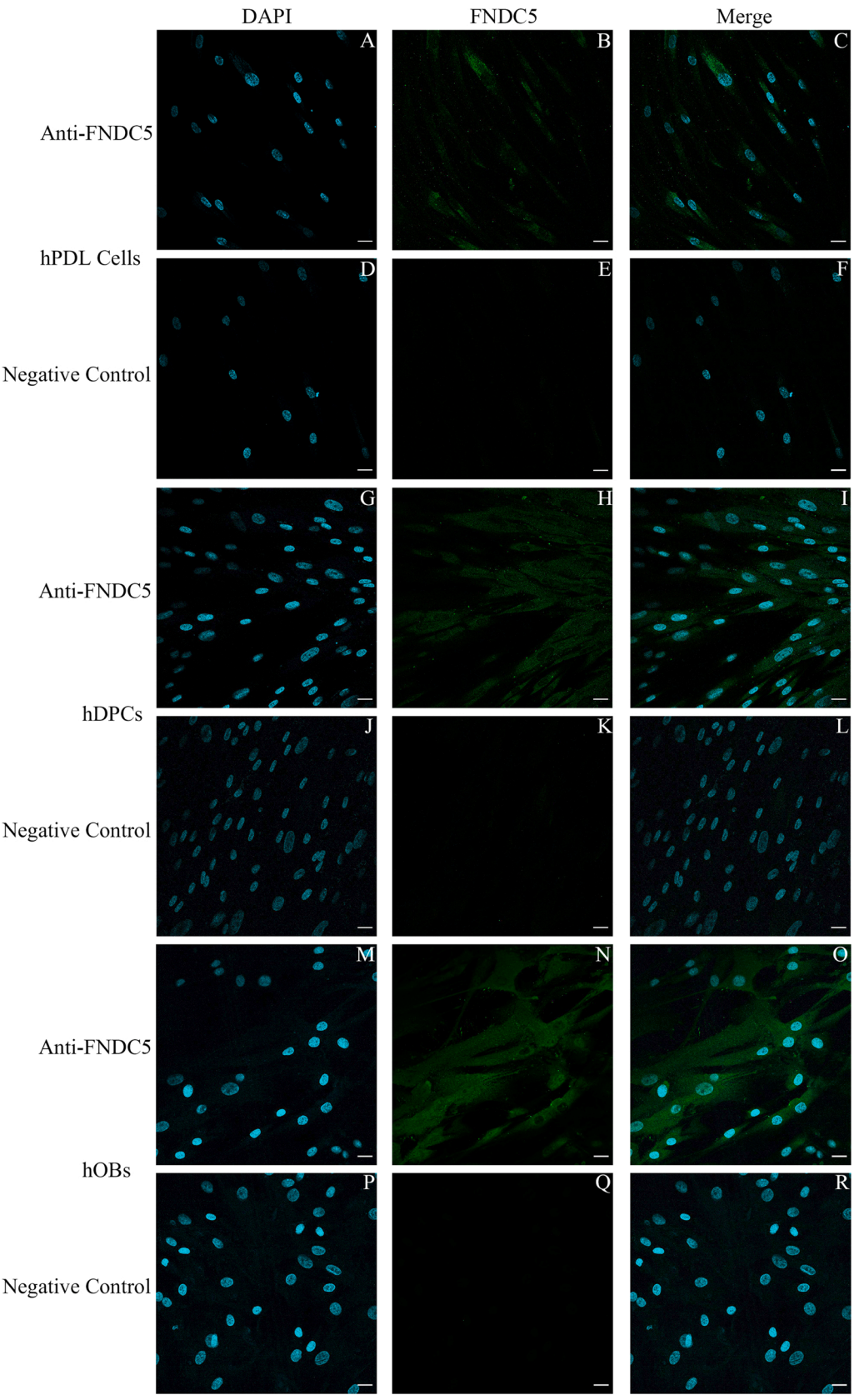

Fig. 6. Immunofluorescence detection of FNDC5/irisin in 2D cultured hPDL cells, hDPCs and hOBs. Cells were immunolabeled with anti-FNDC5 primary antibody (B, C, H, I, N and O), while negative control was not treated with primary anti-FNDC5 antibody (E, F, K, L, Q and R). Nuclei were counterstained with DAPI (A, C, D, F, G, I, J, L, M, O, P and R). Merged images of DAPI and FNDC5 are shown in C, F, I, L, O and R. The images are representative of the respective groups. Scale bar represents 25 μm.

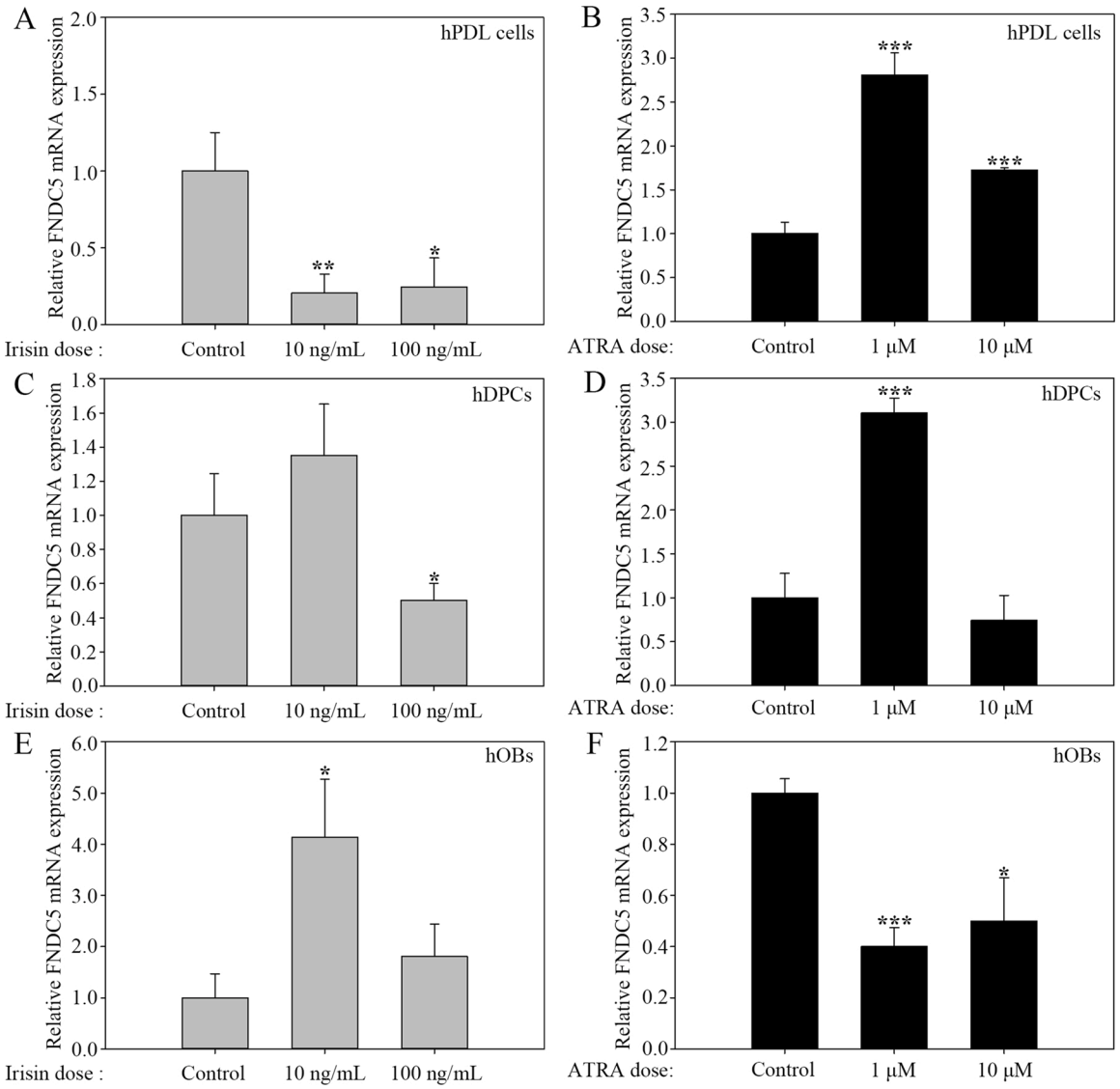

Fig. 7. mRNA expression levels of FNDC5/irisin in hPDL cells, hDPCs and hOBs treated with or without recombinant irisin (10 ng/mL, 100 ng/mL) and ATRA (1 μM, 10 μM). The relative mRNA expression levels of irisin were normalized to GAPDH. (*) $P < 0.05$; (**) $P < 0.01$; (***) $P < 0.001$ *vs* control group. All data present mean ± SD of 3 independent experiments.

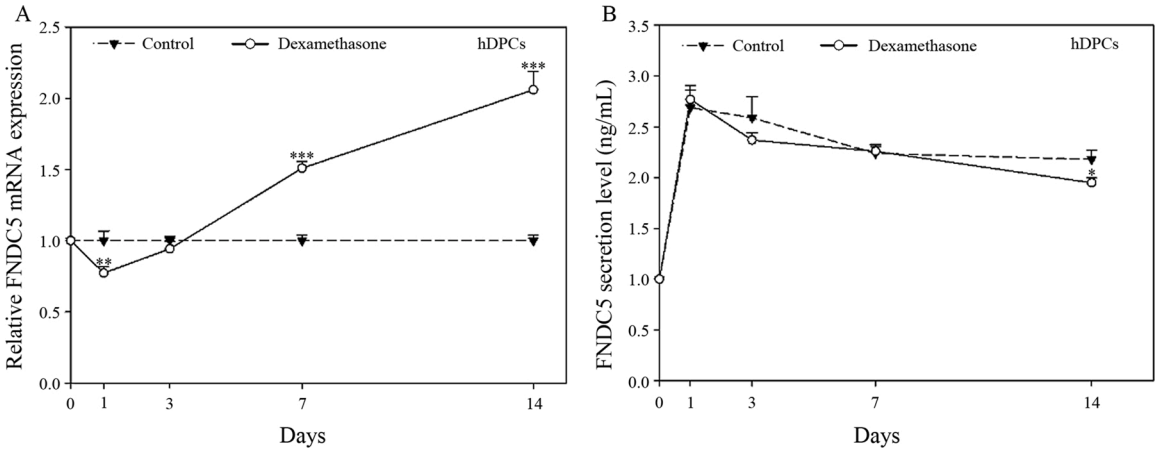

Fig. 8. Expression and secretion of FNDC5/irisin during odontoblast-like differentiation of hDPCs. (A) The mRNA expression levels of FNDC5/irisin from hDPCs over a 14-day odontoblast-like differentiation period. The expression was normalized to GAPDH, (**) $P < 0.01$; (***) $P < 0.001$ *vs* control group. (B) The secretion levels of FNDC5/irisin from hDPCs over a 14-day odontoblast-like differentiation period. (*) $P < 0.05$ *vs* control group. All data present mean ± SD of 3 independent experiments.

other hand, lack of physical activities or disuse of muscles result in severe bone loss (Chestnut, 1993; Colaianni et al., 2014). Likewise, healthy PDL helps to maintain bone mass of the tooth-supporting alveolar bone, whereas diseased periodontal tissues or loss of teeth will cause loss of load, thus resulting in irreversible bone resorption (Berkovitz, 2004; Bodic, Hamel, Lerouxel, Basle, & Chappard, 2005; Di Benedetto, Gigante, Colucci, & Grano, 2013). Therefore, PDL is situated in an environment that resembles that of skeletal muscles. Based on our results that both hPDL cells and rats' PDL sections expressed FNDC5/irisin, we can speculate that FNDC5/irisin expression may be regulated in response to mechanical stimuli of PDL.

In addition to a strong immunofluorescent signal from PDL, FNDC5/irisin was identified to be present in the rat pulp region and to lesser degree in the alveolar bone. We verified these findings by demonstrating that FNDC5/irisin was expressed in 3D spheroids generated from primary hPDL cells, hDPCs and hOBs, mimicking *in vivo* microenvironments (Fontoura et al., 2020; Schröder et al., 2020) as well as in 2D cultured cells. To the authors' knowledge, this is the first demonstration of FNDC5/irisin expression in 3D cultured cells *in vitro*. 2D monolayer cell culturing is the most common culture method, resulting in a homogeneous cell environment that is easy to control, analyze and sustain the ability to proliferate for most types of cells. However, cells are not generally considered to be kept in the natural microenvironment under such circumstances (Fennema, Rivron, Rouwkema, van Blitterswijk, & de Boer, 2013). 3D cultures provide cellular heterogeneity, nutrient and oxygen gradients, cell to cell interactions and matrix deposition so that the *in vivo* environment can be simulated *in vitro* and cells can be induced to behave in a natural environment (Ravi, Paramesh, Kaviya, Anuradha, & Solomon, 2015).

The FNDC5/irisin immunofluorescent signal was barely detected in rat alveolar bone. Preceding research has reported that irisin levels are positively correlated with bone mineral density (BMD) (Singhal et al., 2014; Wu et al., 2018). However, the rat samples in our study were obtained from the tissues around the molars located in the posterior maxilla, which contains lower BMD compared to anterior maxilla and mandible (Devlin, Horner, & Ledgerton, 1998). Moreover, positive correlations between irisin and BMD at different anatomical sites have also been reported (Colaianni et al., 2017), and can thus partly explain our observation. It has been demonstrated previously that murine bone tissues express FNDC5 (Zhang et al., 2017) and that recombinant irisin has a positive effect on proliferation and differentiation of osteoblasts *in vitro* (Pullisaar et al., 2019). However, our study is the first to confirm the expression of FNDC5/irisin in primary human osteoblasts.

To date, the molecular regulation of FNDC5/irisin expression remains largely unknown. FNDC5 is one of the target proteins for peroxisome proliferator-activated receptor-gamma coactivator 1 alpha (PGC-1α), and Boström et al. reported that the expression of PGC-1α stimulated the FNDC5 expression and the secretion of irisin (Boström et al., 2012). Administration of ATRA has been found to induce PGC-1α expression in differentiated 3T3-L1 adipocytes (Mercader et al., 2007) and enhance the gene expression of FNDC5 in C2C12 mouse myoblasts (Abedi-Taleb et al., 2019). We found that ATRA enhanced the expression of FNDC5/irisin in both hPDL cells and hDPCs. However, it attenuated the FNDC5/irisin expression in hOBs. Treatment with recombinant irisin reduced the FNDC5/irisin expression in hPDL cells and hDPCs, while it enhanced the FNDC5/irisin expression in hOBs. The converse effects of recombinant irisin and ATRA on hPDL cells and hDPCs *versus* hOBs in our study may be due to a cell type-specific effect of recombinant irisin and ATRA on the regulation of FNDC5/irisin expression.

Over the past years hDPCs have received broad attention in oral tissue engineering and regeneration owing to their ability to differentiate towards several cell types (Nuti et al., 2016). Dexamethasone treatment has been found to induce odontoblast-like differentiation of hDPCs as evidenced by enhanced expression of alkaline phosphatase (ALP), the major odontoblastic maker dentin sialophosphoprotein, reduced proliferation and enhanced mineralization (Alliot-Licht et al., 2005; Lim et al., 2016; Moretti, Duailibi, Martins, Santos, & Duailibi, 2017). In our study, we found the mRNA expression of FNDC5/irisin to be gradually enhanced in a time-dependent manner over a 14-day period of dexamethasone-induced odontoblast-like differentiation. Conversely, the secretion of FNDC5/irisin was found to be slightly reduced at day 14. Such lack of correlation between the change in FNDC5/irisin mRNA expression and protein secretion has previously been reported. (Roca-Rivada et al., 2013; Tian et al., 2004). Irisin, the secreted form of FNDC5, is proteolytically cleaved and released in response to physical stimulation. It is likely that while treatment with dexamethasone induced an enhanced mRNA expression of FNDC5/irisin in hDPCs, the translation and cleavage of irisin from FNDC5 and thus secretion from hDPCs was not affected.

In conclusion, FNDC5/irisin is expressed in hPDL cells, hDPCs, hOBs, rat PDL and rat dental pulp tissues. Further, FNDC5/irisin production and/or secretion from hPDL cells, hDPCs and hOBs is regulated, indicating that FNDC5/irisin may have autocrine, paracrine and endocrine effects in oral and bone tissues. Finally, the induced odontoblast-like differentiation of hDPCs appeared to affect both expression and secretion of FNDC5/irisin.

Authors' contributions

The conception and experimental design: YY, HP, MG, JER
Supervision: HP, JER
Performance of experiments: YY, MAL, CAH, MS, TXG
Analysis and interpretation of data: YY, HP, MAL, CAH, JER
Manuscript drafting and revision: YY, HP, MAL, CAH, MS, TXG, MG, JER
Final approval of the submitted version: YY, HP, MAL, CAH, MS, TXG, MG, JER

Declaration of Competing Interest

The authors declare that they have no known competing financial interests or personal relationships that could have appeared to influence the work reported in this paper.

Acknowledgments

This work was supported by the Research Council of Norway (project 287953) and Yang Yang (CSC number 201908420242) would like to thank China Scholarship Council (CSC) for personal grant.

References

Abedi-Taleb, E., Vahabi, Z., Sekhavati-Moghadam, E., Khedmat, L., Jazayeri, S., & Saboor-Yaraghi, A. A. (2019). Upregulation of FNDC5 gene expression in C2C12 cells after single and combined treatments of resveratrol and ATRA. *Lipids in Health and Disease, 18*(1), 181. https://doi.org/10.1186/s12944-019-1128-y

Alliot-Licht, B., Bluteau, G., Magne, D., Lopez-Cazaux, S., Lieubeau, B., Daculsi, G., … Guicheux, J. (2005). Dexamethasone stimulates differentiation of odontoblast-like cells in human dental pulp cultures. *Cell and Tissue Research, 321*(3), 391–400. https://doi.org/10.1007/s00441-005-1115-7

Altschul, S. F., Gish, W., Miller, W., Myers, E. W., & Lipman, D. J. (1990). Basic local alignment search tool. *Journal of Molecular Biology, 215*(3), 403–410. https://doi.org/10.1016/s0022-2836(05)80360-2

Amengual, J., Garcia-Carrizo, F. J., Arreguin, A., Musinovic, H., Granados, N., Palou, A., … Ribot, J. (2018). Retinoic acid increases fatty acid oxidation and irisin expression in skeletal muscle cells and impacts Irisin in vivo. *Cellular Physiology and Biochemistry, 46*(1), 187–202. https://doi.org/10.1159/000488422

Aydin, S., Aydin, S., Kuloglu, T., Yilmaz, M., Kalayci, M., Sahin, I., … Cicek, D. (2013). Alterations of irisin concentrations in saliva and serum of obese and normal-weight subjects, before and after 45 min of a Turkish bath or running. *Peptides, 50*, 13–18. https://doi.org/10.1016/j.peptides.2013.09.011

Aydin, S., Aydin, S., Kobat, M. A., Kalayci, M., Eren, M. N., Yilmaz, M., … Baydas, A. (2014). Decreased saliva/serum irisin concentrations in the acute myocardial infarction promising for being a new candidate biomarker for diagnosis of this pathology. *Peptides, 56*, 141–145. https://doi.org/10.1016/j.peptides.2014.04.002

Aydin, S., Kuloglu, T., Aydin, S., Kalayci, M., Yilmaz, M., Cakmak, T., … Ozercan, I. H. (2014). A comprehensive immunohistochemical examination of the distribution of

the fat-burning protein irisin in biological tissues. *Peptides, 61*, 130–136. https://doi.org/10.1016/j.peptides.2014.09.014
Bartold, P. M. (1991). Connective tissues of the periodontium. Research and clinical implications. *Australian Dental Journal, 36*(4), 255–268. https://doi.org/10.1111/j.1834-7819.1991.tb00720.x
Berkovitz, B. K. B. (2004). Periodontal ligament: Structural and clinical correlates. *Dental Update, 31*(1), 46–54. https://doi.org/10.12968/denu.2004.31.1.46
Bodic, F., Hamel, L., Lerouxel, E., Basle, M. F., & Chappard, D. (2005). Bone loss and teeth. *Joint, Bone, Spine, 72*(3), 215–221. https://doi.org/10.1016/j.jbspin.2004.03.007
Boström, P., Wu, J., Jedrychowski, M. P., Korde, A., Ye, L., Lo, J. C., … Spiegelman, B. M. (2012). A PGC1-alpha-dependent myokine that drives brown-fat-like development of white fat and thermogenesis. *Nature, 481*(7382), 463–468. https://doi.org/10.1038/nature10777
Chalisserry, E. P., Nam, S. Y., Park, S. H., & Anil, S. (2017). Therapeutic potential of dental stem cells. *Journal of Tissue Engineering, 8*. https://doi.org/10.1177/2041731417702531, 2041731417702531.
Chestnut, C. H. (1993). Bone mass and exercise. *The American Journal of Medicine, 95*(5, Supplement 1), S34–S36. https://doi.org/10.1016/0002-9343(93)90379-4
Colaianni, G., Brunetti, G., Colucci, S. C., & Grano, M. (2018). Myokine—Irisin—And its effects linking bone and muscle function. *Clinical Reviews in Bone and Mineral Metabolism, 16*(1), 16–21. https://doi.org/10.1007/s12018-017-9240-x
Colaianni, G., Cuscito, C., Mongelli, T., Oranger, A., Mori, G., Brunetti, G., … Grano, M. (2014). Irisin enhances osteoblast differentiation in vitro. *International Journal of Endocrinology, 2014*, Article 902186. https://doi.org/10.1155/2014/902186
Colaianni, G., Notarnicola, A., Sanesi, L., Brunetti, G., Lippo, L., Celi, M., … Grano, M. (2017). Irisin levels correlate with bone mineral density in soccer players. *Journal of Biological Regulators and Homeostatic Agents, 31*(4 suppl 1), 21–28.
Coordinators, N. R. (2016). Database resources of the national center for biotechnology information. *Nucleic Acids Research, 44*(D1), D7–D19. https://doi.org/10.1093/nar/gkv1290
Devlin, H., Horner, K., & Ledgerton, D. (1998). A comparison of maxillary and mandibular bone mineral densities. *The Journal of Prosthetic Dentistry, 79*(3), 323–327. https://doi.org/10.1016/S0022-3913(98)70245-8
Di Benedetto, A., Gigante, I., Colucci, S., & Grano, M. (2013). Periodontal disease: Linking the primary inflammation to bone loss. *Clinical & Developmental Immunology, 2013*, Article 503754. https://doi.org/10.1155/2013/503754
Feller, L., Khammissa, R. A. G., Schechter, I., Thomadakis, G., Fourie, J., & Lemmer, J. (2015). Biological events in periodontal ligament and alveolar bone associated with application of orthodontic forces. *The Scientific World Journal, 2015*, Article 876509. https://doi.org/10.1155/2015/876509
Fennema, E., Rivron, N., Rouwkema, J., van Blitterswijk, C., & de Boer, J. (2013). Spheroid culture as a tool for creating 3D complex tissues. *Trends in Biotechnology, 31*(2), 108–115. https://doi.org/10.1016/j.tibtech.2012.12.003
Fontoura, J. C., Viezzer, C., dos Santos, F. G., Ligabue, R. A., Weinlich, R., Puga, R. D., … Bonorino, C. (2020). Comparison of 2D and 3D cell culture models for cell growth, gene expression and drug resistance. *Materials Science and Engineering C, 107*, Article 110264. https://doi.org/10.1016/j.msec.2019.110264
Forouzanfar, M., Rabiee, F., Ghaedi, K., Beheshti, S., Tanhaei, S., Shoaraye Nejati, A., … Nasr-Esfahani, M. H. (2015). Fndc5 overexpression facilitated neural differentiation of mouse embryonic stem cells. *Cell Biology International, 39*(5), 629–637. https://doi.org/10.1002/cbin.10427
Kawao, N., Moritake, A., Tatsumi, K., & Kaji, H. (2018). Roles of Irisin in the linkage from muscle to bone during mechanical unloading in mice. *Calcified Tissue International, 103*(1), 24–34. https://doi.org/10.1007/s00223-018-0387-3
Lim, H. C., Nam, O. H., Kim, M. J., El-Fiqi, A., Yun, H. M., Lee, Y. M., … Kim, E. C. (2016). Delivery of dexamethasone from bioactive nanofiber matrices stimulates odontogenesis of human dental pulp cells through integrin/BMP/mTOR signaling pathways. *International Journal of Nanomedicine, 11*, 2557–2567. https://doi.org/10.2147/IJN.S97846
Lin, J. D., Jang, A. T., Kurylo, M. P., Hurng, J., Yang, F., Yang, L., … Ho, S. P. (2017). Periodontal ligament entheses and their adaptive role in the context of dentoalveolar joint function. *Dental Materials, 33*(6), 650–666. https://doi.org/10.1016/j.dental.2017.03.007
Livak, K. J., & Schmittgen, T. D. (2001). Analysis of relative gene expression data using real-time quantitative PCR and the 2(-Delta Delta C(T)) Method. *Methods, 25*(4), 402–408. https://doi.org/10.1006/meth.2001.1262
Mercader, J., Madsen, L., Felipe, F., Palou, A., Kristiansen, K., & Bonet, L. (2007). All-trans retinoic acid increases oxidative metabolism in mature adipocytes. *Cellular Physiology and Biochemistry, 20*(6), 1061–1072. https://doi.org/10.1159/000110717
Moretti, R.d. C., Duailibi, M. T., Martins, P. O., Santos, J. A.d., & Duailibi, S. E. (2017). Osteoinductive effects of preoperative dexamethasone in human dental pulp stem cells primary culture. *Future Science OA, 3*(3), FSO184. https://doi.org/10.4155/fsoa-2016-0083
Nuti, N., Corallo, C., Chan, B. M., Ferrari, M., & Gerami-Naini, B. (2016). Multipotent differentiation of human dental pulp stem cells: A literature review. *Stem Cell Reviews and Reports, 12*(5), 511–523. https://doi.org/10.1007/s12015-016-9661-9
Ozaki, S., Kaneko, S., Podyma-Inoue, K. A., Yanagishita, M., & Soma, K. (2005). Modulation of extracellular matrix synthesis and alkaline phosphatase activity of periodontal ligament cells by mechanical stress. *Journal of Periodontal Research Supplement, 40*(2), 110–117. https://doi.org/10.1111/j.1600-0765.2004.00782.x
Pullisaar, H., Colaianni, G., Lian, A. M., Vandevska-Radunovic, V., Grano, M., & Reseland, J. E. (2019). Irisin promotes growth, migration and matrix formation in human periodontal ligament cells. *Archives of Oral Biology, 111*, Article 104635. https://doi.org/10.1016/j.archoralbio.2019.104635
Rabiee, F., Forouzanfar, M., Ghazvini Zadegan, F., Tanhaei, S., Ghaedi, K., Motovali Bashi, M., … Nasr-Esfahani, M. H. (2014). Induced expression of Fndc5 significantly increased cardiomyocyte differentiation rate of mouse embryonic stem cells. *Gene, 551*(2), 127–137. https://doi.org/10.1016/j.gene.2014.08.045
Ravi, M., Paramesh, V., Kaviya, S. R., Anuradha, E., & Solomon, F. D. (2015). 3D cell culture systems: Advantages and applications. *Journal of Cellular Physiology, 230*(1), 16–26. https://doi.org/10.1002/jcp.24683
Roca-Rivada, A., Castelao, C., Senin, L. L., Landrove, M. O., Baltar, J., Belen Crujeiras, A., … Pardo, M. (2013). FNDC5/irisin is not only a myokine but also an adipokine. *PloS One, 8*(4), e60563. https://doi.org/10.1371/journal.pone.0060563
Schröder, M., Riksen, E. A., He, J., Skallerud, B. H., Møller, M. E., Lian, A.-M., … Reseland, J. E. (2020). Vitamin K2 modulates vitamin D-induced mechanical properties of human 3D bone spheroids in vitro. *JBMR Plus, 4*(9), e10394. https://doi.org/10.1002/jbm4.10394
Singhal, V., Lawson, E., Ackerman, K., Fazeli, P., Clarke, H., Lee, H., … Misra, M. (2014). Irisin levels are lower in young amenorrheic athletes compared with eumenorrheic athletes and non-athletes and are associated with bone density and strength estimates. *PloS One, 9*(6), Article e100218. https://doi.org/10.1371/journal.pone.0100218
Tian, Q., Stepaniants, S. B., Mao, M., Weng, L., Feetham, M. C., Doyle, M. J., … Hood, L. E. (2004). Integrated genomic and proteomic analyses of gene expression in mammalian cells. *Molecular & Cellular Proteomics, 3*(10), 960. https://doi.org/10.1074/mcp.M400055-MCP200
Varela-Rodríguez, B. M., Pena-Bello, L., Juiz-Valiña, P., Vidal-Bretal, B., Cordido, F., & Sangiao-Alvarellos, S. (2016). FNDC5 expression and circulating irisin levels are modified by diet and hormonal conditions in hypothalamus, adipose tissue and muscle. *Scientific Reports, 6*(1), 29898. https://doi.org/10.1038/srep29898
Villa, O., Wohlfahrt, J. C., Mdla, I., Petzold, C., Reseland, J. E., Snead, M. L., … Lyngstadaas, S. P. (2015). Proline-rich peptide mimics effects of enamel matrix derivative on rat oral mucosa incisional wound healing. *The Journal of Periodontology, 86*(12), 1386–1395. https://doi.org/10.1902/jop.2015.150207
Wu, L. F., Zhu, D. C., Tang, C. H., Ge, B., Shi, J., Wang, B. H., … Lei, S. F. (2018). Association of plasma Irisin with bone mineral density in a large Chinese population using an extreme sampling design. *Calcified Tissue International, 103*(3), 246–251. https://doi.org/10.1007/s00223-018-0415-3
Zhang, J., Valverde, P., Zhu, X., Murray, D., Wu, Y., Yu, L., … Chen, J. (2017). Exercise-induced irisin in bone and systemic irisin administration reveal new regulatory mechanisms of bone metabolism. *Bone Research, 5*, 16056. https://doi.org/10.1038/boneres.2016.56
Zhu, J., Wang, Y., Cao, Z., Du, M., Hao, Y., Pan, J., … He, H. (2020). Irisin promotes cementoblast differentiation via p38 MAPK pathway. *Oral Diseases, 26*(5), 974–982. https://doi.org/10.1111/odi.13307

II

Irisin reduces orthodontic tooth movement in rats by promoting the osteogenic potential in the periodontal ligament

Yang Yang[1], Helen Pullisaar[2], Astrid Kamilla Stunes[3,4], Liebert Parreiras Nogueira[5], Unni Syversen[3,6], Janne Elin Reseland[1]

[1]Department of Biomaterials, Faculty of Dentistry, University of Oslo, Oslo, Norway

[2]Department of Orthodontics, Faculty of Dentistry, University of Oslo, Oslo, Norway

[3]Department of Clinical and Molecular Medicine, Norwegian University of Science and Technology (NTNU), Trondheim, Norway

[4]Center for Oral Health Services and Research, Mid-Norway (TkMidt), Trondheim, Norway

[5]Oral Research Laboratory, Faculty of Dentistry, University of Oslo, Oslo, Norway

[6]Department of Endocrinology, Clinic of Medicine, St. Olavs University Hospital, 7030 Trondheim, Norway

Summary

Objectives

Positive effects of irisin on osteogenic differentiation of periodontal ligament (PDL) cells have been identified previously, this study aims to examine its effect on orthodontic tooth movement (OTM) *in vivo*.

Materials and methods

The maxillary right first molars of male Wistar rats (n=21) were moved mesially for 14 days, with submucosal injection of two dosages of irisin (0.1 or 1 μg) or PBS (control) every third day. OTM was recorded by feeler gauge and micro-computed tomography (μCT). Alveolar bone and root volume were analyzed using μCT, and plasma irisin levels by ELISA. Histological characteristics of PDL tissues were examined, and the expression of collagen type I, periostin, osteocalcin (OCN), von Willebrand factor (vWF) and fibronectin type III domain-containing protein 5 (FNDC5) in PDL was evaluated by immunofluorescence staining.

Results

Repeated 1 μg irisin injections suppressed OTM on days 6, 9 and 12. No significant differences were observed in OTM in the 0.1 μg irisin group, or in bone morphometric parameters, root volume or plasma irisin, compared to control. Resorption lacunae and hyalinization were found at the PDL-bone interface on the compression side in the control, whereas they were scarce after irisin administration. The expression of collagen type I, periostin, OCN, vWF and FNDC5 in PDL was enhanced by irisin administration.

Limitations

The feeler gauge method may overestimate OTM.

Conclusions

Submucosal irisin injection reduced OTM by enhancing osteogenic potential of PDL, and this effect was more significant on the compression side.

Key words: periodontal ligament, orthodontic tooth movement, irisin, FNDC5, osteogenesis

Introduction

The periodontal ligament (PDL) is an aligned fibrous tissue between the root cementum and the alveolar bone that anchors the tooth and maintains the structural integrity of these mineralized tissues (1). PDL is continuously exposed to physiological mechanical stimuli induced by occlusal forces (2). Furthermore, during orthodontic tooth movement (OTM), remodeling of PDL, alveolar bone, dental pulp, and gingiva occur in response to mechanical loading (3, 4). The orthodontic forces create strain in cells and their surrounding extracellular matrix (ECM), triggering a series of mechanical, chemical, and cellular events, which lead to structural alterations and eventually tooth movement (5). Several chemical substances, such as nonsteroidal anti-inflammatory drugs (NSAIDs) (6), vitamin D (7), adiponectin (8), epidermal growth factor (9), bisphosphonates (10), and fluorides (11) affect this process by interacting with local cells, and thus working in concert with orthodontic forces and exerting inhibitory, additive or synergistic effects on OTM (12, 13).

Irisin is a hormone, which is secreted as a product of fibronectin type III domain-containing protein 5 (FNDC5) from skeletal muscle in response to physical activity (14). Other than its main role in energy metabolism (14), irisin is involved in several other biological functions such as bone homeostasis (15), tumor occurrence and development (16). Beneficial effects of irisin on cells from dental, periodontal and bone tissues were demonstrated previously. Irisin exerts a positive effect on differentiation, mineralization and proliferation of cementoblasts (17). Irisin also promotes odontogenic differentiation, mineralization and angiogenesis in human dental pulp cells, and thus may provide odontogenic and angiogenic effects needed for dental pulp regeneration and healing, as well as in facilitating dentine formation (18). Recently, it was demonstrated that irisin promoted osteogenic differentiation of dental bub-derived mesenchymal stem cells by increasing osteocalcin (OCN) expression (19). For periodontal tissues, recombinant irisin enhanced migration, growth and osteogenic behavior of hPDL cells (20). Further, irisin may accelerate the osteogenic/cementogenic differentiation of hPDL cells partially via p38 signaling pathway (21). Most studies demonstrate a stimulatory effect of irisin on bone formation (15, 22-24). Injection of irisin at a cumulative weekly dose profoundly increased cortical bone mass and strength in mice (22). In addition to irisin's bone

anabolic effect through enhanced osteoblast differentiation, it also exhibits bone catabolic effect through inhibitory effect on osteoclast activation (15).

Based on previous observations, we aim to study the effects of local injection of irisin on the rate of experimental OTM; moreover, analyze the bone morphometric parameters and root volume near the injection site; lastly, compare the protein expression of certain osteogenic and ECM markers in stretched and compressed PDL tissues around mesial roots of maxillary right first molars. This study may elucidate the potential mechanism by which local injection of irisin affects the rate of OTM in murine models.

Materials and methods

Ethics statements

All of the animal experiments in this study were approved by the Norwegian Animal Research Authority (NARA, FOTS ID 25785), and all experimental procedures were performed in accordance with the Animal Welfare Act and under the guidance of ARRIVE guidelines (Animal Research: Reporting of *In Vivo* Experiments).

Animals

Eight-week-old male Wistar rats (n=21), weighing between 286 g and 356 g, were kept in ventilated cages (IVC), with four or three animals per cage, and under 12 h light/dark cycles and standardized conditions. The rats were provided with *ad libitum* access to rat and mouse diet (B&K Universal Ltd, Aldbrough, Hull, UK) along with tap water. All the animals were acclimatized for one week prior to initiation of the experiments.

Experimental design

A split mouth design was used, with the right side of the maxilla as the experimental side and the contralateral side as an internal control, as described previously (25). A closed coil spring (0.008 × 0.030 inches; Ormco, CA, USA) was ligated to the first molar and the eyelet of a modified incisor band, and activated once with approximately 0.5 N force according to a previous

study (8), which resulted in a mesial movement of the maxillary first molar during the experimental period of 14 days (Figure 1A). The force magnitude was measured with a Correx dynamometer (Haag-Streit, Bern, Switzerland).

The animals were consecutively numbered 1 to 21 and randomly assigned using the "RandomNo" function in Microsoft Excel (Microsoft Corporation, https://office.microsoft.com/excel) into three groups (control (phosphate buffered saline (PBS)), 0.1 µg irisin and 1 µg irisin, respectively), each of seven animals. There was no difference in average body weight between the 3 groups. On days 3, 6, 9 and 12 of OTM, solutions of recombinant human irisin (Adipogen, Liestal, Switzerland) dissolved in PBS or plain PBS solution were administered by submucosal injection mesiopalatally to the maxillary right first molars. The experimental groups received 10 µl of either 10 µg/ml irisin (0.1 µg) or 100 µg/ml irisin (1 µg) solutions, whilst the control group received 10 µl of PBS. The animals were anesthetized with ketamine-xylazine (ketamine 50 mg/ml, xylazine 20 mg/ml) given subcutaneously along with isoflurane gas (1 % isoflurane mixed with 30 % O_2/70 % N_2O) prior to orthodontic appliance installation at day 0, and the animals were anesthetized with isoflurane gas during injection at days 3, 6, 9 and 12. At the end of the experiment, all animals were sacrificed by cardiac puncture under the anesthesia via inhalation of isoflurane gas, followed by collection of blood samples.

A feeler gauge (Mitutoyo Co., Kawasaki, Japan) with a minimum measurable distance of 50 µm was used to measure tooth movement between the distal surface of the first molar and the mesial surface of the second molar at days 3, 6, 9, 12, and 14. The animal weights were recorded on the day of orthodontic appliance insertion, during injection at days 3, 6, 9, 12, and prior to sacrifice. After 14 days, blood samples were collected by cardiac puncture during the final anesthesia before the animals were sacrificed. The animals were decapitated, and the heads were stored in 70 % ethanol until further use. The experimental setup is presented in Figure 1B.

Micro-computed tomography (µCT)

The µCT analyses were performed at the end of the experimental OTM at day 14. The orthodontic appliances were removed and the whole maxillae including first, second, and third molars together with the surrounding soft tissues were dissected and further fixed in 4 % formaldehyde (VWR, Radnor, PA, USA) for 48 hours at 4 °C. The dissected rat maxillae were individually wrapped in damp gauze and placed into closed tubes for scanning. The specimens were scanned in a multiscale Skyscan 2211 (Bruker, Belgium) microtomography system, at a voxel size of 10 µm, 60 kV, 60 µA, over 360º with a rotation step of 0.37º and 130 ms exposure time per frame, averaging 4 frames per projection. Tomograms were reconstructed using filtered back-projection at NRecon (v. 1.7.4.6, Bruker).

The scans were aligned in the frontal/coronal (C) plane using the mid-palatal suture. The third molar was defined as a fixed reference point, and at this specific point the transversal (T) and sagittal (S) sections of the maxillae specimens were selected and the 3D dataset aligned accordingly. The movement between maxillary first and third molar at day 14 was measured using the previously defined third molar crown as a fixed reference. The corner points of an enclosed rectangle covering the crowns of both first and third molar in the selected sections were marked, and all the corner points were registered (Figure 2). Subsequently, the midpoints of the cuboids around the crown of the first and third molar were acquired based on these aforementioned coordinates, and the length of the vector between these midpoints was thus calculated. Moreover, at day 14 the smallest distance between the maxillary first and second molars was measured by µCT in order to compare the tooth movement measured by the feeler gauge.

The root volume of the mesial root and the marginal bone mesially to the right first molar were analyzed as they were considered the injection target areas. In each scan, a standardized 3D volume of interest (VOI) was defined using CTAn (1.20.8, Bruker). For the mesial root volume measurement, the upper limit was set at apex, and the lower limit was set at the furcation area, next, the greyscale image was converted into a binary image by applying the automatic threshold function on CTAn, then the VOI was limited to the boundary of the binarized mesial root and further

quantified (Figure 3A). For bone volume and porosity quantification, a volume of interest (VOI) was defined in which the lower limit was set as the marginal alveolar ridge where a fixed cylinder-shaped VOI with 600 µm diameter was selected. The VOI was placed 160 µm mesially to both the mesial and the mesiobuccal roots starting at the marginal bone level and continuing for 500 µm upwards (Figure 3B). The cylinder-shaped VOI containing the alveolar bone was then quantified for bone volume fraction and porosity.

Tissue preparation and histological analyses

After µCT analysis, the specimens were decalcified in 10 % ethylenediamine tetra-acetate (EDTA) (VWR, Radnor, PA, USA) (pH 7.5) at 4°C for 10 weeks, the decalcification degree was monitored by X-ray and needle puncture. The maxillae were subsequently dehydrated in ascending concentrations of ethanol and embedded in paraffin for histological analysis. Parasagittal sections were cut at 5 µm parallel to the long axis of the first molars and mounted onto glass slides. Before staining, sample sections were baked at 60°C for 30 min, de-paraffinized in xylene and rehydrated through a graded ethanol series.

Prior to immunofluorescence staining, the rehydrated tissue sections were permeabilized with 0.1 % Triton X-100 (Sigma-Aldrich, Saint-Louis, Missouri, USA) in PBS for 5 min at room temperature followed by 3 times washing with PBS. Sections were then incubated in Tris-EDTA buffer (pH 9) with 0.05 % Tween 20 overnight at 60°C for antigen retrieval. The sections were washed with PBS 3 times and blocked with 10 % normal goat serum (NGS) (Abcam, Cambridge, United Kingdom) for 1 hour at room temperature in a humidified dark chamber. The sections were incubated with the following primary antibodies, rabbit anti-vWF (1:500, ab287962, Abcam, Cambridge, United Kingdom), mouse anti-collagen type I antibody (1:300, ab90395, Abcam), rabbit anti-periostin antibody (1:300, ab14041, Abcam), mouse anti-OCN antibody (1:200, 33-5400, Thermo Fisher Scientific, Waltham, USA) and rabbit anti-FNDC5 C-terminal antibody (1:200, ab181884, Abcam) in 2 % NGS overnight at 4°C. The sections were then washed 3 times with PBS, and stained with Alexa Fluor 488-conjugated goat anti-rabbit secondary antibody (Invitrogen, Thermo Fisher Scientific, Carlsbad, CA, USA) or Alexa Fluor 568-conjugated goat anti-mouse secondary antibody

(Invitrogen, Thermo Fisher Scientific) at 1:500 dilution in 4 % NGS for 1 hour at room temperature in a humidified dark chamber. After incubation with secondary antibodies, tissue sections were washed 3 times with PBS, counterstained with DRAQ5 Fluorescent Probe Solution (5 mM, 1:1000, 62251, Thermo Fisher Scientific) for 15 min at room temperature. The samples were covered by glass coverslips with Mowiol mounting medium (Mowiol 4-88, Sigma-Aldrich), and imaged using a Leica SP8 confocal microscope at 638 nm, 488 nm and 552 nm excitation, and 665-715 nm, 500-550 nm and 580-630 nm emission filters for DRAQ5, Alexa Fluor 488 and Alexa Fluor 568, respectively. The 10x lens HCX PL Apo CS 10x/0.4 was used to take the overall image for the sagittal sections of maxillary right first molars with surrounding periodontal tissues, while 40x lens HC PL Apo CS2 40x/1.3 was used to take magnified images of PDL, which were then quantified for immunofluorescence intensity.

To quantify and compare the fluorescence intensity of the proteins vWF, collagen type I, periostin, OCN and FNDC5 between the stained PDL tissues from control and treated sample sections, confocal images taken with a 40x objective lens were evaluated using Image J software (NIH, Bethesda, MD, USA; https://imagej.nih.gov/ij/). To quantify the fluorescence intensities, 3 parallel histological sections from each group were selected for staining, and 5 regions of interest from coronal one-third of PDL tissues on both stretched and compressed sides of mesial roots were randomly captured from these 3 sections, thus quantified for their mean intensities, the imaging settings were kept constant while acquiring individual confocal image.

The morphology of the tissue samples was characterized based on a modified Goldner's trichrome staining (26) and H&E staining of the sections. The chemicals included Weigert's hematoxylin solution (Merck KGaA, Merck, Darmstadt, Germany), fuchsine acid (Merck KGaA), orange G (Merck KGaA), tungstophosphoric acid (Merck KGaA), acetic acid (Merck KGaA), Entellan mounting medium (Merck KGaA), chromotrope 2R (Sigma-Aldrich), fast green powder (Sigma-Aldrich) and eosin (Sigma-Aldrich). In brief, the maxillae sections were deparaffinized and rehydrated as previously described, then washed with tap water for 5 min and stained in Weigert's hematoxylin solution for 10 min, followed by another wash with tap water for 10 min. For Goldner's

trichrome staining, sections were subsequently incubated in chromotrope 2R/fuchsine acid for 15 min at room temperature and washed in 1 % acetic acid for 3 times within 2 min. Next, the sections were incubated with Orange G for 7 min at room temperature, followed by washing for 3 times in 1 % acetic acid within 2 min. After that, the sections were incubated in fast green solution for 20 min at room temperature and washed in 1 % acetic acid again in the same manner. While for H&E staining, the sections were then stained with 0.5 % eosin for 3 min followed by 2 min wash after the hematoxylin staining. Next, the samples were dehydrated in 96 % ethanol for 3 min, thereafter in 99 % ethanol for 3 min twice and cleared in xylene for 10 min. Finally, sections were mounted with Entellan mounting medium and covered by cover slips. Images were captured with a Leica DM RBE microscope (Leica Microsystems CMS GmbH, Mannheim, Germany).

Irisin in plasma

The amount of irisin in the blood plasma was quantified after 14 days of OTM using a rat FNDC5/irisin ELISA kit (LifeSpan Biosciences, Seattle, Washington, USA) according to manufacturer's instructions. The plates were read at the wavelength of 450 nm using a spectrophotometer (BioTek, Winooski, USA), and the concentrations of circulating irisin were determined by comparing the optical density values of the tested samples to the standard curve.

Statistics

Statistical analysis was conducted using GraphPad Prism Version 9.5.0 (525). The normality distribution of the experimental results was tested by the Kolmogorov-Smirnov test, while the equality of group variance was tested by Brown Forsythe test, followed by one-way analysis of variance (ANOVA) with Dunnett's post hoc test for differences between groups. Where the equal variance and/or the normality test failed, the Kruskal-Wallis one-way ANOVA on ranks (Dunn's method) was performed. All data are presented as mean ± standard deviation (SD), a probability value of ≤ 0.05 is considered significant.

Results

Weight changes and plasma irisin

There was no difference in mean body weight between groups at any of the time points analyzed. However, the average weight in the control group was significantly reduced (p=0.0007) from day 0 to day 3 (314±11.7 g and 273±32.1 g, respectively), while no significant differences were observed between days 0, 6, 9, and 12. Thus, it is suggested that the rats in all groups remained healthy during OTM treatment.

The circulating levels of irisin were measured to determine if the injections had local or systemic effects. The injections appeared to have local effects only, as neither 0.1 μg (31.34±3.91 pg/mL) nor 1 μg irisin (24.36±3.54 pg/mL) resulted in significantly altered plasma levels of irisin compared to that of the control group (30.84±11.51 pg/mL).

Tooth movement

The maxillary right first molar in the 1 μg irisin group moved significantly less compared to the control group at days 6, 9 and 12. The average tooth movement of control group was found to be 0.23 mm, 0.33 mm and 0.39 mm at days 6, 9 and 12, respectively, while average tooth movement of the group injected with 1 μg irisin was found to be 0.15 mm (p=0.013), 0.21 mm (p=0.037) and 0.24 mm (p=0.049) at days 6, 9 and 12, respectively, however, no significant differences were observed between the 1 μg irisin group and control group at days 3 and 14 (Figure 4A). Although a trend of reduced OTM was recorded between the 0.1 μg irisin group and control group at days 6, 9, 12, and 14, this failed to reach statistical significance (Figure 4A). With regard to μCT measurements, no significant difference was observed between the control and the irisin groups at day 14 (Figure 4B and 4C).

Bone and root volume effects

It was hypothesized that the local injection of irisin might influence the bone and root close to the administration site. The mesial alveolar bone and mesial tooth root, without including PDL and tooth structures, were chosen for analysis of bone morphometric parameters and root volume as

they were closest to the injection site. However, bone volume fraction, porosity and mesial root volume did not differ between the control and irisin treated groups after 14 days of treatment (Figure 4D-F).

Histological analysis

By histological staining, the PDL appeared to be disorganized and sparse on the compression side in the control group, in contrast to a denser and well-organized PDL on the compression side in the two groups given irisin (Figure 5). Bone resorption lacunae (indicated by red arrows) were observed at the PDL-bone interface on the compression side in control group (Figure 5A), while the PDL-bone interfaces were smoother, with no obvious lacunae on the compression sides in animals given 0.1 μg and 1 μg irisin (Figure 5B and C). In addition, hyalinization areas (pointed to by black arrows) were present at the PDL-bone interface on the compression side in the control group (Figure 5D), whereas osteoblasts (pointed to by black arrows) were lining the PDL-bone interfaces on the compression side in the two irisin groups (Figure 5E and F). However, there was no observed difference in morphology on the tensional sides between the control and intervention groups (data not shown).

Immunofluorescence staining analysis

The coronal one-third areas of PDL were chosen for analysis, and the expression of the ECM markers collagen type I and periostin (Figure 6), the osteogenic marker OCN (Figure 7), angiogenic marker vWF (Figure 8), and FNDC5 (Figure 9) was evaluated by fluorescence staining on both tension and compression sides of the mesial root of maxillary right first molar after 14 days of OTM.

There were no significant differences in the levels of collagen type I expression on the tension side between the irisin treatment groups and the control group, whilst it was significantly enhanced on the compression side (2.42-fold ($p=0.0003$) and 2.39-fold ($p=0.0004$)) in the two irisin groups, respectively, compared to the control group (Figure 6A and 6B). The expression of periostin was significantly enhanced on the tension side (1.4-fold ($p=0.023$)) in the 1 μg irisin group compared to the control group. Moreover, both irisin groups exhibited significantly increased periostin

expression on the compression side compared to the control group (4.61-fold ($p<0.0001$) and 6.37-fold ($p<0.0001$), respectively) (Figure 6A and 6C).

The levels of OCN were 1.25-fold ($p=0.042$) increased on the tension side in the 0.1 μg irisin dosage group compared to the control group. On the compression side, both irisin groups displayed significantly enhanced levels of OCN compared to control (1.94-fold ($p<0.0001$) and 2.09-fold ($p<0.0001$), respectively) (Figure 7A and 7B).

The levels of vWF, which is a vascular endothelial cell marker, were significantly decreased by 0.33-fold ($p=0.042$) in the group given 0.1 μg irisin compared to control on the tension side, and significantly increased by 2.16-fold ($p<0.0001$) and 2.67-fold ($p<0.0001$) in both irisin groups compared to control on the compression side (Figure 8A and 8B).

Immune detection of the non-secreted C-terminal region of FNDC5 demonstrated that both 0.1 and 1 μg irisin induced significantly enhanced levels of FNDC5 expression on the tension side compared to the control group (both 1.6-fold; $p<0.0001$ and $p=0.0176$, respectively). Similarly, on the compression side, both dosages of irisin induced a significant 2.9-fold ($p<0.0001$) and 2.46-fold ($p<0.0001$) increase in FNDC5 expression compared to control group (Figure 9A and 9B).

Discussion

In orthodontic practice, the unwanted movement of anchor teeth and relapse of previously moved teeth are of major concern, thus identification of pharmacological agents that may counteract these undesired events may be of clinical significance (27, 28). In the present study, we demonstrated that submucosal injection of 1 μg irisin transiently reduced OTM in an experimental murine orthodontic model. No systemic or local negative effects of irisin administration were observed.

Feeler gauge measurements demonstrated that irisin induced a significant reduction in OTM at days 6, 9 and 12, however, not on day 14, measured by both feeler gauge and μCT. These two measurement methods have different accuracy levels. The feeler gauge method represents a

relatively simple and quick, somewhat operator-dependent measurement technique, which enables the rats to be under a light and reversible gas inhalation anesthesia. However, its accuracy is limited to a minimum measurable distance of 0.05 mm (8). On the other hand, μCT represents a more sophisticated, somewhat less operator-dependent measurement technique with relatively high accuracy. The OTM between first and second molars was measured by feeler gauge, while the μCT technique measured the OTM between first and second molars, as well as between first and third molars. The measurements between first and second molars showed similar trend by both feeler gauge and μCT, indicating that the two measurement techniques are comparable. However, the OTM measurement readings by μCT were smaller compared to feeler gauge. The latter might stem from the periodontal ligament flexibility allowing insertion of bigger feeler gauge blades into the gap between first and second molars, thus leading to an overestimation of tooth movement. Therefore, the feeler gauge measurements should be carried out with meticulous care without applying excessive force to the blades.

On the other hand, the group treated with 0.1 μg irisin showed a non-significant trend with reduced OTM when measured between the first and second molars with both feeler gauge and μCT, but the same was not observed with μCT measurement between the first and third molars. It cannot be excluded that the measurement between first and third molars made with the μCT on day 14 showed a higher OTM due to the gradual resumption of the natural distal movement of the maxillary third molars (29). Consequently, the inhibitory effect on tooth movement induced by 0.1 μg irisin may have been masked.

The non-sustained reduction of OTM at day 14 might also be due to a dose–response relationship in terms of irisin application frequency and dosage. Previous study has reported that out of 5 different irisin dosages ranging from 0.1 to 15 μg/kg, the injection dose starting from 0.5 μg/kg irisin induced substantial physiological changes in rat brain (30). This is one of the few studies done on the effect of irisin in soft tissues *in vivo*, and the two dosages (0.1 and 1 μg) used in our study were within this range. However, irisin dosages applied to bone have been reported to be higher; in mice, injection of 100 μg/kg recombinant irisin for 1 week increased strength and mass of cortical

bone (22), and another study from the same research group has further proved that injection of 100 μg/kg recombinant irisin weekly for 4 weeks prevented disuse-induced bone loss and retrieved bone mass in mice (31). We cannot rule out that the utilized injected dosages of irisin in the present study might have been below the so-called optimal irisin dosage of effect, which was suggested to be 500 μg/kg daily according to a systematic review (32). As far as we know, our study is the first one exploring the role of irisin in OTM, therefore, further research is needed to identify the optimum irisin dose that impacts the periodontal remodeling process during OTM.

Another contributing factor may be the observed hyalinization, as it is associated with a lag phase in orthodontics and may temporarily stop OTM until the hyalinized tissues are cleaned (33, 34). In the 1 μg irisin group an interesting tooth movement trend was observed, from notably reduced tooth movement at day 6 to a notably increased tooth movement trend at day 14. It can be speculated that 1 μg dosage of irisin might have negatively affected the removal of hyalinization in the early phase of the experimental OTM, but once the hyalinization was removed the tooth movement increased. However, the similar OTM trend was not observed in the 0.1 μg group at day 14, hence it further supports the irisin concentration, frequency and duration of application may impact the OTM differentially.

In the present study, local submucosal injection of irisin did not induce substantial changes in alveolar bone architecture in terms of bone volume fraction and porosity. Previous studies have shown that irisin administration might increase bone mineral density more in rodents with osteoporosis compared to healthy ones (35). Accordingly, since the rats were healthy in the present study, more consequential bone anabolic effect of irisin regarding OTM might be expected in periodontally compromised teeth. The anti-catabolic effect of irisin was demonstrated by markedly fewer bone resorption lacunae at the PDL-bone interface on the compression side in the irisin groups compared to control. This finding suggests that irisin might attenuate the activity of osteoclasts, which is in line with a previous study showing that irisin inhibits osteoclast differentiation via downregulation of RANK (36). Further, during OTM, the interaction between innate immune cells and osteoclasts is crucial (37). To promote the formation of osteoclasts, the ratio of M1/M2

macrophages is increased, thus leading to a more pronounced pro-inflammatory effect (38, 39). This increase is further facilitated by the pyrin domain-containing protein 3 (NLRP3) inflammasome produced by PDL cells (40). Irisin has been shown to inhibit the polarization of M1 macrophages and promote repolarization of M2 macrophages, thus reducing the secretion of interleukin (IL)-1β, IL-18 and tumor necrosis factor-α to exert an anti-inflammatory effect (41). On the other hand, irisin has also been found to suppress apoptosis in osteoblasts of osteoporotic rats through inhibiting NLRP3 (42). Seeing these in context, we may speculate that irisin might inhibit osteoclastogenesis at PDL-bone interface on the compression side by attenuating inflammatory reaction induced by immune cells.

To elucidate the potential cellular mechanisms involved in irisin-mediated OTM, expression of several important markers related to periodontal remodeling was assessed by immunofluorescence staining. Collagen type I is a major structural protein of ECM responsible for mechanical properties in connective tissues, while periostin is strongly expressed in collagen-rich tissues constantly subjected to mechanical loading. Periostin can directly bind to collagen type I, enhancing the collagen fibrillogenesis and therefore the mechanical properties of connective tissues (43). OCN is the most abundant non-collagenous protein expressed in periodontal tissues, and it may serve as a biological index reflecting the activity of osteoblasts during bone formation (44, 45). Moreover, since the development of vasculature is essential for osteogenesis to take place, expression of an angiogenic marker vWF, which is routinely used for identification of blood vessel formation (46, 47), was analyzed.

It has been shown that there is a negative correlation between mechanical properties of PDL and the tooth mobility. Teeth tend to be more immobile with stiffer PDL, and more mobile with mechanically weak and disorganized PDL (48). The elevated expression of collagen type I and periostin on the compression side and elevated expression of periostin on the tension side by 1 μg irisin reflect increased ECM deposition and stiffness in PDL in the presence of irisin. Moreover, the denser and well-organized PDL on the compression side visualized by histological analysis in the

two irisin-treated groups further supports this finding. Taken together, our findings suggest that irisin may inhibit tooth mobility by enhancing the mechanical properties of PDL.

The rate of OTM also largely depends on the remodeling of alveolar bone, and the rate of alveolar bone remodeling is determined by the activity of bone cells including osteoclasts and osteoblasts (49). It is well established that active bone formation on the tension side and bone resorption on the compression side lead to rapid OTM (50). Therefore, through interfering with the osteoclast activity or stimulating the osteoblast activity in the alveolar bone remodeling, the OTM rate may be reduced (51, 52). Both dosages of irisin induced significant increase in osteogenic marker OCN and angiogenic marker vWF on the compression side, while only 0.1 μg irisin increased OCN on the tension side. In addition, by histological staining, significant resorption lacunae were observed at the PDL-bone interface on the compression side of the control group, while smoother interfaces were present in the two irisin groups, indicating a reduced osteoclast activity by irisin administration. Further, the well-aligned osteoblasts at the PDL-bone interface in the two irisin groups imply an enhanced osteogenic activity. These findings are in line with previous studies demonstrating that irisin could both stimulate osteoblastic lineage cell differentiation and inhibit osteoclastogenesis (36, 53). Thus, the suppressed OTM in our study may also be attributed to the inhibited osteoclast activity and enhanced osteoblast activity by irisin application. However, specific quantification of osteoclasts at the PDL-bone interface could not be reliably performed because frontal resorption of bone may cause changes in the structure at the PDL-bone interface leading to increased irregularity, which does not allow for accurate numerical assessment (54).

The protein structure of FNDC5 comprises an N-terminal signal sequence, a short transmembrane region termed as irisin domain, and a C-terminal domain. The C-terminal tail of FNDC5 is in the cytoplasm, while the extracellular N-terminal part is proteolytically cleaved and released into circulation as irisin (55, 56). Hence, primary antibody against C-terminal FNDC5 was used for immunofluorescent staining in the present study. The FNDC5 expression was markedly increased in PDL by 0.1 and 1 μg irisin in both PDL tension and compression sides compared to the control group. However, no significant differences in the circulating levels of irisin were found between

control and irisin groups. Hence, we speculate that irisin may exert its osteogenesis stimulatory effect to reduce OTM by directly targeting PDL tissues. However, our findings may not necessarily translate to a clinical setting given the limitations in a rodent model. Since orthodontic treatment is a long course, more studies looking at irisin application frequency, dosage and duration are needed to bring this therapeutic from bench to chairside.

In conclusion, local injection of recombinant irisin may inhibit OTM transiently by enhancing the ECM deposition, osteogenic potential and thus mechanical properties of PDL mainly on the compression side.

Figures

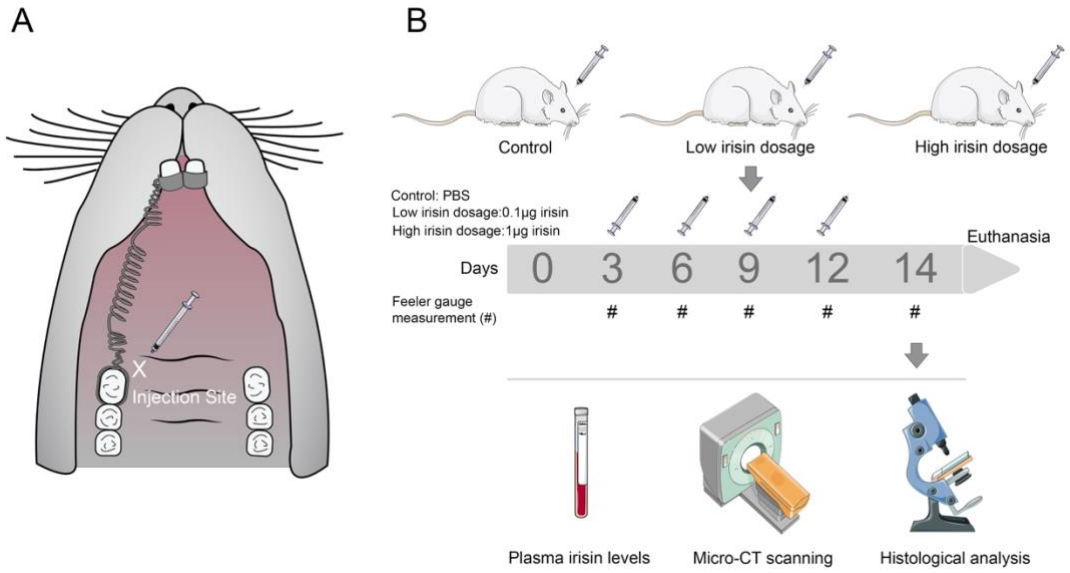

Figure 1. A. An intraoral schematic illustration depicting the injection site and the orthodontic appliance. B. The flow chart of the experimental setup. # represents the performance of OTM measurement by feeler gauge. Parts of the figure were generated using Servier Medical Art, provided by Servier, licensed under a Creative Commons Attribution 3.0 unported license.

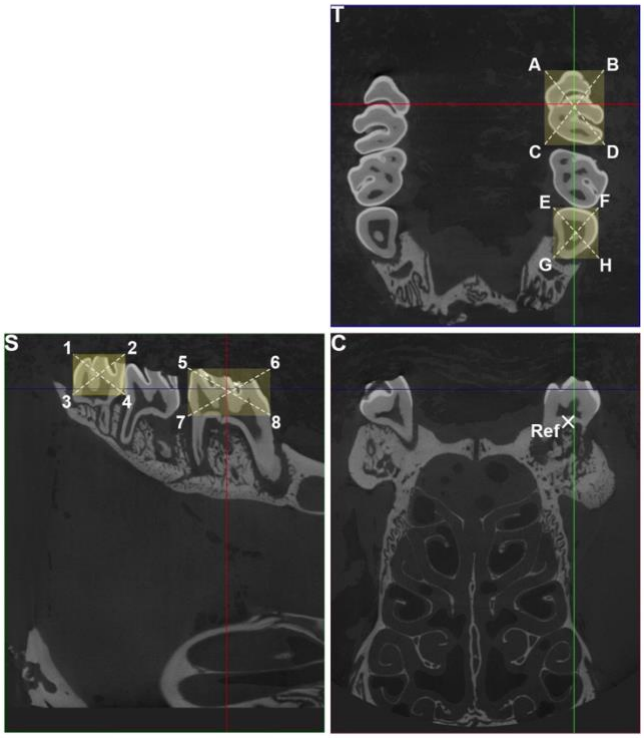

Figure 2. Tooth movement measured by μCT. The corner point coordinates of an enclosed rectangle covering the crown of both first and third molar in the chosen sections were marked and registered (A-H in the transversal view; 1-8 in the sagittal view). According to these points the midpoints of cuboids around the molars were acquired. The length between the two midpoints was thus measured. The scans were aligned in the frontal/coronal plane using the mid-palatal suture. The third molar was defined as a fixed reference point, and at this specific point the transversal and sagittal sections of the maxillae specimens were selected, and the 3D dataset aligned accordingly. In addition, the smallest distance between the first and second molars was measured. T: transversal, C: coronal, S: sagittal.

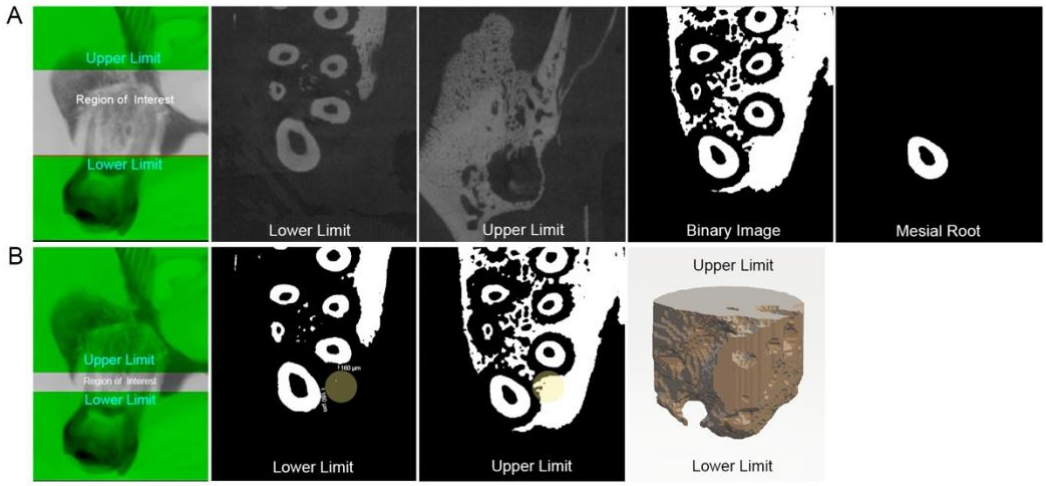

Figure 3. A. Root volume measured by µCT. The VOI was defined, the raw µCT scan image was converted into binary image, then the VOI was shrunk and limited to the mesial root and quantified. B. Bone morphometric parameters measured by µCT. The VOI was set as a 600 µm diameter cylinder placed 160 µm mesially to both the mesial and the mesiobuccal roots starting from the marginal alveolar bone and continuing upwards for 500 µm. The cylinder-shaped VOI containing the alveolar bone was quantified for bone volume fraction and porosity.

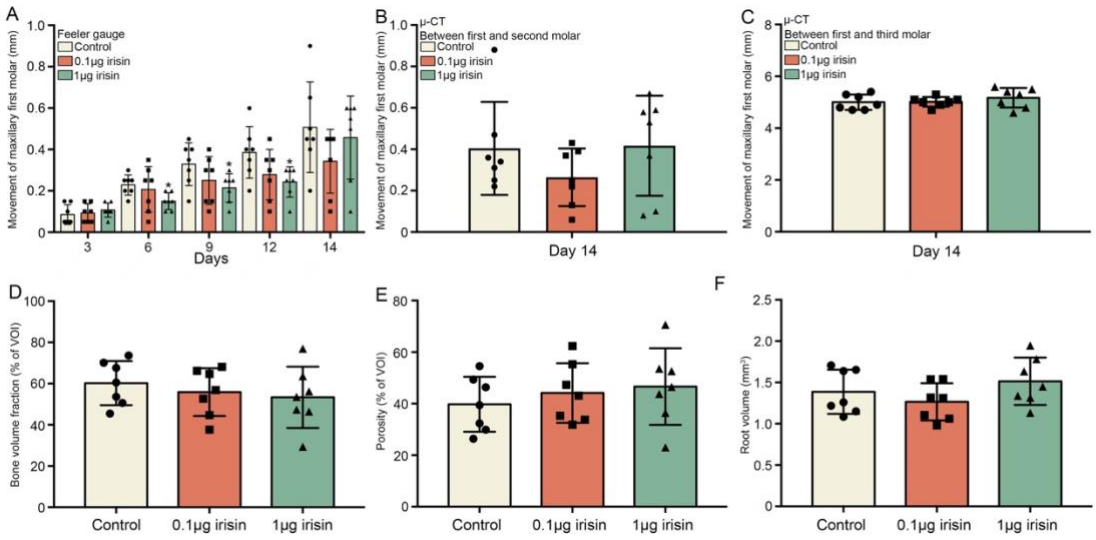

Figure 4. A. Tooth movement measured by feeler gauge (mm) between first and second molar at days 6, 9 and 12 was significantly decreased in the irisin injected group (1 µg) in contrast with control group. No significant changes were observed at other time points. Significantly different from control at *, $p \leq 0.05$. B. Tooth movement between first and second molars measured by µCT at day 14. No significant difference was observed between control and irisin-treated groups. C. Tooth movement measured by µCT scanning on day 14 between first and third molar. No significant difference was observed between control and irisin treated groups. D. Comparison of bone volume fraction measured at the alveolar ridge mesial to the maxillary right first molar. E. Comparison of porosity measured at the alveolar ridge mesial to the maxillary right first molar. F. Comparison of mesial root volume of maxillary right first molar. No significant changes were found in bone volume

fraction, porosity and root volume between control and irisin treated groups (n=7 for each group, one-way ANOVA).

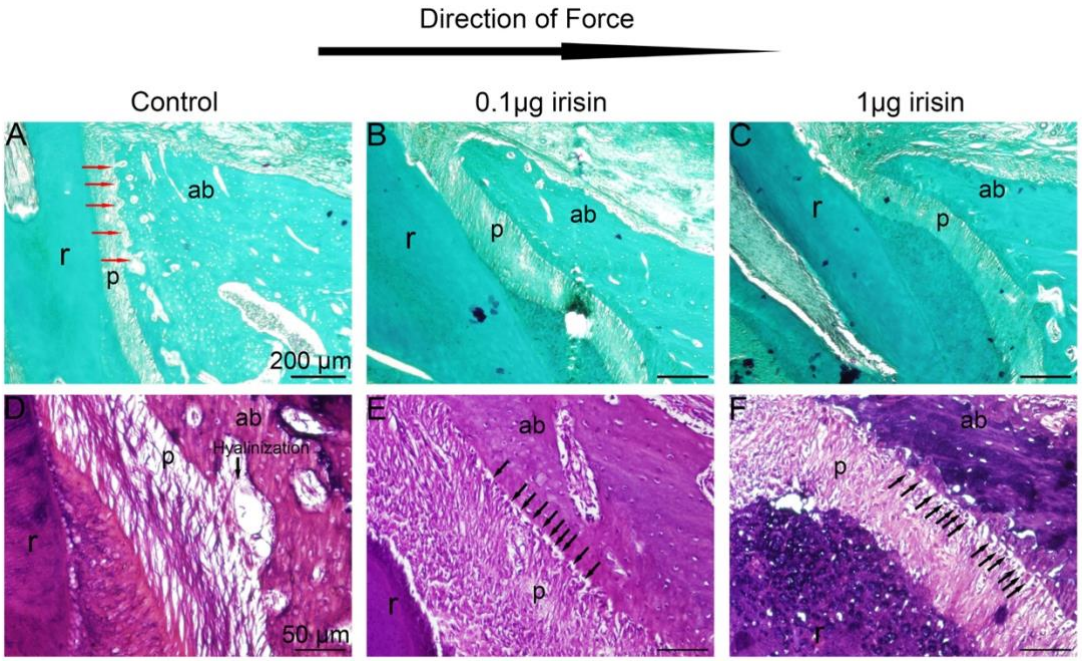

Figure 5. Histologically stained sections displaying periodontal tissues near injection site. Sagittal sections of periodontal tissues were stained with Goldner's trichrome staining (A-C) and H&E staining (D-F). Big black arrow indicates the direction of applied force; small red arrows indicate resorption pits at PDL-bone interface; small black arrows indicate hyalinization areas and osteoblasts lining the PDL-bone interface. r: root; p: periodontal ligament; ab: alveolar bone.

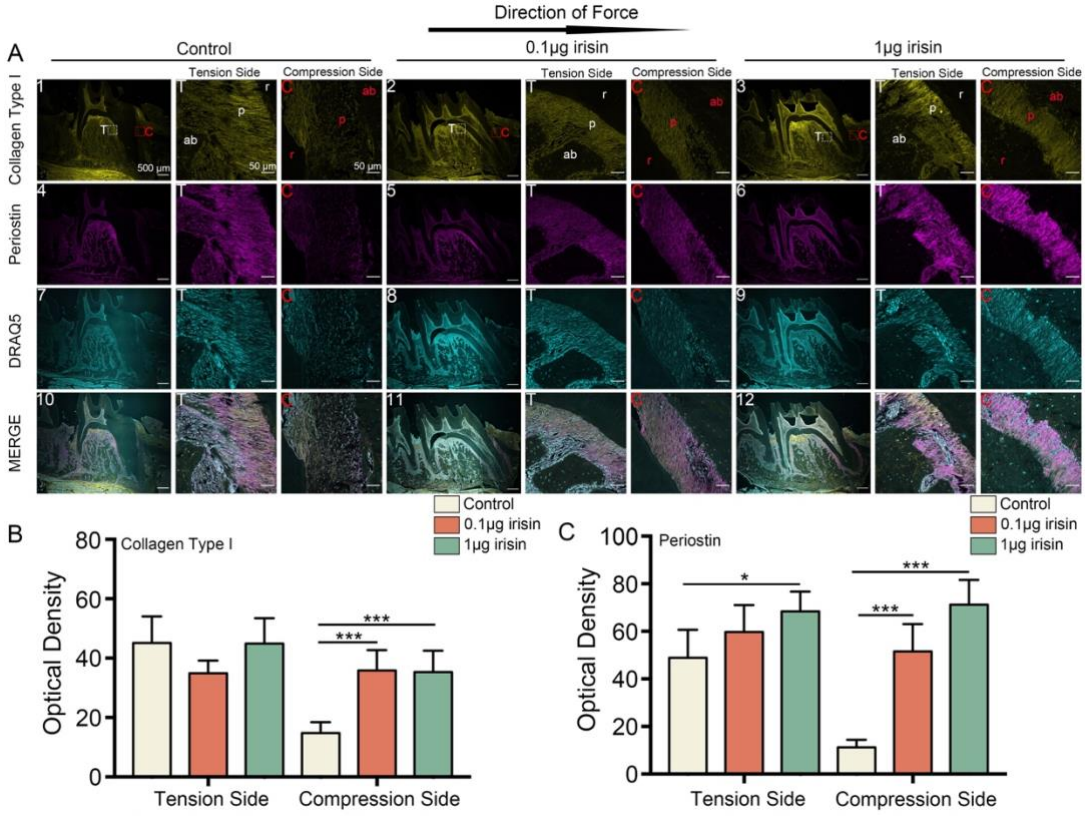

Figure 6. Confocal images of sagittal sections of maxillary right first molars from control and irisin-treated groups co-stained with collagen type I and periostin, and quantification of immunofluorescence intensity. A. Histological sections of maxillary right first molars were assessed by immunofluorescence staining against collagen type I (1-3), periostin (4-6), nuclei were counter stained with DRAQ5 (7-9), merged images are presented in 10-12. Boxed areas are shown at a higher magnification, white boxes indicate tension side while red boxes indicate compression side. T: tension side, C: compression side. B. Quantification of collagen type I fluorescence intensity. C. Quantification of periostin fluorescence intensity. Significantly different from control at * $p \leq 0.05$ and *** $p \leq 0.001$. Mean fluorescence intensities were measured from five random regions of interest for each group, one-way ANOVA was used for statistical analysis.

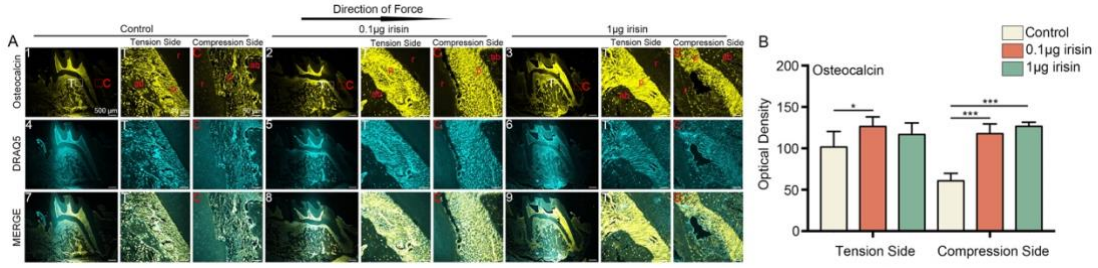

Figure 7. Confocal images of sagittal sections of maxillary right first molars from control and irisin-treated groups stained with OCN, and quantification of immunofluorescence intensity. A. Histological sections of maxillary right first molars were assessed by immunofluorescence staining against OCN (1-3), nuclei were counterstained with DRAQ5 (4-6) and merged images are displayed in 7-9. Boxed areas are shown at a higher magnification, white boxes indicate tension side while red boxes indicate compression side. T: tension side, C: compression side. B. Quantification of OCN

fluorescence intensity. Significantly different from control at * p≤0.05 and *** p≤0.001. Mean fluorescence intensities were measured from five random regions of interest for each group, one-way ANOVA was used for statistical analysis.

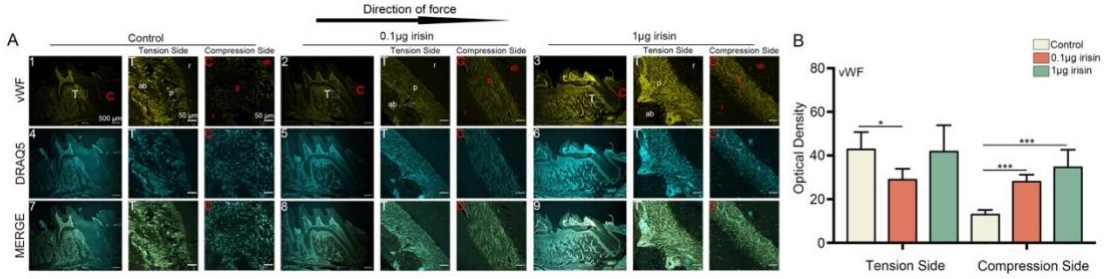

Figure 8. Confocal images of sagittal sections of maxillary right first molars from control and irisin-treated groups stained with vWF, and quantification of immunofluorescence intensity. A. Histological sections of maxillary right first molars were assessed by immunofluorescence staining against vWF (1-3), nuclei were counterstained with DRAQ5 (4-6) and merged images are displayed in 7-9. Boxed areas are shown at a higher magnification, white boxes indicate tension side while red boxes indicate compression side. T: tension side, C: compression side. B. Quantification of vWF fluorescence intensity. Significantly different from control at * p≤0.05 and *** p≤0.001. Mean fluorescence intensities were measured from five random regions of interest for each group, one-way ANOVA was used for statistical analysis.

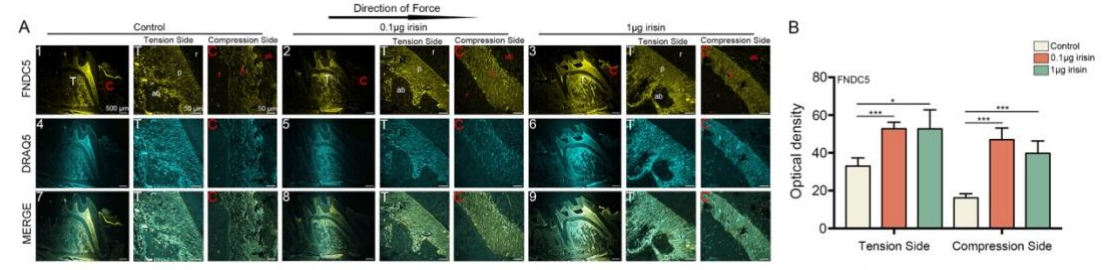

Figure 9. Confocal images of sagittal sections of maxillary right first molars from control and irisin-treated groups stained with FNDC5, and quantification of immunofluorescence intensity. A. Histological sections of maxillary right first molars were assessed by immunofluorescence staining against FNDC5 (1-3), nuclei were counterstained with DRAQ5 (4-6) and merged images are displayed in 7-9. Boxed areas are shown at a higher magnification, white boxes indicate tension side while red boxes indicate compression side. T: tension side, C: compression side. B. Quantification of FNDC5 fluorescence intensity. Significantly different from control at * p≤0.05 and *** p≤0.001. Mean fluorescence intensities were measured from five random regions of interest for each group, one-way ANOVA was used for statistical analysis.

Author contributions

YY: participated in the experimental design, performed experiments and drafted the manuscript.

HP, AKS, LPN, US: performed the experiments and edited the manuscript.

JER: launched this project, designed the experiments and contributed in editing this manuscript.

Declaration of Competing Interest

The authors declare that there are no potential competing financial interests or personal relationships that could have appeared to influence the study reported in this paper.

Funding

This work was supported by the Research Council of Norway [287953]; and grants from the Liaison Committee between the Central Norway Regional Health Authority and the Norwegian University of Science and Technology.

Acknowledgements

Yang Yang (CSC number 201908420242) would like to thank China Scholarship Council (CSC) for a personal grant. Gratitude goes to Professor Vaska Vandevska Radunovic, Department of Orthodontics, Faculty of Dentistry, University of Oslo, for providing technical support on establishment of murine models. Acknowledgement goes to Catherine Anne Heyward, Oral Research Laboratory, Faculty of Dentistry, University of Oslo, for providing instructions in histology.

Data availability

The data supporting the findings of the present study are available from the corresponding author upon request.

References

1. De Jong, T., Bakker, A., Everts, V., Smit, T. (2017) The intricate anatomy of the periodontal ligament and its development: Lessons for periodontal regeneration. *Journal of Periodontal Research*, 52(6),965-974.
2. Matsuda, N., Yokoyama, K., Takeshita, S., Watanabe, M. (1998) Role of epidermal growth factor and its receptor in mechanical stress-induced differentiation of human periodontal ligament cells in vitro. *Archives of Oral Biology*, 43(12),987-997.
3. Garlet, T.P., Coelho, U., Silva, J.S., Garlet, G.P. (2007) Cytokine expression pattern in compression and tension sides of the periodontal ligament during orthodontic tooth movement in humans. *European journal of oral sciences*, 115(5),355-362.
4. Krishnan, V., Davidovitch, Z.e. (2006) Cellular, molecular, and tissue-level reactions to orthodontic force. *American Journal of Orthodontics and Dentofacial Orthopedics*, 129(4),469.e461-469.e432.
5. Krishnan, V., Davidovitch, Z. (2009) On a path to unfolding the biological mechanisms of orthodontic tooth movement. *Journal of Dental Research*, 88(7),597-608.
6. Chumbley, A.B., Tuncay, O.C. (1986) The effect of indomethacin (an aspirin-like drug) on the rate of orthodontic tooth movement. *American Journal of Orthodontics*, 89(4),312-314.
7. Collins, M.K., Sinclair, P.M. (1988) The local use of vitamin d to increase the rate of orthodontic tooth movement. *American Journal of Orthodontics and Dentofacial Orthopedics*, 94(4),278-284.
8. Haugen, S., Aasarød, K.M., Stunes, A.K., Mosti, M.P., Franzen, T., Vandevska-Radunovic, V., Syversen, U., Reseland, J.E. (2017) Adiponectin prevents orthodontic tooth movement in rats. *Archives of Oral Biology*, 83,304-311.
9. Saddi, K.R.G.C., Alves, G.D., Paulino, T.P., Ciancaglini, P., Alves, J.B. (2008) Epidermal growth factor in liposomes may enhance osteoclast recruitment during tooth movement in rats. *The Angle Orthodontist*, 78(4),604-609.
10. Igar, K., Adachi, H., Mitani, H., Shinoda, H. (1996) Inhibitory effect of the topical administration of a bisphosphonate (risedronate) on root resorption incident to orthodontic tooth movement in rats. *Journal of Dental Research*, 75(9),1644-1649.
11. Hellsing, E., Hammarström, L. (1991) The effects of pregnancy and fluoride on orthodontic tooth movements in rats. *The European Journal of Orthodontics*, 13(3),223-230.
12. Diravidamani, K., Sivalingam, S.K., Agarwal, V. (2012) Drugs influencing orthodontic tooth movement: An overall review. *Journal of pharmacy & bioallied sciences*, 4(Suppl 2),S299-S303.
13. Almpani, K., Kantarci, A. (2016) Nonsurgical methods for the acceleration of the orthodontic tooth movement. *Tooth movement*, 18,80-91.
14. Boström, P.*, et al.* (2012) A pgc1-α-dependent myokine that drives brown-fat-like development of white fat and thermogenesis. *Nature*, 481(7382),463-468.
15. Xue, Y.*, et al.* (2022) Myokine irisin promotes osteogenesis by activating bmp/smad signaling via αv integrin and regulates bone mass in mice. *International journal of biological sciences*, 18(2),572-584.
16. Zhang, D., Tan, X., Tang, N., Huang, F., Chen, Z., Shi, G. (2020) Review of research on the role of irisin in tumors. *OncoTargets and therapy*, 13,4423-4430.
17. Zhu, J., Wang, Y., Cao, Z., Du, M., Hao, Y., Pan, J., He, H. (2020) Irisin promotes cementoblast differentiation via p38 mapk pathway. *Oral Diseases*, 26(5),974-982.
18. Son, J., Choi, S., Jang, J., Koh, J., Oh, W., Hwang, Y., Lee, B. (2021) Irisin promotes odontogenic differentiation and angiogenic potential in human dental pulp cells. *International Endodontic Journal*,

54(3),399-412.
19. Posa, F., Colaianni, G., Di Cosola, M., Dicarlo, M., Gaccione, F., Colucci, S., Grano, M., Mori, G. (2021) The myokine irisin promotes osteogenic differentiation of dental bud-derived mscs. *Biology*, 10(4),295.
20. Pullisaar, H., Colaianni, G., Lian, A.-M., Vandevska-Radunovic, V., Grano, M., Reseland, J.E. (2020) Irisin promotes growth, migration and matrix formation in human periodontal ligament cells. *Archives of Oral Biology*, 111,104635.
21. Huang, X., Xiao, J., Wang, X., Cao, Z. (2022) Irisin attenuates p. Gingivalis-suppressed osteogenic/cementogenic differentiation of periodontal ligament cells via p38 signaling pathway. *Biochemical and Biophysical Research Communications*.
22. Colaianni, G.*, et al.* (2015) The myokine irisin increases cortical bone mass. *Proceedings of the National Academy of Sciences*, 112(39),12157-12162.
23. Chen, X., Sun, K., Zhao, S., Geng, T., Fan, X., Sun, S., Zheng, M., Jin, Q. (2020) Irisin promotes osteogenic differentiation of bone marrow mesenchymal stem cells by activating autophagy via the wnt//β-catenin signal pathway. *Cytokine*, 136,155292.
24. Yang, J., Yu, K., Liu, D., Yang, J., Tan, L., Zhang, D. (2021) Irisin enhances osteogenic differentiation of mouse mc3t3-e1 cells via upregulating osteogenic genes. *Experimental and Therapeutic Medicine*, 21(6),1-7.
25. Franzen, T.J., Brudvik, P., Vandevska-Radunovic, V. (2013) Periodontal tissue reaction during orthodontic relapse in rat molars. *The European Journal of Orthodontics*, 35(2),152-159.
26. Luna, L.G. Histopathologic methods and color atlas of special stains and tissue artifacts: Amer Histolabs Pub Department; 1992.
27. Keles, A., Grunes, B., DiFuria, C., Gagari, E., Srinivasan, V., Darendeliler, M.A., Muller, R., Kent Jr, R., Stashenko, P. (2007) Inhibition of tooth movement by osteoprotegerin vs. Pamidronate under conditions of constant orthodontic force. *European journal of oral sciences*, 115(2),131-136.
28. Kouskoura, T., Katsaros, C., von Gunten, S. (2017) The potential use of pharmacological agents to modulate orthodontic tooth movement (otm). *Frontiers in Physiology*, 8.
29. King, G.J., Keeling, S.D., McCoy, E.A., Ward, T.H. (1991) Measuring dental drift and orthodontic tooth movement in response to various initial forces in adult rats. *American Journal of Orthodontics and Dentofacial Orthopedics*, 99(5),456-465.
30. Asadi, Y., Gorjipour, F., Behrouzifar, S., Vakili, A. (2018) Irisin peptide protects brain against ischemic injury through reducing apoptosis and enhancing bdnf in a rodent model of stroke. *Neurochemical Research*, 43(8),1549-1560.
31. Colaianni, G.*, et al.* (2017) Irisin prevents and restores bone loss and muscle atrophy in hind-limb suspended mice. *Scientific Reports*, 7(1),1-16.
32. Alzoughool, F., Al-Zghoul, M.B., Al-Nassan, S., Alanagreh, L., Mufleh, D., Atoum, M. (2020) The optimal therapeutic irisin dose intervention in animal model: A systematic review. *Vet World*, 13(10),2191-2196.
33. Kurol, J., Owman-Moll, P. (1998) Hyalinization and root resorption during early orthodontic tooth movement in adolescents. *The Angle Orthodontist*, 68(2),161-166.
34. Iino, S., Sakoda, S., Ito, G., Nishimori, T., Ikeda, T., Miyawaki, S. (2007) Acceleration of orthodontic tooth movement by alveolar corticotomy in the dog. *American Journal of Orthodontics and Dentofacial Orthopedics*, 131(4),448. e441-448. e448.
35. Pereira, L.J., Andrade, E.F., Barroso, L.C., Lima, R.R.d., Macari, S., Paiva, S.M., Silva, T.A. (2022)

Irisin effects on bone: Systematic review with meta-analysis of preclinical studies and prospects for oral health. *Brazilian Oral Research*, 36.

36. Ma, Y.*, et al.* (2018) Irisin promotes proliferation but inhibits differentiation in osteoclast precursor cells. *The FASEB Journal*, 32(11),5813-5823.

37. Gao, Y., Min, Q., Li, X., Liu, L., Lv, Y., Xu, W., Liu, X., Wang, H. (2022) Immune system acts on orthodontic tooth movement: Cellular and molecular mechanisms. *BioMed Research International*, 2022.

38. He, D., Liu, F., Cui, S., Jiang, N., Yu, H., Zhou, Y., Liu, Y., Kou, X. (2020) Mechanical load-induced h2s production by periodontal ligament stem cells activates m1 macrophages to promote bone remodeling and tooth movement via stat1. *Stem Cell Research & Therapy*, 11(1),1-14.

39. He, D.*, et al.* (2015) Enhanced m1/m2 macrophage ratio promotes orthodontic root resorption. *Journal of Dental Research*, 94(1),129-139.

40. Zhang, J., Liu, X., Wan, C., Liu, Y., Wang, Y., Meng, C., Zhang, Y., Jiang, C. (2020) Nlrp3 inflammasome mediates m1 macrophage polarization and il-1β production in inflammatory root resorption. *Journal of Clinical Periodontology*, 47(4),451-460.

41. Han, Z., Ma, J., Han, Y., Yuan, G., Jiao, R., Meng, A. (2023) Irisin attenuates acute lung injury by suppressing the pyroptosis of alveolar macrophages. *International Journal of Molecular Medicine*, 51(4),32.

42. Xu, L., Shen, L., Yu, X., Li, P., Wang, Q., Li, C. (2020) Effects of irisin on osteoblast apoptosis and osteoporosis in postmenopausal osteoporosis rats through upregulating nrf2 and inhibiting nlrp3 inflammasome. *Experimental and Therapeutic Medicine*, 19(2),1084-1090.

43. Norris, R.A.*, et al.* (2007) Periostin regulates collagen fibrillogenesis and the biomechanical properties of connective tissues. *Journal of Cellular Biochemistry*, 101(3),695-711.

44. Han, X.-L., Meng, Y., Kang, N., Lv, T., Bai, D. (2008) Expression of osteocalcin during surgically assisted rapid orthodontic tooth movement in beagle dogs. *Journal of Oral and Maxillofacial Surgery*, 66(12),2467-2475.

45. Brito, M.V., Pérez, M.A.Á., Rodríguez, F.J.M. (2013) Osteocalcin expression in periodontal ligament when inducing orthodontic forces. *Revista odontológica mexicana*, 17(3),152-155.

46. Fang, T.D.*, et al.* (2005) Angiogenesis is required for successful bone induction during distraction osteogenesis. *Journal of Bone and Mineral Research*, 20(7),1114-1124.

47. Zanetta, L., Marcus, S.G., Vasile, J., Dobryansky, M., Cohen, H., Eng, K., Shamamian, P., Mignatti, P. (2000) Expression of von willebrand factor, an endothelial cell marker, is up-regulated by angiogenesis factors: A potential method for objective assessment of tumor angiogenesis. *International journal of cancer*, 85(2),281-288.

48. Madan, M.S., Liu, Z.J., Gu, G.M., King, G.J. (2007) Effects of human relaxin on orthodontic tooth movement and periodontal ligaments in rats. *American Journal of Orthodontics and Dentofacial Orthopedics*, 131(1),8. e1-8. e10.

49. Huang, H., Williams, R.C., Kyrkanides, S. (2014) Accelerated orthodontic tooth movement: Molecular mechanisms. *American Journal of Orthodontics and Dentofacial Orthopedics*, 146(5),620-632.

50. Ren, A., Lv, T., Kang, N., Zhao, B., Chen, Y., Bai, D. (2007) Rapid orthodontic tooth movement aided by alveolar surgery in beagles. *American Journal of Orthodontics and Dentofacial Orthopedics*, 131(2),160. e161-160. e110.

51. Han, G., Chen, Y., Hou, J., Liu, C., Chen, C., Zhuang, J., Meng, W. (2010) Effects of simvastatin on relapse and remodeling of periodontal tissues after tooth movement in rats. *American Journal of*

Orthodontics and Dentofacial Orthopedics, 138(5),550. e551-550. e557.

52. Liu, X.-c., Wang, X.-x., Zhang, L.-n., Yang, F., Nie, F.-j., Zhang, J. (2020) Inhibitory effects of resveratrol on orthodontic tooth movement and associated root resorption in rats. *Archives of Oral Biology*, 111,104642.

53. Qiao, X., Nie, Y., Ma, Y., Chen, Y., Cheng, R., Yin, W., Hu, Y., Xu, W., Xu, L. (2016) Irisin promotes osteoblast proliferation and differentiation via activating the map kinase signaling pathways. *Scientific Reports*, 6(1),1-12.

54. Araujo, A.S., Fernandes, A.B.N., Maciel, J.V.B., Netto, J.d.N.S., Bolognese, A.M. (2015) New methodology for evaluating osteoclastic activity induced by orthodontic load. *Journal of Applied Oral Science*, 23,19-25.

55. Cao, R.Y., Zheng, H., Redfearn, D., Yang, J. (2019) Fndc5: A novel player in metabolism and metabolic syndrome. *Biochimie*, 158,111-116.

56. Arhire, L.I., Mihalache, L., Covasa, M. (2019) Irisin: A hope in understanding and managing obesity and metabolic syndrome. *Frontiers in Endocrinology*, 10,524.

III

Received: 11 July 2022 | Revised: 24 November 2022 | Accepted: 27 December 2022

DOI: 10.1111/jre.13094

ORIGINAL ARTICLE

Journal of PERIODONTAL RESEARCH WILEY

Recombinant irisin enhances the extracellular matrix formation, remodeling potential, and differentiation of human periodontal ligament cells cultured in 3D

Yang Yang[1] | Tianxiang Geng[1] | Athina Samara[1] | Ole Kristoffer Olstad[2] | Jianying He[3] | Anne Eriksson Agger[1] | Bjørn Helge Skallerud[3] | Maria A. Landin[4] | Catherine Anne Heyward[4] | Helen Pullisaar[5] | Janne Elin Reseland[1]

[1]Department of Biomaterials, Faculty of Dentistry, University of Oslo, Oslo, Norway

[2]Department of Medical Biochemistry, Oslo University Hospital, Oslo, Norway

[3]Department of Structural Engineering, Faculty of Engineering, Norwegian University of Science and Technology (NTNU), Trondheim, Norway

[4]Oral Research Laboratory, Faculty of Dentistry, University of Oslo, Oslo, Norway

[5]Department of Orthodontics, Faculty of Dentistry, University of Oslo, Oslo, Norway

Correspondence
Janne Elin Reseland, Department of Biomaterials, Faculty of Dentistry, University of Oslo, Oslo, Norway.
Email: j.e.reseland@odont.uio.no

Funding information
China Scholarship Council, Grant/Award Number: 201908420242; Research Council of Norway, Grant/Award Number: 287953

Abstract

Background: Irisin is expressed in human periodontal ligament (hPDL), and its administration enhances growth, migration and matrix deposition in hPDL cells cultured in monolayers in vitro.

Objectives: To identify whether irisin affects the gene expression patterns directing the morphology, mechanical properties, extracellular matrix (ECM) formation, osteogenic activity and angiogenic potential in hPDL cell spheroids cultured in 3D.

Materials and Methods: Spheroids of primary human hPDL cells were generated in a rotational 3D culture system and treated with or without irisin. The gene expression patterns were evaluated by Affymetrix microarrays. The morphology of the spheroids was characterized using histological staining. Mechanical properties were quantified by nanoindentation. The osteogenic and angiogenic potential of spheroids were assessed through immunofluorescence staining for collagen type I, periostin fibronectin and von Willebrand factor (vWF), and mRNA expression of osteogenic markers. The secretion of multiple myokines was evaluated using Luminex immunoassays.

Results: Approximately 1000 genes were differentially expressed between control and irisin-treated groups by Affymetrix. Several genes related to ECM organization were differentially expressed, and multiple deubiquitinating enzymes were upregulated in the irisin-exposed samples analyzed. These represent cellular and molecular mechanisms indicative of a role for irisin in tissue remodeling. Irisin induced a rim-like structure on the outer region of the hPDL spheroids, ECM-related protein expression and the stiffness of the spheroids were enhanced by irisin. The expression of osteogenic and angiogenetic markers was increased by irisin.

Conclusions: Irisin altered the morphology in primary hPDL cell-derived spheroids, enhanced its ECM deposition, mechanical properties, differentiation and remodeling potential.

KEYWORDS
extracellular matrix, irisin, mechanical properties, osteogenesis, periodontal ligament cells, three-dimensional culture

1 | INTRODUCTION

Irisin was first identified in 2012 by a research group from Harvard University, which reported that PPAR-γ co-activator-1α (*PGC1-α*) stimulated the expression of fibronectin type III domain-containing protein 5 (*FNDC5*) in skeletal muscle, this newly characterized myokine was then cleaved and secreted into the blood circulation in response to physical activities and was named irisin.[1] It was thus considered that its primary physiological role was the regulation of metabolism and energy homeostasis. It also promotes the activity of insulin and reduces insulin resistance, these effects improve the metabolic profile in tissues and increase energy expenditure, making irisin a promising research target for treating metabolic diseases.[1–3] Irisin has also been found to be associated with osteogenesis, as injections of cumulative weekly dose of recombinant irisin significantly boosted cortical bone mass and bone strength, enhanced osteogenesis, and the relative osteogenic genes concomitant with a decrease in osteoblastic inhibitors.[4] Further, irisin is known to induce bone matrix deposition by stimulating osteocalcin expression in dental bud-derived mesenchymal stem cells.[5]

It has been documented that irisin is expressed in human PDL cells and rat PDL tissues.[6] The PDL is a highly organized fibrous connective tissue firmly anchored to the teeth and the inner wall of the alveolar bone.[7,8] The main role of PDL is to provide support for the teeth to help them function normally and resist external forces, which is in close relation with the mechanical properties of the tissue. Its structure features a fibrous stroma consisting of cells, blood vessels and nerves, and the fibrous stroma is primarily made of collagens.[9] Among these the most predominant component is collagen type I[10,11] associated with osteoblast-like characteristics of PDL cells.[12] Additionally, collagen type I largely impacts the mechanical properties of ligaments and tendons due to its molecule structure and physical arrangements into fibers.[13] Till now, little is known regarding the role of irisin in PDL cells regarding its ECM and differentiation potential, to the best of our knowledge, it has only been reported that irisin treatment can promote growth, migration and matrix formation in hPDL cells cultured in 2D.[14]

Tissue structure, function and pathology are commonly studied using monolayer cell culture methods (2D), but which can differ significantly in morphology, cell-to-cell and cell-to-matrix interaction and differentiation compared to 3D-cultured cells.[15] The 3D setup helps cells assemble into a tissue-like structure, reflects the in vivo cellular structure and mirrors cellular responses, which will enable greater cell-to-cell contacts and intercellular signaling. Similar to in vivo developmental processes 3D cell assembly induces differentiation to form more complicated structures that mimic a physiological microenvironment.[16,17] This transit from conventional 2D to 3D culture of PDL cells usually requires extracellular scaffolds or biomaterials.[18–20] Recently, a rotating cell culture system (RCCS) has been introduced as a novel method to generate 3D cells, offering a facile, reproducible and high-throughput platform.[21] The mechanical properties of 3D-generated osteospheres using RCCS were previously evaluated in response to different treatments,[22,23] and it was also shown that hPDL cells could form 3D spheroids in RCCS.[6]

There is a need for alternative regenerative strategies to restore the structures and functions of tooth-supporting tissues in patients with periodontal diseases. In the present research, we performed Affymetrix analysis to profile the mRNA expression patterns between 3D hPDL cell spheroids treated with and without irisin, to identify the role of irisin in gene regulation and biological functions in tissue-mimetic 3D-cultured hPDL cells. Furthermore, we examined the effects of irisin administration on the morphology, mechanical properties, ECM formation, differentiation potential and the secretion of myokines from 3D hPDL cell spheroids.

2 | MATERIALS AND METHODS

2.1 | Generation of 3D hPDL cell spheroids

Commercially available primary human PDL (hPDL) cells (Lonza) were maintained in Dulbecco's modified Eagle's medium (Sigma-Aldrich) supplemented with 10% fetal bovine serum, 200 mM GlutaMAX (Gibco, Thermo Fisher Scientific) and 100 μg/ml penicillin/100 IU μg/ml streptomycin (Lonza). The medium was refreshed every three days, and cells were subcultured and seeded in T75 flasks. Cells in passage 4–8 were used to generate 3D hPDL cell spheroids. Approximately 6.5×10^6 hPDL cells were subcultured in CelVivo 10 ml bioreactors (CelVivo), and the 3D hPDL cell spheroids were acquired in the rotational 3D cell culture system (CelVivo) in a humidified atmosphere with 5% CO_2 at 37°C at the rotation speed of 2 rpm. Once the spheroids formed, 10 ng/ml recombinant irisin (Adipogen) or equal volume of sterile MilliQ water (control for recombinant irisin) were administered to the culture medium. The spheroids were cultured for 14 days, culture medium was refreshed 24 h prior harvest and collected at day 1, 3, 7 and 14 for Luminex assay. Spheroids were harvested at day 14 and stored at −80°C prior to further analyses.

2.2 | RNA extraction, cDNA synthesis and qPCR analysis

Total RNA was extracted from 3D hPDL cell spheroids using TRIzol (Ambion, Life Technologies) method,[24] and the cDNA was synthesized using a Revert Aid First Strand cDNA Synthesis Kit (K1622, Thermo

Fisher Scientific) according to manufacturer's instructions. qPCR analysis was performed using IQ SYBR Green Supermix (Bio Rad) in a total volume of 20 μl (1 ng cDNA) in a CFX384 Touch Real-Time PCR Detection System (Bio Rad). The $^{\Delta\Delta}$Ct method[25] was adopted to calculate the relative mRNA levels of the genes that were normalized to GAPDH. Primers used in this study were synthesized by Invitrogen (Thermo Fisher Scientific), and are listed as follows: *GAPDH*, forward 5′-CTCTGCTCCTCCTGTTCGAC-3′, reverse 5′-ACGACCAAATC CGTTGACTC-3′; collagen type I, forward 5′-CATCTCCCCTTCGT TTTTGA-3′, reverse 5′-CCAAATCCGATGTTTCTGCT-3′; fibronectin, forward 5′-GATGCTCCCACTAACCTCCA-3′, reverse 5′-CGGTC AGTCGGTATCCTGTT-3′; Periostin, forward 5′-GCCCTGGTTATATG AGAATGGA-3′, reverse 5′-ATGCCCAGGTGCCATAAAC-3′; alkaline phosphatase (*ALP*), forward 5′-GACAAGAAGCCCTTCACTGC-3′, reverse 5′-AGACTGCGCCTGGTAGTTGT-3′; osteocalcin (*OCN*), forward 5′-GCAAGTAGCGCCAATCTAGG-3′, reverse 5′-GCTTCACC CTCGAAATGGTA-3′; bone morphogenetic protein 2 (*BMP2*), forward 5′-TCAAGCCAAACACAAACAGC-3′, reverse 5′-AGCCACAA TCCAGTCATTCC-3′; Runt-related transcription factor 2 (*RUNX2*), forward 5′-TTACTTACACCCCGCCAGTC-3′, reverse 5′-CACTCTGG CTTTGGGAAGAG-3′; osterix (*OSX*), forward 5′-TACCCCATCTCCCT TGACTG-3′, reverse 5′-GCTGCAAGCTCTCCATAACC-3′.

2.3 | Microarray analysis

Microarray analyses were performed using the Affymetrix GeneChip Clariom S Human Arrays (Affymetrix). Total RNA (150 ng) was subjected to the GeneChip WT PLUS Reagent Kit (WT PLUS Kit), following the manufacturer's protocol for whole-genome gene expression analysis (Affymetrix). Biotinylated and fragmented single-stranded cDNAs were hybridized to the GeneChips. The arrays were washed and stained using an FS-450 fluidics station (Affymetrix). Signal intensities were detected by a Hewlett Packard 3000 7G gene array scanner. The scanned images were processed using the Affymetrix GeneChip Command Console software, and the CEL files were imported into Partek Genomics Suite software (Partek). The robust multichip analysis (RMA) algorithm was applied for the generation of signal values and normalization.

2.4 | Differential gene expression analysis

Differential expression analysis was performed using the R package: limma (version 3.52.4).[26] A threshold of mRNA was used for $p < .05$ and |log2 fold change [FC]| > 0.5. Volcano plot and expression heat map were visualized using ggplot2 (version 3.3.3).

2.5 | Functional enrichment analysis

Functional enrichment analysis was performed on the factors obtained from the differential analysis using the clusterProfiler package (version 3.14.3).[27] Gene ontology (GO) enrichments (including biological process (BP), cellular component (CC) and molecular function (MF)). Networks of protein–protein association were performed with STRING DB[28] (http://string-db.org).

2.6 | Ingenuity pathways analysis (IPA)

Microarray analysis raw data were uploaded to IPA system (http://www.ingenuity.com/, Redwood City, CA, USA) to classify genes into signaling pathways.

2.7 | Histological analysis of 3D hPDL cell spheroids

The hPDL cell spheroids were harvested and washed 3 times in PBS, fixed in 4% paraformaldehyde for 15 min, then embedded in optimal cutting temperature (OCT) compound (Leica). 7-μm thickness serial sections of the spheroids were acquired with a CryoStar™ NX70 Cryostat (Thermo Fisher Scientific), mounted onto glass slides and stored at −20°C for further use.

To characterize the morphology of the hPDL cells in the spheroids, a modified version of Goldner's trichrome method was adopted to stain the sections. Weigert's hematoxylin solution, fuchsine acid, orange G, tungstophosphoric acid, acetic acid and Entellan mounting medium were purchased from Merck KGaA (Merck), chromotrope 2R and fast green powder were purchased from Sigma (Sigma-Aldrich). In brief, spheroid sections were washed in tap water for 5 min, stained in hematoxylin solution for 5 min and washed again with water for 5 min. Sections were then incubated in chromotrope 2R/fuchsine acid for 15 min, followed by 2 min wash in 1% acetic acid for 3 times. Afterwards, sections were stained with orange G for 7 min, washed in 1% acetic acid, stained with fast green for 20 min and washed in 1% acetic acid. After dehydration in 96% and 99% ethanol, samples were mounted with Entellan mounting medium and covered by cover slips. Images were captured with a Leica DM RBE microscope (Leica Microsystems CMS GmbH).

For immunofluorescence analysis, sections of hPDL cell spheroids were firstly permeabilized with 0.1% Triton X-100 (Sigma-Aldrich) diluted in PBS for 5 min at room temperature. Sections were washed with PBS, blocked with 10% normal goat serum (NGS) (Abcam) for 1 h at room temperature in a humidified dark chamber. Sections were then incubated with rabbit anti-periostin antibody (1:300, ab14041, Abcam), mouse anti-collagen type I antibody (1:300, ab90395, Abcam), rabbit anti-fibronectin antibody (1:300, ab2413, Abcam) and rabbit anti-von Willebrand factor (vWF) antibody (1:1000, ab6994, Abcam) in 2% NGS overnight at 4°C. On the following day, sections were washed 3 times with PBS, stained with Alexa Fluor 488-conjugated goat anti-rabbit secondary antibody (Invitrogen, Thermo Fisher Scientific), Alexa Fluor 568-conjugated goat anti-mouse secondary antibody (Invitrogen, Thermo Fisher Scientific) at 1:500 dilution or Alexa Fluor 568-conjugated phalloidin

(Invitrogen, Thermo Fisher Scientific) at 1:400 dilution in 4% NGS for 1 h at room temperature. After incubation, sections were washed 3 times with PBS, stained with 300 nM 4′,6-diamidino-2-phenylindole (DAPI) (Sigma-Aldrich) for 20 min at room temperature, and covered by glass slips with Mowiol mounting medium, which was made from Mowiol 4-88 (Sigma-Aldrich) according to Cold Spring Harbor protocol.[29] Confocal images were captured with a Leica SP8 confocal microscope (Leica Microsystems CMS GmbH) using 405, 488 and 552 nm excitation, and 420–480, 500–550 and 580–630 nm emission filters for DAPI, Alexa Fluor 488 and Alexa Fluor 568, respectively. Optical density of confocal images taken at 40× objective lens was measured with IMAGE J software (NIH; https://imagej.nih.gov/ij/). For each image, 5 random regions of interest (ROI) were captured and quantified for their mean intensity and the imaging settings were kept constant during individual acquisition of confocal image.

2.8 | Mechanical testing of 3D hPDL cell spheroids

The mechanical properties of the 3D hPDL cell spheroids were characterized via nanoindentation using Hysitron TI950 TriboIndenter® (Hysitron). The conventional nanoindentation was not applicable due to the irregular geometry of the spheroids. Therefore, a so-called flat punch method for compression test of particle-like materials was adopted.[30] The spheroids were placed on a silicon chip and compressed by a diamond flat punch with a diameter of 1.08 mm, comparable with sample size, as illustrated in a previous study.[22] The set up for nanoindentation and the calculation of nominal stress and strain were performed as previously described.[23]

2.9 | Immunoassay: quantification of secreted proteins in the cell culture medium

A simultaneous quantification of the concentration of biomarkers in 25 µl aliquots of cell culture media after 1, 3, 7 and 14 days of culture were determined using the human myokine magnetic bead panel (HMYOMAG-56K) (Millipore). This multianalyte profiling of the protein levels in the culture medium from 3D hPDL cell spheroids treated with or without irisin were performed using the Luminex 200 system (Luminex) employing xMAP (multianalyte profiling) technology. Acquired fluorescence data were then analyzed using the XPONENT 3.1 software (Luminex), and the analyses were performed according to the manufacturer's instructions.

2.10 | Statistical analysis

Statistical analysis was performed using SIGMAPLOT software (version 14.0, Systat Software). Data from qPCR, mean intensities from the confocal images were compared between the two groups using unpaired Student's *t* test as both normality test and equality test passed. A probability of ≤.05 was considered significant. All experiments were performed in triplicates except for mean intensities from the confocal images ($n = 5$).

3 | RESULTS

3.1 | Differential gene expression and functional analysis of 3D hPDL cell spheroids exposed to irisin

Approximately 1000 genes were significantly up- or downregulated after irisin treatment for 14 days (FC ≥ |0.5|, p-value<.05) compared to untreated controls. Of these, 535 genes showed significant upregulation and 667 genes showed significant downregulation compared to untreated control. The top 50 up- and downregulated genes were visualized as a heat map (Figure 1A) and box plots (Figure S1), and were also used to perform principal component analysis (PCA), at the PC2, where the differentially expressed genes (DEGs) were significantly distinguished among the irisin-exposed and control groups (76.5%) (Figure 1B). Of all the genes with significant differences, a total of 15 genes encoding proteins were found to be interlinked (Figure S2).

The biological functions most significantly associated with irisin treatment in 3D hPDL cell spheroids were identified using Gene Ontology/Kyoto Encyclopedia of Genes and Genomes (GO/KEGG analysis) and listed in Table 1. In addition, the ten most up- and downregulated genes are listed in Table 2. In the GO/KEGG analysis, we found four biological process (BP) and one molecular function (MF) show significant aggregation: extracellular matrix organization, extracellular structure organization, negative regulation of nucleocytoplasmic transport, collagen catabolic process and bitter taste receptor activity (Table 1). All these BP and MF were downregulated upon treatment with irisin. Notably, several matrix metalloproteinases (MMPs) *MMP-1*, *MMP-3*, *MMP-13* and *MMP-17* were implicated in extracellular matrix organization, extracellular structure organization, and collagen catabolic process (Figure 1C). Interestingly, *TAS2R46*, *TAS2R10*, *TAS2R4*, *TAS2R20*, *TAS2R60* and *TAS2R38*, which belong to bitter taste receptor family, were also observed to be differentially expressed (Figure 1C).

Several ubiquitination related genes were found among those that were differentially significantly expressed after irisin exposure (also shown in the heat map, and $p < .05$). Further, microarray dataset exploration showed that *USP53* was significantly downregulated while *USP2*, *USP43*, and several members of the USP17L family were significantly upregulated upon irisin exposure. Among the USP17L family members, in the hPDL spheroids studied here, the most differentially significantly upregulated family members compared to the control were *USP17L11*, *USP17L22* and *USP17L29*; the highest mRNA expression among the *USP17L* family members was documented for *USP17L13* and *USP17L17* (Figure S3A,B).

Similarly, due to their overrepresentation among the most significant DEGs, the datasets were mined for significant differential expression of zinc-finger proteins (ZNFs) family members ($p < .05$).

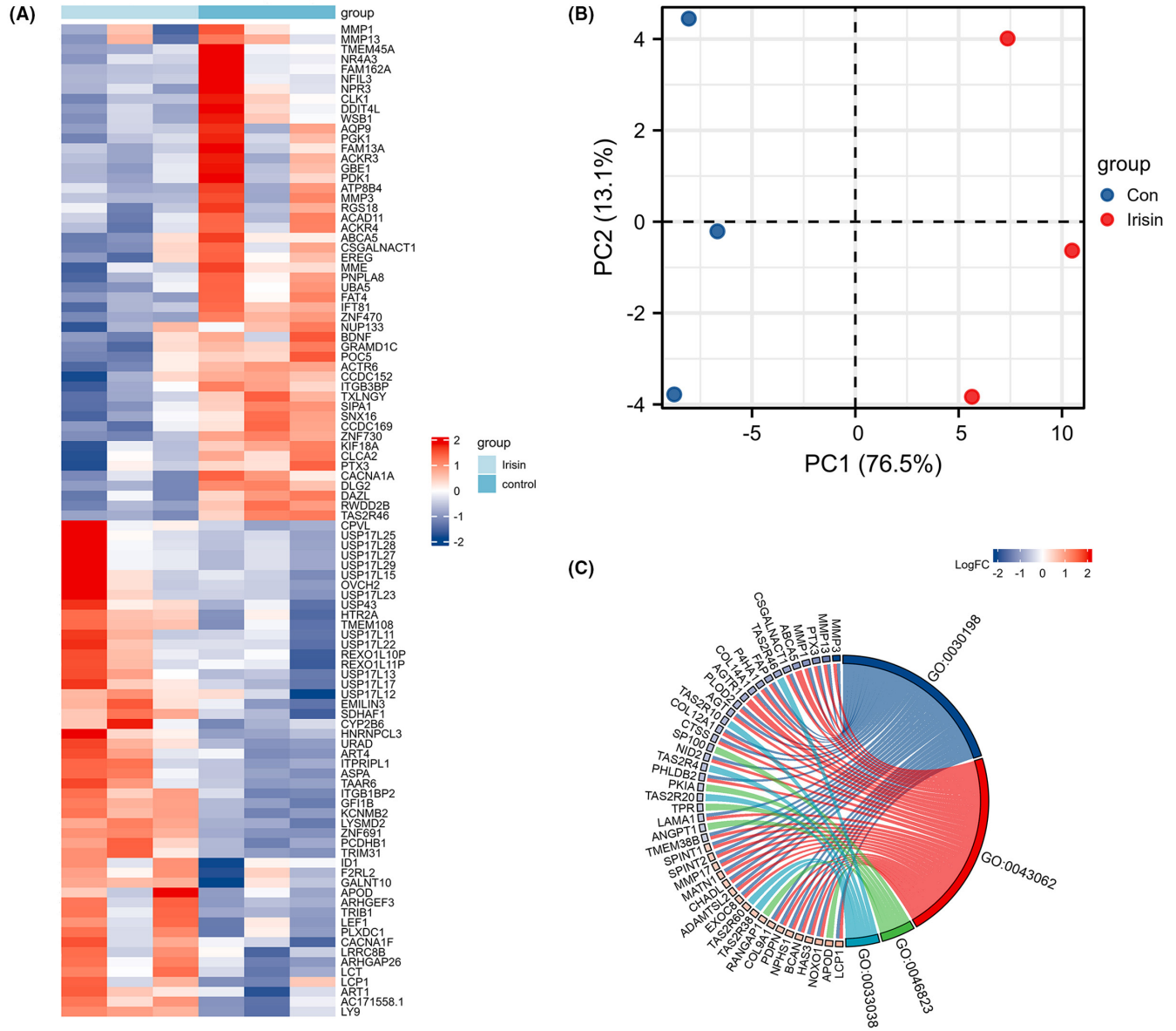

FIGURE 1 Analysis of Differentially Expressed Genes (DEGs). (A) Cluster analysis heatmap of top 50 up- and downregulated mRNAs (FC ≥ |0.5| and *p*-value < .05) expressed in irisin-treated and control 3D hPDL cell spheroids. Each column represents data from one 3D spheroid and each row represents individual genes, red color is used to represent genes which were upregulated, and blue color is used to represent genes which were downregulated. The color key is indicated on the right side of the heat map. (B) Principal component analysis based on top 50 significantly up- and downregulated DEGs. (C) GO/KEGG analysis based on DEGs.

ZNF691 and *ZNF367* were the two most significantly upregulated genes, while *ZNF14*, *ZNF248*, *ZNF331*, *ZNF470* and *ZNF730* were the most significantly downregulated genes of the ZNF family in the hPDL spheroids treated with irisin (Figure S3A,C).

3.2 | Enriched canonical pathways detected using IPA

The list of enriched canonical signaling pathways significantly associated with irisin treatment is presented in (Figure 2). A total of 13 pathways were identified by applying the −log(*p*-value) > 1.3 threshold and ranked according to their −log(*p*-value). Among these pathways, it was observed that coronavirus replication pathway, actin cytoskeleton signaling, integrin signaling, aldosterone signaling in epithelial cells, signaling by Rho-family GTPases, and bladder cancer signaling were upregulated, while valine degradation I, GDNF family ligand-receptor interactions, thyroid cancer signaling, paxillin signaling, autophagy, apelin adipocyte signaling pathway, and tRNA charging were downregulated.

3.3 | Morphology of 3D hPDL cell spheroids

The spheroids exhibited a homogeneous nearly round-shaped appearance. Goldner's trichrome and phalloidin staining of sections indicated an internal organization of cells and ECM in loose tubular structure, which was separated by well distributed strip-like tissues

TABLE 1 Biological process and molecular functions by GO/KEGG analysis

Ontology	ID	Description	GeneRatio	BgRatio	*p*-Value	*q*-Value	*z*-Score
BP	GO:0030198	Extracellular matrix organization	30/606	368/18 670	3.91 e-06	0.017	−0.365
BP	GO:0043062	Extracellular structure organization	32/606	422/18 670	8.48 e-06	0.018	−0.707
BP	GO:0046823	Negative regulation of nucleocytoplasmic transport	6/606	20/18 670	3.00 e-05	0.042	−0.816
BP	GO:0030574	Collagen catabolic process	3/38	47/18 670	.000118572	0.07312585	−1.732
MF	GO:0033038	Bitter taste receptor activity	6/608	23/17 697	9.82 e-05	0.072	−0.816

TABLE 2 Top 10 up- and downregulated genes induced by 10 ng/ml irisin in the 3D hPDL cell spheroids compared to untreated controls

10 most upregulated genes			10 most downregulated genes		
Gene symbol	Fold change	*p*-Value	Gene symbol	Fold change	*p*-Value
PLXDC1	1.22	.012	MMP3	−2.20	.020
AC171558.1	1.18	.001	NR4A3	−2.20	.047
LEF1	1.15	.013	CLCA2	−1.68	.003
USP17L22	1.15	.016	PDK1	−1.62	.030
USP17L11	1.12	.023	MME	−1.56	.005
USP17L27	1.08	.039	ATP8B4	−1.50	.030
USP17L29	1.08	.039	MMP13	−1.41	.045
USP17L13	1.08	.002	ACKR3	−1.39	.045
REXO1L10P	1.07	.016	KIF18A	−1.39	.001
USP17L23	1.04	.025	PGK1	−1.37	.011

(Figure 3). By contrast, a rim-like structure was observed on the outer area of the irisin-treated spheroids (Figure 3A,B).

3.4 | Irisin enhances the extracellular matrix deposition in 3D hPDL cell spheroids

Irisin was found to promote ECM formation in spheroids, identified by significantly enhanced collagen type I deposition, compared to control (1.35-fold) ($p = .009$) (Figure 4A,B). The periostin level, which has been proved to mediate biomechanical properties of connective tissues and ECM formation,[31] was also enhanced by irisin in the 3D hPDL cell spheroids by 1.2-fold after 14 days ($p = .006$) (Figure 4A,C). Fibronectin, which is vital in regulating the composition and organization of ECM,[32] was also increased by 1.35-fold in comparison with control ($p = .001$) after 14 days of incubation in the irisin-exposed spheroids (Figure 5A,B). Notably, a similar rim-like structure was also well-characterized around the spheroids exposed to irisin in these stained samples (indicated by arrows, Figures 4A and 5A).

3.5 | Irisin enhances the mechanical properties of 3D hPDL cell spheroids

Since collagen type I has an impact on the mechanical properties of PDL tissues, we thus investigated whether irisin affected the stiffness of hPDL cell spheroids. The potential effects of irisin treatment on the mechanical properties of the 3D hPDL cell spheroids are described by the nominal stress–strain response assessment (Figure 6). The tangent stiffness was obtained by the linearly connecting the stress at each cyclic peak on the loading part of the stress–strain curves. There is a sharp turning point at around strain 0.025 for the irisin-treated sample, that turning point might be due to the liquid in the spheroids being squeezed out during nanoindentation. From the stress–strain curve, it is obvious that the irisin-treated hPDL cell spheroid is much stronger than the control counterpart, demonstrating a strengthening effect of irisin on the mechanical stiffness.

3.6 | Irisin induces osteogenic behavior of 3D hPDL cell spheroids

As the ECM deposition affects osteogenesis, we evaluated the mRNA expression of several ECM and osteogenic markers genes to compare osteogenic potential of 3D hPDL cell spheroids exposed or not exposed to irisin. After 14 days of culture, irisin induced a 5.7-fold ($p < .0001$) in the mRNA expression of the ECM markers collagen type I (Figure 7A) and a 2.5-fold ($p < .0001$) increase in fibronectin (Figure 7B) compared with control. In contrast, the mRNA expression of periostin was reduced by 0.8-fold ($p = .0003$) compared to control (Figure 7C). Similarly, *OCN* (Figure 7E), *BMP2* (Figure 7F), *RUNX2* (Figure 7G) and *OSX* (Figure 7H) were enhanced

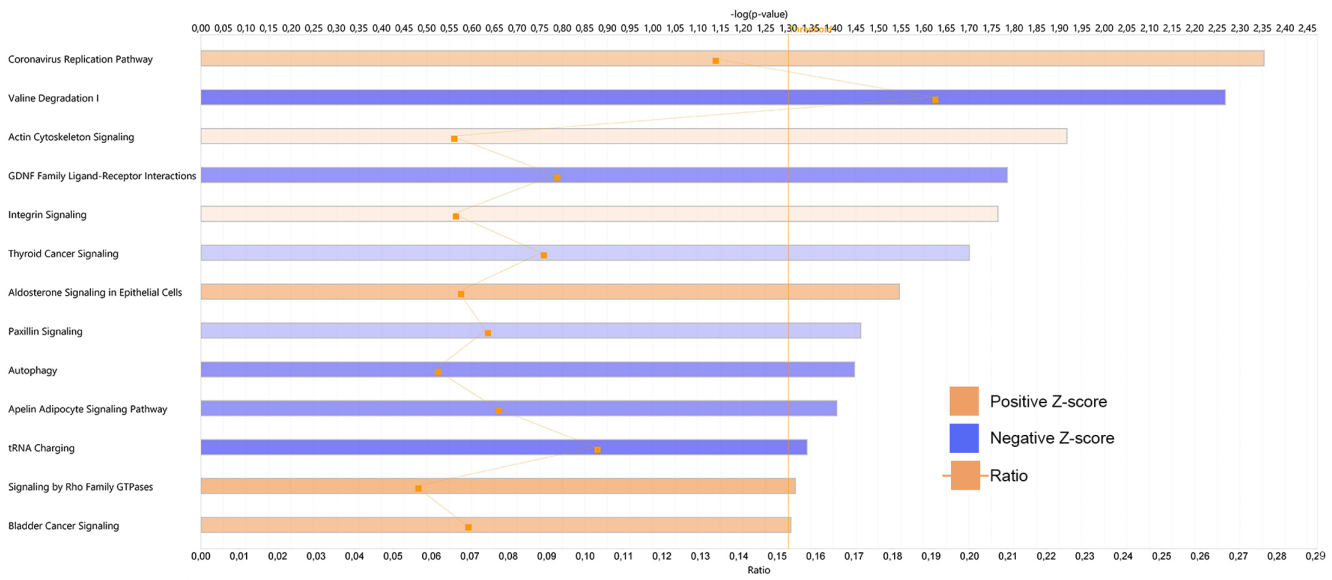

FIGURE 2 Histogram of 13 canonical pathways. The *Y*-axis represents the −log(*p*-value), *X*-axis indicates each of the representative canonical pathways. Orange bar indicates positive *Z*-score, blue bar indicates negative *Z*-score. Ratio (differential orange line and box markers) refers to the number of molecules in a given pathway that meet the −log(*p*-value) threshold 1.3 divided by the total number of molecules that make up the pathway from within the IPA knowledge database.

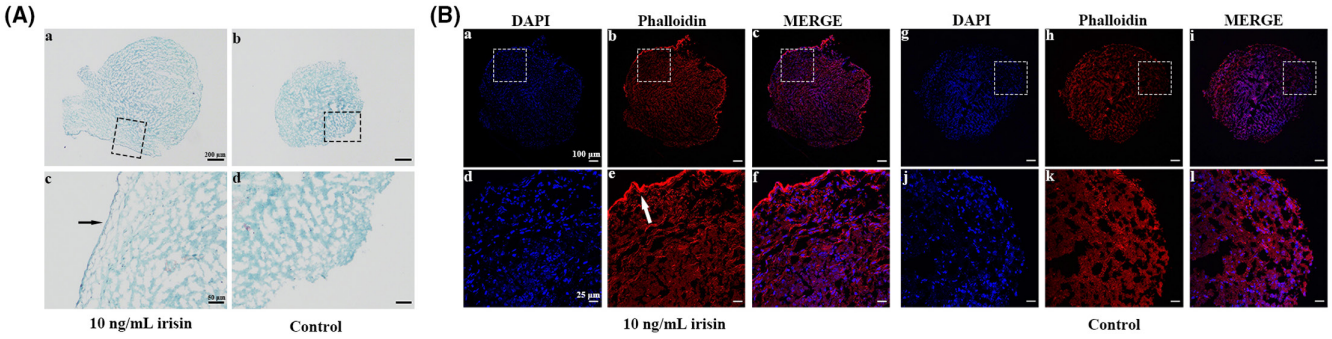

FIGURE 3 Morphological characterization of 3D hPDL cells treated with and without 10 ng/ml irisin by Goldner trichrome method and phalloidin. (A) Goldner trichrome staining (a and b) showed that spheroids treated with 10 ng/mL irisin developed a rim-like tissue around the spheroid while control spheroids did not. Boxed areas are shown at a higher magnification (c and d). Arrows indicated the rim-like tissues. (B) Likewise, similar rim-like tissues were observed in phalloidin-stained spheroid supplemented with irisin but not pronounced in control (b, e, h and k), nuclei are counterstained with DAPI (a, d, g and j), merged images of phalloidin and DAPI are shown in c, f, i and l. Boxed areas are shown at a higher magnification (d, e, f, j, k and l). Arrows indicated the rim-like tissues.

by 2-fold ($p = .0002$), 1.6-fold ($p = .0002$), 1.8-fold ($p < .0001$) and 3-fold ($p < .0001$), respectively. However, the expression of the early marker of osteoblast differentiation, *ALP* (Figure 7D), was reduced by 0.8-fold ($p = .048$) in irisin-treated hPDL cell spheroids.

3.7 | Irisin promotes the angiogenic potential of 3D hPDL cell spheroids

Angiogenesis, which refers to the formation of new blood vessels, plays an important role in guiding bone and dental tissue regeneration.[33] To achieve periodontal tissue regeneration, the combination of angiogenic and osteoinductive to promote bone formation has emerged as a novel approach.[34] Additionally, the angiogenic effect of irisin has previously been described in vivo and in vitro using human umbilical vein endothelial cells.[35] Here we demonstrate for the first time the ability of irisin to induce angiogenic activity in 3D cultured hPDL cell spheroids. The expression of the vascular endothelial cell marker vWF, was enhanced by 1.8-fold in the spheroids cultured with irisin compared with control at day 14, as evidenced by confocal laser scanning microscopy imaging and fluorescence intensity quantification ($p = .0004$) (Figure 8A,B).

3.8 | Irisin regulates myokines secretion from 3D hPDL cell spheroids

The concentration of osteonectin in the culture medium from the hPDL cell spheroids exposed to irisin was lower compared to control both on day 3 ($p = .0192$) and on day 14 (Figure 9A). The secretion

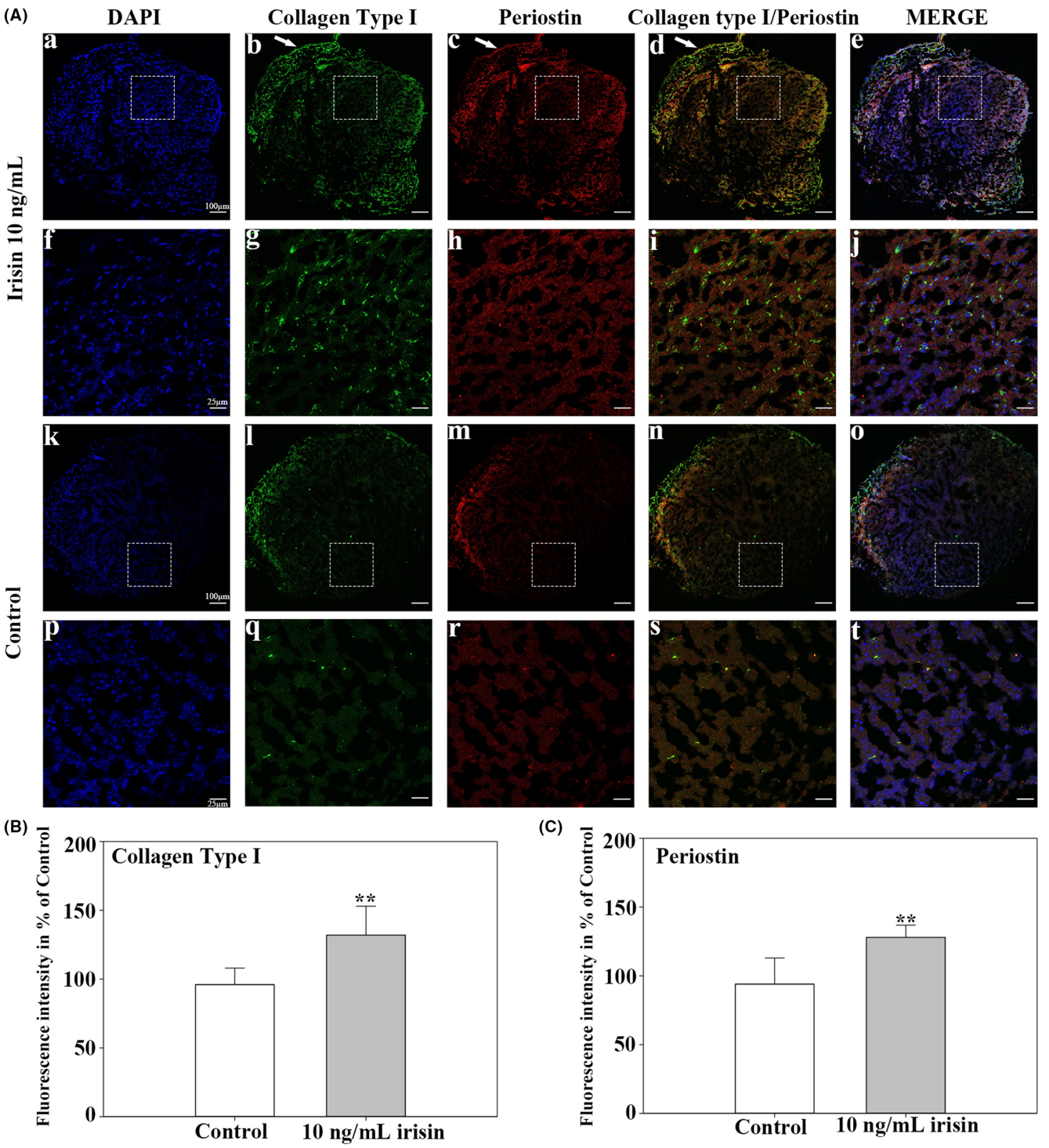

FIGURE 4 Confocal images of 3D hPDL cell spheroid sections treated with and without 10 ng/ml irisin immunolabeled with Collagen type I and Periostin and quantification of immunofluorescence intensity. (A) Histological sections of spheroids were analyzed by immunofluorescence staining for Collagen type I and Periostin (b, c, g, h, l, m, q and r), nuclei were counterstained with DAPI (a, f, k and p), merged images of Collagen type I and Periostin are shown in d, i, n and s, merged images of nuclei, Collagen type I and Periostin are presented in e, j, o and t. Boxed areas are shown at a higher magnification in f, g, h, i, j, p, q, r, s and t. Arrows indicate rim-like tissues. (B) Quantification of Collagen type I fluorescence intensity in % of control. (C) Quantification of Periostin fluorescence intensity in % of control. Mean fluorescence intensities were measured from five random regions of interest in each section. Significantly different from control at $^{*}p \leq .05$, $^{**}p \leq .01$ and $^{***}p \leq .001$.

of leukemia inhibitory factor (LIF) in culture medium from spheroids treated with irisin was increased at day 3 ($p = .0439$) but thereafter attenuated significantly at day 7 ($p = .0004$) and day 14 ($p = .0018$) compared to control (Figure 9B). Secretion of interleukin 6 (IL-6) was significantly reduced from spheroids with irisin at day 1 ($p = .0001$), day 7 ($p = .0025$) and day 14 ($p = .0024$), when compared to the

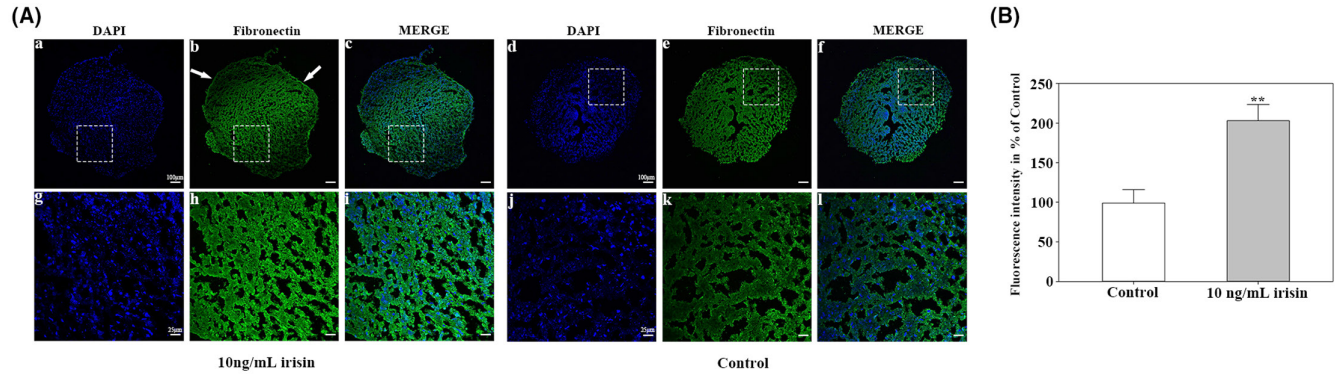

FIGURE 5 Confocal images of 3D hPDL cell spheroid sections treated with and without 10 ng/mL irisin immunolabeled with fibronectin and quantification of immunofluorescence intensity. (A) Histological sections of spheroids were analyzed by immunofluorescence staining for fibronectin (b, h, e and k), nuclei were counterstained with DAPI (a, g, d and j), merged images of fibronectin and nuclei are shown in c, i, f and l. Boxed areas are shown at a higher magnification in g, h, i, j, k and l. Arrows indicate the rim-like tissues. (B) Quantification of fibronectin fluorescence intensity in % of control. Mean fluorescence intensities were measured from five random regions of interest in each section. Significantly different from control at $^{*}p \leq .05$, $^{**}p \leq .01$ and $^{***}p \leq .001$.

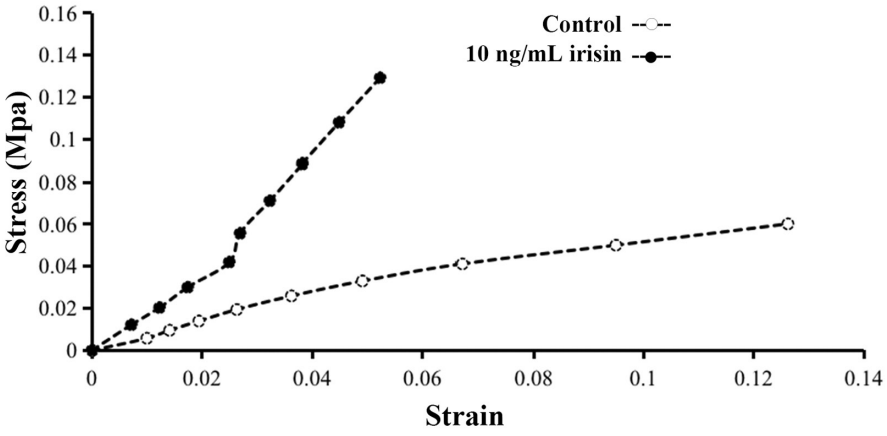

FIGURE 6 The stress–strain relationship from 3D hPDL cell spheroids treated with and without 10 ng/ml irisin.

control (Figure 9C). The concentrations of the other factors tested (apelin, BDNF, erythropoietin, FABP3, FGF-21, fractalkine/CX3CL1, follistatin-like protein 1, IL-15, irisin, myostatin/GDF8, oncostatin M, osteocrin/musclin) were lower than the set levels of detection for the analyses.

4 | DISCUSSION

To the authors' best knowledge, this is the first study on the effects of recombinant irisin on different biological behaviors of 3D cultured hPDL cells.

We used Affymetrix microarray analysis to profile the mRNA expression patterns between 3D hPDL cell spheroids under standard culture conditions or exposed to irisin. The mRNA expression profiling identified approximately 1000 mRNAs that were differentially expressed between the two groups, suggesting that irisin is involved in gene regulation in hPDL cells. Further, the GO/KEGG analysis screened out some important biological processes (BPs) related to ECM remodeling, and these BPs shared several MMPs family genes. MMPs are a family of zinc-binding metalloproteinases that can degrade all ECM components,[36] and these collagenases can be enhanced by chronic inflammation (IL-1 and TNFα).[37] In periodontal diseases, degradation of collagen fibers is induced by MMPs released by the PDL cells in response to inflammatory stimuli.[11] Based on GO/KEGG results, *MMP-1*, *MMP-3* and *MMP-13* are all downregulated in irisin-treated 3D hPDL cell spheroids, this indicates that irisin induces a negative transcriptional regulation of collagenase genes, which conforms to a previous study that irisin decreased *MMP-1* and *MMP-13* expression in osteoarthritic chondrocytes.[38] These findings support a role of irisin in ECM integrity maintenance by inhibiting the breakdown of collagens in the 3D hPDL cell spheroids and alleviating periodontal inflammation.

Additionally, bitter taste receptor activity is identified by GO/KEGG analysis. Bitter taste-sensing type 2 receptor family subtypes (TAS2Rs) play key roles in perceiving bitterness and are distributed throughout the body including periodontal ligament, and thus termed non-lingual receptors.[39] TAS2Rs have been associated with immune response and microbiome regulation.[40] The role of TAS2Rs family in PDL is unknown, however, it was recently shown that in human dental pulp stem cells (DPSCs), *TAS2Rs* were correlated to odontoblastic differentiation in an inflammatory microenvironment, mediating the

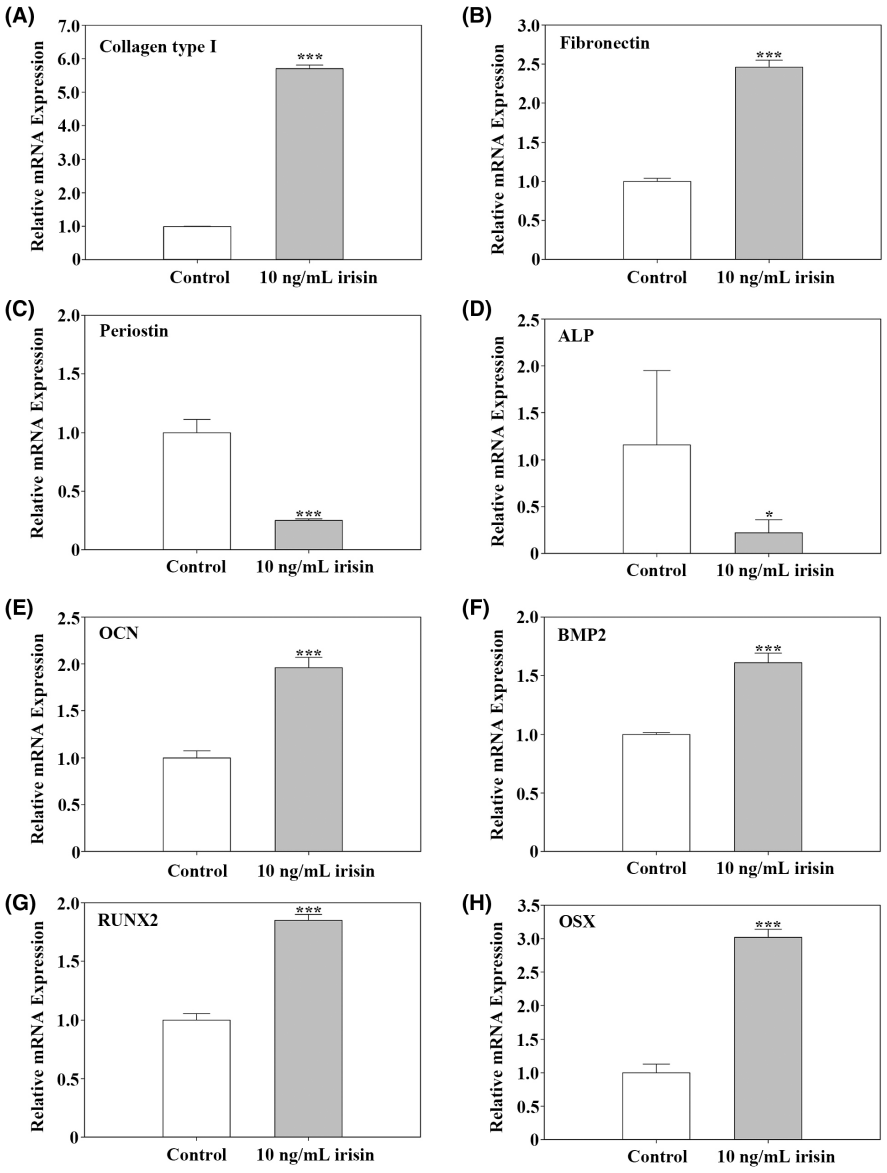

FIGURE 7 Relative mRNA expression levels for ECM and osteoblast differentiation marker genes collagen type I (A), fibronectin (B), periostin (C), *ALP* (D), *OCN* (E), *BMP2* (F), *RUNX2* (G), *OSX* (H) in 3D hPDL cell spheroids treated with and without irisin are normalized to reference gene *GAPDH* and presented as fold change relative to controls. All values represent the mean ± SD of 3 independent experiments. Significantly different from control at $^{*}p \leq .05$, $^{**}p \leq .01$ and $^{***}p \leq .001$.

increase in intracellular Ca2+ via conventional G protein-coupled receptors (GPCR) signaling.[41] Upon irisin exposure *TAS2R10* was downregulated in the 3D hPDL cell spheroids presented here, while in the DPSC study reported that when *TAS2R10* was silenced, odontoblastic differentiation of hDPSCs was reduced.[41] This could thus, also infer that in the 3D hPDL culture model, irisin exposure mediated effects on differentiation.

Intriguingly, the microarray dataset analyses, also documented a role for irisin in ubiquitination in the hPDL cells under spheroid culture. *USP53* was significantly downregulated while *USP2* and *USP43* and several members of the ubiquitin specific peptidase 17 like family (*USP17L*) were significantly upregulated in the irisin-exposed samples analyzed. The roles of these enzyme in bone development have been under intense study.[42] *UPS53* was previously described to enhance Wnt/β-catenin signaling in mesenchymal stem cells (MSCs) undergoing osteogenic differentiation,[43] while its knockdown increased osteoblast numbers and decreased adipocyte counts, in mice.[44] *USP43* abundance was previously shown to increases with increasing cell density and found in cells close to E-cadherin at sites of cell–cell contacts.[45] These findings document a multiparametric and possibly causal role of irisin in ubiquitination, where its functions might also be mediated via these deubiquitinating enzymes to regulate cellular processes, including cell proliferation, differentiation progress and cell migration.

Irisin exposure further affected the expression of several ZNF genes in the hPDL spheroids. Targeted microarray dataset mining identified that *ZNF691* and *ZNF367* were the most significantly upregulated genes in the irisin-exposed spheroids; *ZNF14*, *ZNF248*, *ZNF331*, *ZNF470* and *ZNF730* were the most significantly downregulated genes of the ZNF family in the hPDL spheroids treated with irisin. Further studies will investigate the effect of irisin on the corresponding pathways. However, it remains to be interested that although the function of the majority of ZNF genes in hPDL cells is largely unknown, in other cell models their functions are considered crucial in proliferation, development and differentiation.[46]

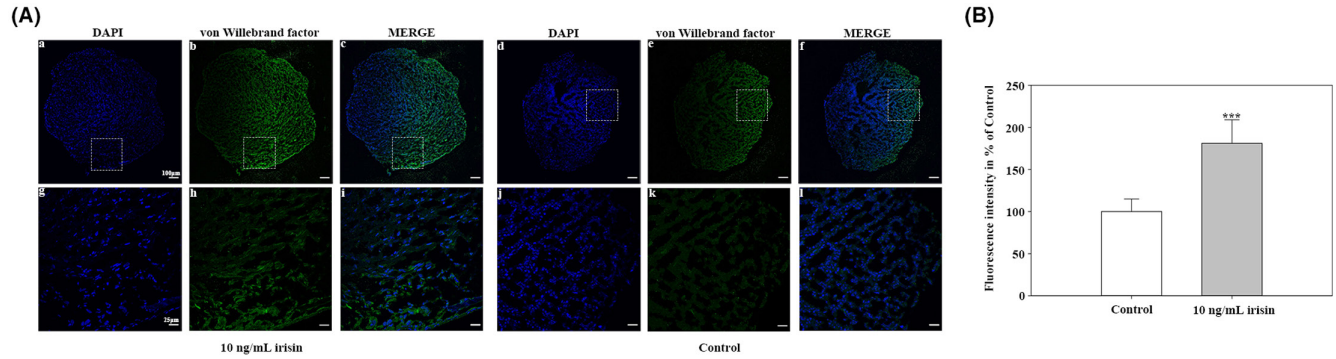

FIGURE 8 Confocal images of 3D hPDL cell spheroid sections treated with and without 10 ng/ml irisin immunolabeled with vWF and quantification of immunofluorescence intensity. (A) Histological sections of spheroids were analyzed by immunofluorescence staining for vWF (b, h, e and k), nuclei were counterstained with DAPI (a, g, d and j), merged images of vWF and nuclei are shown in c, i, f and l. Boxed areas are shown at a higher magnification in g, h, i, j, k and l. (B) Quantification of vWF fluorescence intensity in % of control. Mean fluorescence intensities were measured from five random regions of interest in each section. Significantly different from control at $^{*}p \leq .05$, $^{**}p \leq .01$ and $^{***}p \leq .001$.

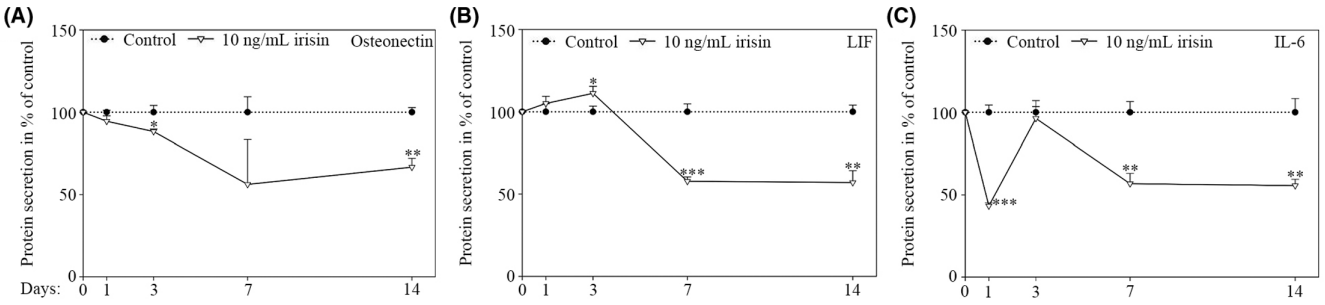

FIGURE 9 Secretion of (A) osteonectin, (B) LIF, and (C) IL-6 to culture medium from 3D-cultured hPDL cell spheroids treated with and without irisin is shown in percentage of control at day 0, 1, 3, 7 and 14. Values represent the mean ± SD. Significantly different from control at $^{*}p \leq .05$, $^{**}p \leq .01$ and $^{***}p \leq .001$.

The IPA analysis also identified several important signaling pathways involved upon irisin exposure. Interestingly, we found that coronavirus replication pathway was activated upon irisin treatment, though irisin has been reported to counteract the adverse effects of COVID-19 during the various disease stages,[47] no research up to date has studied its role on coronavirus-infected hPDL cells yet. The actin cytoskeleton rearrangement is key to both withstanding extracellular mechanical strain and intracellular structural support, and inhibition of actin cytoskeleton leads to down regulation of collagen type I,[48] the activation of actin cytoskeleton signaling may suggest reinforcement of ECM by irisin. Integrins affect an array of signal transduction cascades which mediate cell survival, proliferation, differentiation and organ development.[49] It is also noteworthy that irisin was recently identified as a ligand for the integrins αVβ5, αVβ1, and α5β1 expressed on mesenchymal cells.[50,51] Rho-family GTPases are of critical importance in integrating intracellular signals downstream of mechano-sensors, hence promoting re-organization of the actin cytoskeleton which is necessary for cell-shape alterations and eventually migration.[52] Valine is one of the branched-chain amino acids that is needed to synthesize proteins, it can enhance mammary cell growth.[53] The irisin-induced upregulation of Rho-family GTPases and downregulation of valine degradation I signaling indicate that irisin promotes migration and helps maintain the cell growth in 3D hPDL cell spheroids, which is in line with previous study of hPDL cells cultured in 2D.[14]

An increase of several ECM-related markers like collagen type I, periostin and fibronectin was observed by immunofluorescent staining. Periostin is able to directly bind to collagen type I and form a complex, thus enhancing their assembly into ECM and contributing to the mechanical strength of connective tissues.[31,54] Fibronectin is one of the main elements in basement membrane (BM), which comprises the ECM along with interstitial matrix, BM structure is more compact and less porous,[55] the upregulation of fibronectin expression upon irisin treatment implies that irisin may induce a less porous, more organized structure in the spheroids, which could explain the formation of thickened rim-like tissue around irisin-treated spheroids. In addition, the rim-like structure can also be observed in irisin-exposed spheres stained with ECM markers, which further proves that irisin may regulate the morphology of 3D hPDL cell spheroids. The PCR analysis showed that mRNA expression levels of collagen type I and fibronectin were

upregulated in the irisin-treated spheroids, but periostin showed a contradictory trend compared to immunofluorescence quantification. The contradictory results are probably due to the molecules half-lives and the multiple post-transcriptional mechanisms involved, making it difficult to correlate protein expression to mRNA.[56–58]

The PDL is a complicated tissue reinforced by fibers which responds to force in a viscoelastic manner.[59] Its composition mainly consists of collagen fibers along with a few blood vessels and nerve endings.[60] The collagen components are able to resist tension and the fibrous proteins are embedded into the highly hydrated viscous ground substance, which forms the ECM. The ground substances, especially collagen type I, is responsible for the PDL's viscoelastic properties when subject to loading.[13,61] We have observed an increase in both ECM deposition and mechanical strength in the irisin-treated hPDL spheroids, which suggests that irisin may grant the hPDL cell spheroids stiffer mechanical properties by enhancing the deposition of ground substances.

Irisin induced a significant increase in the mRNA expressions of several important osteogenesis-related markers like *RUNX2*, *OSX*, *BMP2* and *OCN*. In contrast, *ALP* was downregulated in the irisin-treated spheroids, which might be explained by *ALP* being produced early in the differentiation phase, before the mineralization takes place. Its expression has been demonstrated to be highest in matrix maturation phase, but as the cultures progress into the mineralization phase, markers like *OCN* are upregulated while the *ALP* expression declines.[62,63] These findings support an osteogenesis-stimulatory role of irisin in 3D hPDL cell spheroids.

Vasculature is essential for bone development, remodeling and homeostasis, to ensure successful osteogenesis, vascularization is required.[64] The PDL itself is a highly vascularized tissue, the vascular activity is important in periodontal remodeling,[65] moreover, the putative role of irisin on promoting osteogenic potential and remodeling of PDL tissues also requires stimulation of blood vessel formation. vWF is a large glycoprotein best known for its critical role in platelet binding to the sub-endothelium during hemostasis, it is widely used as a specific endothelial marker and routinely used to verify vessels in tissue sections.[66] The hPDL cell spheroids treated with irisin demonstrated a significant increase in vWF expression compared with control at day 14, indicating that irisin promoted the angiogenic potential in the spheroids. Taken together, these data further prove that irisin enhances osteogenic differentiation of 3D hPDL cell spheroids.

In the current study, secretion of several myokines like osteonectin, LIF and IL-6 were affected by irisin administration. Osteonectin is a glycoprotein secreted by osteoblasts during bone formation. It shows affinity for both collagen and calcium and is reported to modify the interaction of cells with ECM by increasing the expression of collagenase, stomelysin and metalloproteinases, which are capable of degrading ECM.[67,68] Osteonectin exhibited continued decrease in secretion from irisin-treated hPDL cell spheroids over the 14-day culture, this suggests that ECM degradation may be inhibited by irisin in 3D hPDL cell spheroids. LIF is a multifunctional cytokine which belongs to the IL-6 superfamily, and it can induce inflammation, thus likely to play a regulatory role.[69] The secretion of LIF from irisin-treated hPDL cell spheroids demonstrated a slight increase early in culture but a sharp decrease later on. IL-6 is a pleiotropic pro-inflammatory cytokine, its secretion is promoted in response to inflammation,[70,71] in our study, irisin treatment kept the secretion of IL-6 from 3D hPDL cell spheroids at lower levels throughout the 14-day culture except on day3, in comparison with control. We can thus infer that irisin treatment may influence the ECM remodeling and possibly have a role in alleviating inflammation in 3D hPDL cell spheroids.

5 | CONCLUSIONS

Our study primarily demonstrates that irisin may serve as a clear switch that induces differential expression of a plethora of genes in 3D-cultured hPDL cells, and that these genes are associated with an array of cellular and biological functions. More specifically, administration of irisin increased the ECM deposition, mechanical properties, osteogenic behavior, angiogenic activity and may have a role of alleviating inflammation 3D hPDL cell spheroids, indicating a role for irisin in PDL remodeling and repair. In conclusion, irisin may have a potential role in a therapeutic strategy to restore the structures and functions of periodontal tissues in patients with periodontal diseases.

AUTHOR CONTRIBUTIONS

YY participated in the experimental design, performed experiments, and drafted the manuscript. TXG, AS, OKO, JYH, AEA, BSS, MAL, CAH, and HP participated in experiments, data analysis, and editing of the manuscript. JER initiated the project, designed the setup of experiments, contributed to data analysis and editing of the manuscript.

ACKNOWLEDGEMENT

Yang Yang (CSC number 201908420242) would like to thank China Scholarship Council (CSC) for a personal grant.

FUNDING INFORMATION

We acknowledge the financial support from Research Council of Norway for project no. 287953.

CONFLICT OF INTEREST

The authors declare that they have no known competing financial interests or personal relationships that could have appeared to influence the work reported in this paper.

DATA AVAILABILITY STATEMENT

The Affymetrix data that support the findings of this study are openly available in Gene Expression Omnibus at https://www.ncbi.nlm.nih.gov/geo/query/acc.cgi?acc=GSE206938, reference number GSE206938.

ORCID

Yang Yang https://orcid.org/0000-0003-0427-0764
Athina Samara https://orcid.org/0000-0001-6931-1972
Ole Kristoffer Olstad https://orcid.org/0000-0003-4476-3061
Jianying He https://orcid.org/0000-0001-8485-7893
Anne Eriksson Agger https://orcid.org/0000-0002-9180-1297
Bjørn Helge Skallerud https://orcid.org/0000-0003-4062-8014
Maria A. Landin https://orcid.org/0000-0002-9674-7728
Catherine Anne Heyward https://orcid.org/0000-0002-1567-787X
Helen Pullisaar https://orcid.org/0000-0002-5117-4604
Janne Elin Reseland https://orcid.org/0000-0001-5743-4297

REFERENCES

1. Boström P, Wu J, Jedrychowski MP, et al. A PGC1-α-dependent myokine that drives brown-fat-like development of white fat and thermogenesis. *Nature*. 2012;481(7382):463-468.
2. Castillo-Quan JI. From white to brown fat through the PGC-1α-dependent myokine irisin: implications for diabetes and obesity. *Dis Model Mech*. 2012;5(3):293-295.
3. Chen N, Li Q, Liu J, Jia S. Irisin, an exercise-induced myokine as a metabolic regulator: an updated narrative review. *Diabetes Metab Res Rev*. 2016;32(1):51-59.
4. Colaianni G, Cuscito C, Mongelli T, et al. The myokine irisin increases cortical bone mass. *Proc Natl Acad Sci*. 2015;112(39):12157-12162.
5. Posa F, Colaianni G, Di Cosola M, et al. The myokine irisin promotes osteogenic differentiation of dental bud-derived MSCs. *Biology*. 2021;10(4):295.
6. Yang Y, Pullisaar H, Landin MA, et al. FNDC5/irisin is expressed and regulated differently in human periodontal ligament cells, dental pulp stem cells and osteoblasts. *Arch Oral Biol*. 2021;124:105061.
7. de Jong T, Bakker AD, Everts V, Smit TH. The intricate anatomy of the periodontal ligament and its development: lessons for periodontal regeneration. *J Periodontal Res*. 2017;52(6):965-974.
8. Beertsen W, McCulloch CAG, Sodek J. The periodontal ligament: a unique, multifunctional connective tissue. *Periodontol 2000*. 1997;13(1):20-40.
9. Berkovitz BKB. The structure of the periodontal ligament: an update. *Eur J Orthod*. 1990;12(1):51-76.
10. Watanabe Y, Komatsu K. Biomechanical and morphological studies on the periodontal ligament of the rat molar after treatment with α-amylase in vitro. *Connect Tissue Res*. 1997;36(1):35-49.
11. Sapna G, Gokul S, Bagri-Manjrekar K. Matrix metalloproteinases and periodontal diseases. *Oral Dis*. 2014;20(6):538-550.
12. Somerman MJ, Young MF, Foster RA, Moehring JM, Imm G, Sauk JJ. Characteristics of human periodontal ligament cells in vitro. *Arch Oral Biol*. 1990;35(3):241-247.
13. Liu SH, Yang RS, al-Shaikh R, Lane JM. Collagen in tendon, ligament, and bone healing. A current review. *Clin Orthop Relat Res*. 1995;318:265-278.
14. Pullisaar H, Colaianni G, Lian A-M, Vandevska-Radunovic V, Grano M, Reseland JE. Irisin promotes growth, migration and matrix formation in human periodontal ligament cells. *Arch Oral Biol*. 2020;111:104635.
15. Yamada KM, Cukierman E. Modeling tissue morphogenesis and cancer in 3D. *Cell*. 2007;130(4):601-610.
16. Edmondson R, Broglie JJ, Adcock AF, Yang L. Three-dimensional cell culture systems and their applications in drug discovery and cell-based biosensors. *Assay Drug Dev Technol*. 2014;12(4):207-218.
17. Knight E, Przyborski S. Advances in 3D cell culture technologies enabling tissue-like structures to be created in vitro. *J Anat*. 2015;227(6):746-756.
18. Inanc B, Elcin AE, Elcin YM. Osteogenic induction of human periodontal ligament fibroblasts under two- and three-dimensional culture conditions. *Tissue Eng*. 2006;12(2):257-266.
19. Li M, Yi J, Yang Y, Zheng W, Li Y, Zhao Z. Investigation of optimal orthodontic force at the cellular level through three-dimensionally cultured periodontal ligament cells. *Eur J Orthod*. 2016;38(4):366-372.
20. Moritani Y, Usui M, Sano K, et al. Spheroid culture enhances osteogenic potential of periodontal ligament mesenchymal stem cells. *J Periodontal Res*. 2018;53(5):870-882.
21. Zwezdaryk KJ, Warner JA, Machado HL, Morris CA, Höner zu Bentrup K. Rotating cell culture systems for human cell culture: human trophoblast cells as a model. *J Vis Exp*. 2012;(59):3367. doi:10.3791/3367
22. Haugen S, He J, Sundaresan A, et al. Adiponectin reduces bone stiffness: verified in a three-dimensional artificial human bone model in vitro. *Front Endocrinol*. 2018;9(236):1-12.
23. Schröder M, Riksen EA, He J, et al. Vitamin K2 modulates vitamin D-induced mechanical properties of human 3D bone spheroids In vitro. *JBMR Plus*. 2020;4(9):e10394.
24. Rio DC, Ares M, Hannon GJ, Nilsen TW. Purification of RNA using TRIzol (TRI reagent). *Cold Spring Harb Protoc*. 2010;2010(6):pdb.prot5439.
25. Livak KJ, Schmittgen TD. Analysis of relative gene expression data using real-time quantitative PCR and the 2−ΔΔCT method. *Methods*. 2001;25(4):402-408.
26. Ritchie ME, Phipson B, Wu D, et al. Limma powers differential expression analyses for RNA-sequencing and microarray studies. *Nucleic Acids Res*. 2015;43(7):e47.
27. Love MI, Huber W, Anders S. Moderated estimation of fold change and dispersion for RNA-seq data with DESeq2. *Genome Biol*. 2014;15(12):1-21.
28. Szklarczyk D, Gable AL, Lyon D, et al. STRING v11: protein–protein association networks with increased coverage, supporting functional discovery in genome-wide experimental datasets. *Nucleic Acids Res*. 2019;47(D1):D607-D613.
29. Mowiol embedding medium. *Cold Spring Harb Protoc*. 2010;2010(1):pdb.rec12110.
30. He J, Zhang Z, Kristiansen H. Nanomechanical characterization of single Micron-sized polymer particles. *J Appl Polym Sci*. 2009;113(3):1398-1405.
31. Norris RA, Damon B, Mironov V, et al. Periostin regulates collagen fibrillogenesis and the biomechanical properties of connective tissues. *J Cell Biochem*. 2007;101(3):695-711.
32. Sottile J, Hocking DC. Fibronectin polymerization regulates the composition and stability of extracellular matrix fibrils and cell-matrix adhesions. *Mol Biol Cell*. 2002;13(10):3546-3559.
33. Baru O, Nutu A, Braicu C, et al. Angiogenesis in regenerative dentistry: are we far enough for therapy? *Int J Mol Sci*. 2021;22(2):929.
34. Fraser D, Caton J, Benoit DS. Periodontal wound healing and regeneration: insights for engineering new therapeutic approaches. *Front Dent Med*. 2022;3:815810.
35. Liao Q, Qu S, Tang L-x, et al. Irisin exerts a therapeutic effect against myocardial infarction via promoting angiogenesis. *Acta Pharmacol Sin*. 2019;40(10):1314-1321.
36. Quintero-Fabián S, Arreola R, Becerril-Villanueva E, et al. Role of matrix metalloproteinases in angiogenesis and cancer. *Front Oncol*. 2019;9:1370.
37. Herouy Y, Mellios P, Bandemir E, et al. Inflammation in stasis dermatitis upregulates MMP-1, MMP-2 and MMP-13 expression. *J Dermatol Sci*. 2001;25(3):198-205.
38. Vadalà G, Di Giacomo G, Ambrosio L, et al. Irisin recovers osteoarthritic chondrocytes in vitro. *Cell*. 2020;9(6):1478.
39. Xi R, Zheng X, Tizzano M. Role of taste receptors in innate immunity and oral health. *J Dent Res*. 2022;101(7):759-768.
40. Tuzim K, Korolczuk A. An update on extra-oral bitter taste receptors. *J Transl Med*. 2021;19(1):1-33.

41. Kang W, Wang Y, Li J, et al. TAS2R supports odontoblastic differentiation of human dental pulp stem cells in the inflammatory microenvironment. *Stem Cell Res Ther*. 2022;13(1):374.
42. Pan Y, Tang Y, Gu H, Ge W. Ubiquitin modification in osteogenic differentiation and bone formation: from mechanisms to clinical significance. *Front Cell Dev Biol*. 2022;10:1033223.
43. Baek D, Park KH, Lee KM, et al. Ubiquitin-specific protease 53 promotes osteogenic differentiation of human bone marrow-derived mesenchymal stem cells. *Cell Death Dis*. 2021;12(3):238.
44. Hariri H, Addison WN, St-Arnaud R. Ubiquitin specific peptidase Usp53 regulates osteoblast versus adipocyte lineage commitment. *Sci Rep*. 2021;11(1):8418.
45. Prescott JA, Balmanno K, Mitchell JP, Okkenhaug H, Cook SJ. IKKα plays a major role in canonical NF-κB signalling in colorectal cells. *Biochem J*. 2022;479(3):305-325.
46. Cassandri M, Smirnov A, Novelli F, et al. Zinc-finger proteins in health and disease. *Cell Death Dis*. 2017;3(1):17071.
47. Alves HR, Lomba GSB, Gonçalves-de-Albuquerque CF, Burth P. Irisin, exercise, and COVID-19. *Front Endocrinol*. 2022;13:879066.
48. Qin Z, Fisher GJ, Voorhees JJ, Quan T. Actin cytoskeleton assembly regulates collagen production via TGF-β type II receptor in human skin fibroblasts. *J Cell Mol Med*. 2018;22(9):4085-4096.
49. Zhang Y, Wang H. Integrin signalling and function in immune cells. *Immunology*. 2012;135(4):268-275.
50. Myint PK, Ito A, Appiah MG, et al. Irisin supports integrin-mediated cell adhesion of lymphocytes. *Biochem Biophys Rep*. 2021;26:100977.
51. Kim H, Wrann CD, Jedrychowski M, et al. Irisin mediates effects on bone and fat via αV integrin receptors. *Cell*. 2018;175(7):1756-68.e17.
52. Sadok A, Marshall CJ. Rho GTPases: masters of cell migration. *Small GTPases*. 2014;5:e29710.
53. Zhang J, He W, Yi D, et al. Regulation of protein synthesis in porcine mammary epithelial cells by l-valine. *Amino Acids*. 2019;51(4):717-726.
54. Kudo A, Kii I. Periostin function in communication with extracellular matrices. *J Cell Commun Signal*. 2018;12(1):301-308.
55. Kular JK, Basu S, Sharma RI. The extracellular matrix: structure, composition, age-related differences, tools for analysis and applications for tissue engineering. *J Tissue Eng*. 2014;5:2041731414557112.
56. Koussounadis A, Langdon SP, Um IH, Harrison DJ, Smith VA. Relationship between differentially expressed mRNA and mRNA-protein correlations in a xenograft model system. *Sci Rep*. 2015;5(1):10775.
57. Maier T, Güell M, Serrano L. Correlation of mRNA and protein in complex biological samples. *FEBS Lett*. 2009;583(24):3966-3973.
58. Greenbaum D, Colangelo C, Williams K, Gerstein M. Comparing protein abundance and mRNA expression levels on a genomic scale. *Genome Biol*. 2003;4(9):1-8.
59. Jónsdóttir S, Giesen E, Maltha J. Biomechanical behaviour of the periodontal ligament of the beagle dog during the first 5 hours of orthodontic force application. *Eur J Orthod*. 2006;28(6):547-552.
60. Embery G. An update on the biochemistry of the periodontal ligament. *Eur J Orthod*. 1990;12(1):77-80.
61. Fill TS, Carey JP, Toogood RW, Major PW. Experimentally determined mechanical properties of, and models for, the periodontal ligament: critical review of current literature. *J Dent Biomech*. 2011;2011:312980.
62. Vimalraj S. Alkaline phosphatase: structure, expression and its function in bone mineralization. *Gene*. 2020;754:144855.
63. Lian JB, Stein GS. Concepts of osteoblast growth and differentiation: basis for modulation of bone cell development and tissue formation. *Crit Rev Oral Biol Med*. 1992;3(3):269-305.
64. Saran U, Gemini Piperni S, Chatterjee S. Role of angiogenesis in bone repair. *Arch Biochem Biophys*. 2014;561:109-117.
65. Rygh P, Bowling K, Hovlandsdal L, Williams S. Activation of the vascular system: a main mediator of periodontal fiber remodeling in orthodontic tooth movement. *Am J Orthod*. 1986;89(6):453-468.
66. Zanetta L, Marcus SG, Vasile J, et al. Expression of Von Willebrand factor, an endothelial cell marker, is up-regulated by angiogenesis factors: a potential method for objective assessment of tumor angiogenesis. *Int J Cancer*. 2000;85(2):281-288.
67. Tremble PM, Lane TF, Sage EH, Werb Z. SPARC, a secreted protein associated with morphogenesis and tissue remodeling, induces expression of metalloproteinases in fibroblasts through a novel extracellular matrix-dependent pathway. *J Cell Biol*. 1993;121(6):1433-1444.
68. Rosset EM, Bradshaw AD. SPARC/osteonectin in mineralized tissue. *Matrix Biol*. 2016;52–54:78-87.
69. Weber MA, Schnyder-Candrian S, Schnyder B, et al. Endogenous leukemia inhibitory factor attenuates endotoxin response. *Lab Invest*. 2005;85(2):276-284.
70. Kaur S, Bansal Y, Kumar R, Bansal G. A panoramic review of IL-6: structure, pathophysiological roles and inhibitors. *Bioorg Med Chem*. 2020;28(5):115327.
71. Hou T, Tieu BC, Ray S, et al. Roles of IL-6-gp130 signaling in vascular inflammation. *Curr Cardiol Rev*. 2008;4(3):179-192.

SUPPORTING INFORMATION

Additional supporting information can be found online in the Supporting Information section at the end of this article.

How to cite this article: Yang Y, Geng T, Samara A, et al. Recombinant irisin enhances the extracellular matrix formation, remodeling potential, and differentiation of human periodontal ligament cells cultured in 3D. *J Periodont Res*. 2023;58:336-349. doi:10.1111/jre.13094